2022

Evaluating Energy-based Trait Shifts and Population Level Impacts of Big Brown Bats (Eptesicus fuscus) with Long-term Exposure to Pseudogymnoascus destructans

Molly C. Simonis
Wright State University

EVALUATING ENERGY-BASED TRAIT SHIFTS AND POPULATION LEVEL IMPACTS OF BIG BROWN BATS (*EPTESICUS FUSCUS*) WITH LONG-TERM EXPOSURE TO *PSEUDOGYMNOASCUS DESTRUCTANS*

A Dissertation submitted in partial fulfillment of the

requirements for the degree of

Doctor of Philosophy

by

MOLLY C. SIMONIS

M.S., Wright State University, 2018

B.S., University of Dayton, 2009

2022

Wright State University

WRIGHT STATE UNIVERSITY
GRADUATE SCHOOL

April 8th, 2022

I HEREBY RECOMMEND THAT THE DISSERTATION PREPARED UNDER MY SUPERVISION BY Molly C. Simonis ENTITLED Evaluating energy-based trait shifts and population level impacts of big brown bats (*Eptesicus fuscus*) with long-term exposure to *Pseudogymnoascus destructans* BE ACCEPTED IN PARTIAL FULFILLMENT OF THE REQUIREMENTS FOR THE DEGREE OF Doctor of Philosophy.

_____
Megan Rúa, Ph.D.
Dissertation Director

_____
Lynn Hartzler, Ph.D.
Dissertation Director

_____
Don Cipollini, Ph.D.
Director, ES Ph.D. Program

_____
Barry Milligan, Ph.D.
Vice Provost for Academic Affairs
Dean of the Graduate School

Committee on Final Examination:

_____
Volker Bahn, Ph.D.

_____
Lisa Cooper, Ph.D.

_____
Joe Johnson, Ph.D.

ABSTRACT

Simonis, Molly C. Ph.D. Environmental Sciences Ph.D. Program, Wright State University, 2022. Evaluating energy-based trait shifts and population level impacts of big brown bats (*Eptesicus fuscus*) with long-term exposure to *Pseudogymnoascus destructans*

Disturbances in environment can lead to a wide range of host physiological responses. These responses can either allow hosts to adjust to new conditions in their environment or can reduce their survival, and can subsequently cause host traits to shift. Small mammals are particularly vulnerable to stochastic disturbances, like a pathogen introduction, because of their high energy demands. Studies examining host responses to pathogens often focus on species highly susceptible to infection that typically have high mortality rates, leading to a gap in understanding the responses of less susceptible species. My dissertation evaluates the energy balance of *Eptesicus fuscus* (big brown bats), a species considered less susceptible to the introduced fungal pathogen *Pseudogymnoascus destructans* (*Pd*) which causes white-nose syndrome in North American hibernating bats. I quantified changes in body mass, energy expenditures and capture rates of *E. fuscus* over long-term *Pd* exposure time. Using 30 years of data for 24,129 individual *E. fuscus* captures across the eastern US, I found *E. fuscus* body mass decreased with increasing latitude once *Pd* was established on the landscape (5+ years). When measuring whole-animal energy expenditures of 19 *E. fuscus* in lab settings using open-flow respirometry, I found that *E. fuscus* with long-term exposure to *Pd* have increases or no change to torpid metabolic rates across a wide range of ambient

temperatures. Finally, capture rates of *E. fuscus* increased with *Pd* exposure, and lactating and post-lactating bats capture rates increased with increasing latitude in the eastern US. Taken together, these results suggest that *E. fuscus* may have a combination of pathogen and intraspecific competitive pressures impacting their populations, particularly in northern latitudes. This dissertation highlights how introduced pathogens can cause spatially variable responses in less susceptible hosts over time, and other ecological pressures may contribute to those responses. Future efforts for understanding the degree of persistence of less susceptible wildlife host populations are critical for predicting how and why their populations change following emerging infectious disease outbreaks and epidemics.

TABLE OF CONTENTS

List of Figures

LIST OF TABLES

ACKNOWLEDGEMENTS

I am extremely grateful for my advisors, Dr. Megan Rúa and Dr. Lynn Hartzler. I am so fortunate to have not just one, but two, strong female advisors over the past four years for this degree. You have both dramatically influenced my growth as a scientist and as a person. I am grateful for your kindness, guidance and continued encouragement throughout my PhD. I thank my committee members, Dr. Volker Bahn, Dr. Lisa Cooper and Dr. Joe Johnson. Thank you for your kindness, support, encouragement on this dissertation, side projects and collaborations. Thank you to my family for being supportive throughout my graduate schooling and encouraging my academic adventures. I am enormously thankful for my fellow graduate student friends Aaron Onufrak, Ashley Julian, Adam Reed, Dr. Leon Katona, Marty Black, Michaela Woods, Dr. Sara Seibert, and Yasmeen Samar. Finally, I also thank my friends outside of academia, Dr. Alecia Klemas, Becky Crow, Bridget Brown, Candace Dalmagne-Rouge, Cyndi Treasure, Deb Oexmann, Jon Treasure and Sarah Stankavich, for their ongoing support.

CHAPTER 1

INTRODUCTION

Disturbances, such as pathogen introductions, in an environment can cause hosts to have a wide range of physiological responses (Carroll and Corneli, 1999; Strauss *et al.*, 2006). These responses can either allow organisms to adjust to new conditions in their environment or negatively impact their survival. Consequently, disturbances like a pathogen introduction can cause host traits to shift from their original values (Fig. 1.1). Energy-based traits (e.g. mass, fat, metabolism) have a wide range of responses to selective pressures imposed by pathogens on host populations (Carroll and Corneli, 1999; Schlaepfer et al., 2005; Strauss et al., 2006; West-Eberhard, 2003). These responses create gradients of host suitability, susceptibility, resistance and tolerance across inter- and intraspecific hosts and can drive fluctuating coevolutionary dynamics over time (Rabajante *et al.* 2015; Mason 2016; Cortez *et al.* 2017; Downs *et al.* 2019). When it comes to highly susceptible, low resistant and low tolerant hosts, energy-based trait responses, such as decreases to body condition and/or increases to energy expenditures due to infections, are well described (Altizer *et al.* 2004; Voyles *et al.* 2007; Verant *et al.* 2014; Poorten & Rosenblum 2016; McGuire *et al.* 2017). However, there are clear knowledge gaps in understanding responses of energy-based traits for less susceptible hosts despite their importance for structuring pathogen dynamics and their increased

contribution to diversity following a pathogen introduction and subsequent emerging infectious disease (Gervasi *et al.* 2015; VanderWaal & Ezenwa 2016).

Small mammals are particularly vulnerable to stochastic events in the environment. With high mass-specific metabolic rates, small mammals have high daily energy demands with relatively little energy storage capacity (Hill *et al.* 2016). Because small mammals lose more energy in the form of body heat to their environment relative to larger mammals, it costs small mammals more energy to maintain a warm body temperature (T_b) across all ambient temperatures (T_a; Hill *et al.* 2016). These relatively greater energy costs compared to larger mammals require small mammals to eat larger amounts of food to offset those losses and maintain a stable T_b from within. Therefore, when a disruption like an introduced pathogen requires small mammals to compensate with additional energy, small mammals must be able to make up for those additive energy costs in order to survive.

To combat the energetic costs of defending a warm body temperature, regardless of a disruption in the environment, many small mammals are heterothermic and can switch from being homeothermic to poikilothermic (having a variable T_b with T_a). To maintain a stable warm T_b as homeothermic endotherms, small mammals must expend energy outside of their thermoneutral zone (TNZ; range of T_a within which an animal has a basal metabolic rate and expends no additional energy to maintain T_b). This can be particularly challenging in colder climates when food availability is scarce (*e.g.*, during winter months). Therefore, many small mammals reduce the energetic costs by decreasing the heat gradient between their body and their environment, combatting energetic costs of maintaining a warm, stable T_b by using poikilothermy as an

endothermic strategy. This allows small mammals to torpor in colder T_a. Torpor can be brief (hours) or extend into longer bouts (days to weeks) throughout winter, known as hibernation. While torpid, sensory and motor functions are depleted, protein synthesis, mitosis and active membrane transport ceases and immune functions are decreased or halted (Sulkin *et al.* 1966; Kolaeva *et al.* 1980; Nedergaard *et al.* 1990; Marjanovic & Willis 1992; Frerichs *et al.* 1998; Burton & Reichman 1999; Humphries *et al.* 2003). While poikilothermy can reduce energy expenditures for small mammals, their vulnerability to disruptions like a pathogen increases during torpor since these disruptions can take advantage of host inactivity in environments where they hibernate (Wang & Wolowyk 1988).

There is a general risk for starvation for small mammals during hibernation. This is because small mammals rely on fat stores alone for survival in cold winter months when food is scarce, so survival is positively correlated with the amount of fat small mammals obtain before entering hibernation (Brigham 1987; Speakman & Thomas 2003; Willis *et al.* 2005; Jonasson & Willis 2017). Small mammals must undergo periodic arousals where they increase energy expenditures in order to adjust metabolic imbalances that are more easily corrected when they homeothermic and defend a warm stable body temperature (Ruf & Geiser 2015). These periodic arousals can account for over half, and even up to 85%, of energy expenditures throughout hibernation (Geiser 2007; Jonasson & Willis 2012). A pathogen introduction into a small mammal's hibernating environment has the potential to disrupt the energetic cost savings of torpor by triggering arousals to mount immune responses (Prendergast *et al.* 2002; Fig. 1.2). Therefore, if a small mammal has not eaten enough prior to hibernation to support additional energy

expenditures due to pathogen exposure during hibernation, they risk starvation from early fat store depletion. Unless small mammals can compensate for the additional energetic costs from introduced pathogen exposure and infections, it is likely host populations will suffer over time (Willis 1982, 2015; Geiser 2013).

In North America, temperate hibernating bats are currently threatened by the introduced fungal pathogen *Pd*, which causes white-nose syndrome (WNS; Blehert *et al.*, 2008; Lorch *et al.*, 2011). *Pd* was introduced from Eurasia to New York, USA, but first detected in winter 2006. It has subsequently spread across North America (Blehert *et al.* 2009; Leopardi *et al.* 2015; Drees *et al.* 2017; White Nose Syndrome Response Team 2022; Fig. 1.3). *Pd* exhibits optimal growth between 12 °C and 16 °C (Verant *et al.* 2012), making hibernacula like caves the perfect environment for *Pd* to thrive. *Pd* infects the epithelial tissue of bats wings and muzzles while they hibernate (Blehert *et al.* 2009; Meteyer *et al.* 2009; Lorch *et al.* 2011). In species that are highly susceptible to *Pd* infection, WNS increases periodic arousal frequency, decreases torpor bout duration, increases metabolic rates, increases evaporative water loss, and causes hypotonic dehydration and respiratory acidosis during hibernation, ultimately leading to death from energy depletion (Lorch *et al.* 2011; Reeder *et al.* 2012; Cryan *et al.* 2013; Verant *et al.* 2014; McGuire *et al.* 2017). Outside of hibernating months, highly susceptible species surviving hibernation with *Pd* infections have increased energy expenditures in the spring when they emerge from hibernation and begin to heal winter infections (Meierhofer *et al.* 2018; Fuller *et al.* 2020). The detrimental consequences of WNS to the physiology of infected bats has devastated populations of highly susceptible North American temperate bat species with estimated declines over 90% (Frick *et al.* 2010a, 2015, 2017; Cheng *et*

al. 2021). Surviving North American temperate bat populations are also likely incurring the same consequences to their physiology annually throughout their life stages, although research into this phenomenon is lacking.

Eptesicus fuscus (big brown bats) are a North American temperate bat species that is considered less susceptible with some resistance to *Pd* infection (Frank *et al.*, 2014; Moore *et al.*, 2018). Although *E. fuscus* populations are estimated to have decreased up to 50% following *Pd* introduction, their populations persist in greater numbers than highly susceptible species despite annual *Pd* exposure and infections during hibernation (Turner *et al.* 2011; Simonis *et al.* 2020; Cheng *et al.* 2021). As a large-bodied temperate bat species, *E. fuscus*' ability to survive *Pd* infections is predicted to be due, in part, to their greater body mass relative to other highly susceptible bat species (Haase *et al.* 2021). Additionally, when infected with *Pd*, *E. fuscus* extend their torpor bout durations during hibernation compared to when they are not infected, which likely contributes to their winter survival with *Pd* infections (Moore *et al.* 2018). *E. fuscus* also do not change their periodic arousal frequency during hibernation when exposed to *Pd* compared to before *Pd* introduction, supporting some degree of resistance to *Pd* (Frank *et al.* 2014).

Even though *E. fuscus* may have some physiological traits that contribute to their lowered susceptibility and higher resistance to *Pd* infections, their repeated and annual exposure to *Pd* in winter months could have damaging cumulative effects as they go through their annual life stages in combination with *Pd* exposure (Fig. 1.4). Unfortunately, due to their ability to persist in greater numbers compared to highly susceptible species, long-term impacts to *E. fuscus* abundance and energy-based traits may go unnoticed. This is concerning because as a species less susceptible to *Pd*

infection, *E. fuscus* are greater contributors North American bat diversity following *Pd* introduction. Therefore, to understand the full extent of *Pd* impacts on North American bat populations over time, it is critical to have more knowledge into how less susceptible, resistant *E. fuscus* populations and their energy-based traits are changing.

The overarching goal of my dissertation is to identify changes in energy-based traits of small mammal hosts during prolonged exposure to an introduced pathogen, and relate those traits to long-term host population level impacts of the pathogen. To achieve this goal, the chapters of my dissertation aim to understand changes to host energy-intake traits (Chapter 2), host energy-expenditure traits (Chapter 3) and host populations (Chapter 4) with long-term pathogen exposure. This dissertation uses the *Pd* / North American temperate bat system to meet these aims and quantifies changes to energy based-traits and the capture rates of *E. fuscus* with long-term *Pd* exposure. In Chapter 2, I quantify changes to *E. fuscus* body mass over long-term *Pd* exposure across the eastern US. In Chapter 3, I quantify changes to the torpid energy expenditures of *E. fuscus* a decade after the introduction of *Pd*. In Chapter 4, I quantify changes to the capture rates and demographic structure of *E. fuscus* over *Pd* exposure time across the eastern US. This dissertation will advance our understanding for how and why the energy-based traits of less susceptible small mammal hosts change with long-term pathogen exposure as wildlife pathogen introductions become more prominent on the landscape (Daszak *et al.* 2001; Jones *et al.* 2008).

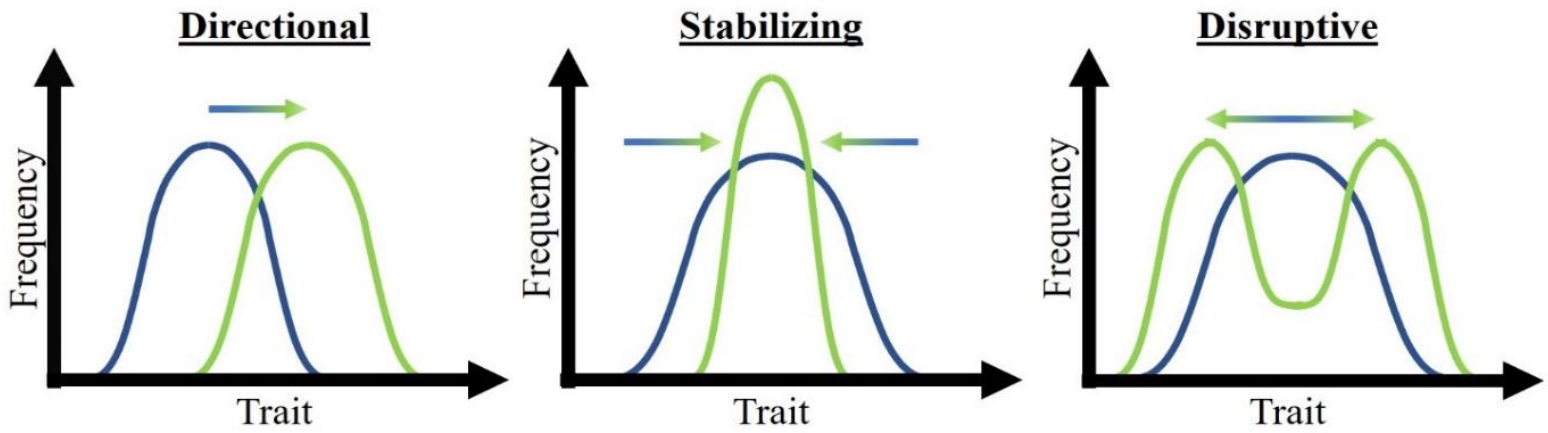

Figure 1.1. Directional, stabilizing and disruptive trait selection occur over time when an organism's environment is disturbed. Plasticity throughout an organism's population can provide insight into selection when the environmental disturbance is initiated and continued. Blue lines indicate initial trait distributions while green lines represent trait distributions after disturbance.

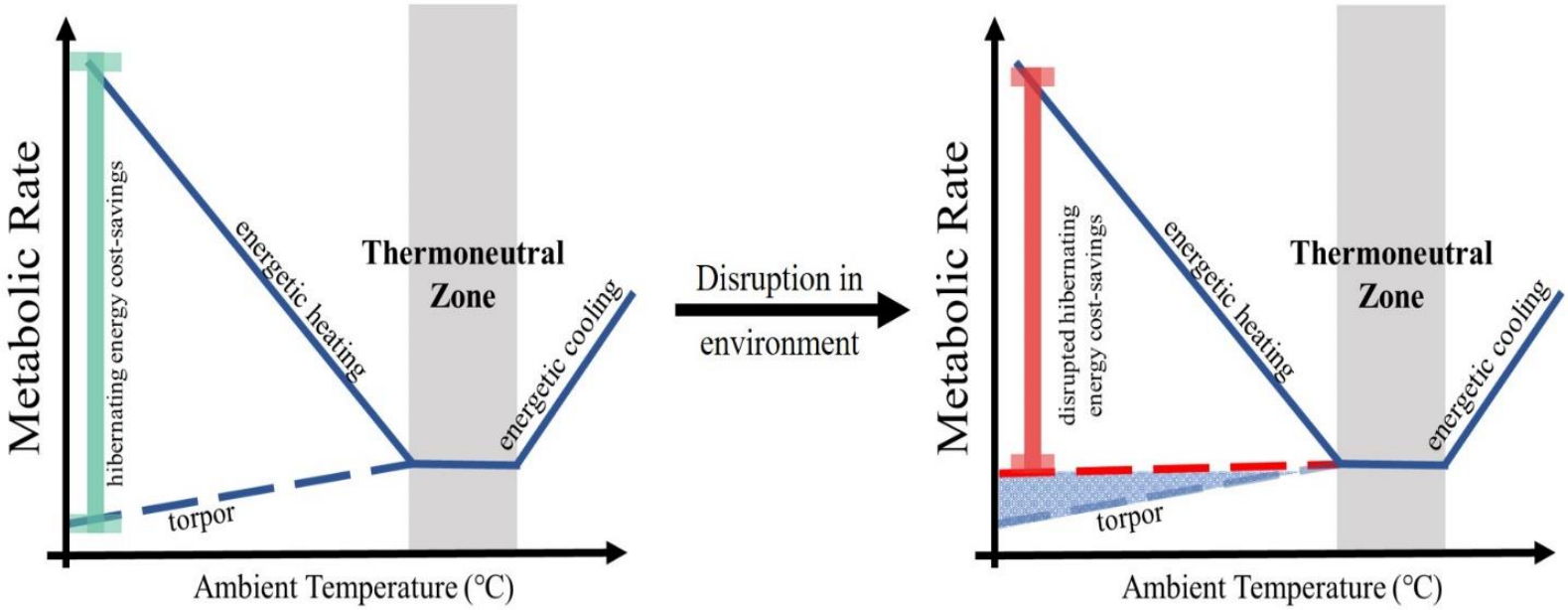

Figure 1.2. Energy savings decrease during hibernation when torpor is disrupted. This can be caused by disruptions such as pathogen interactions, human interference and/or climate change.

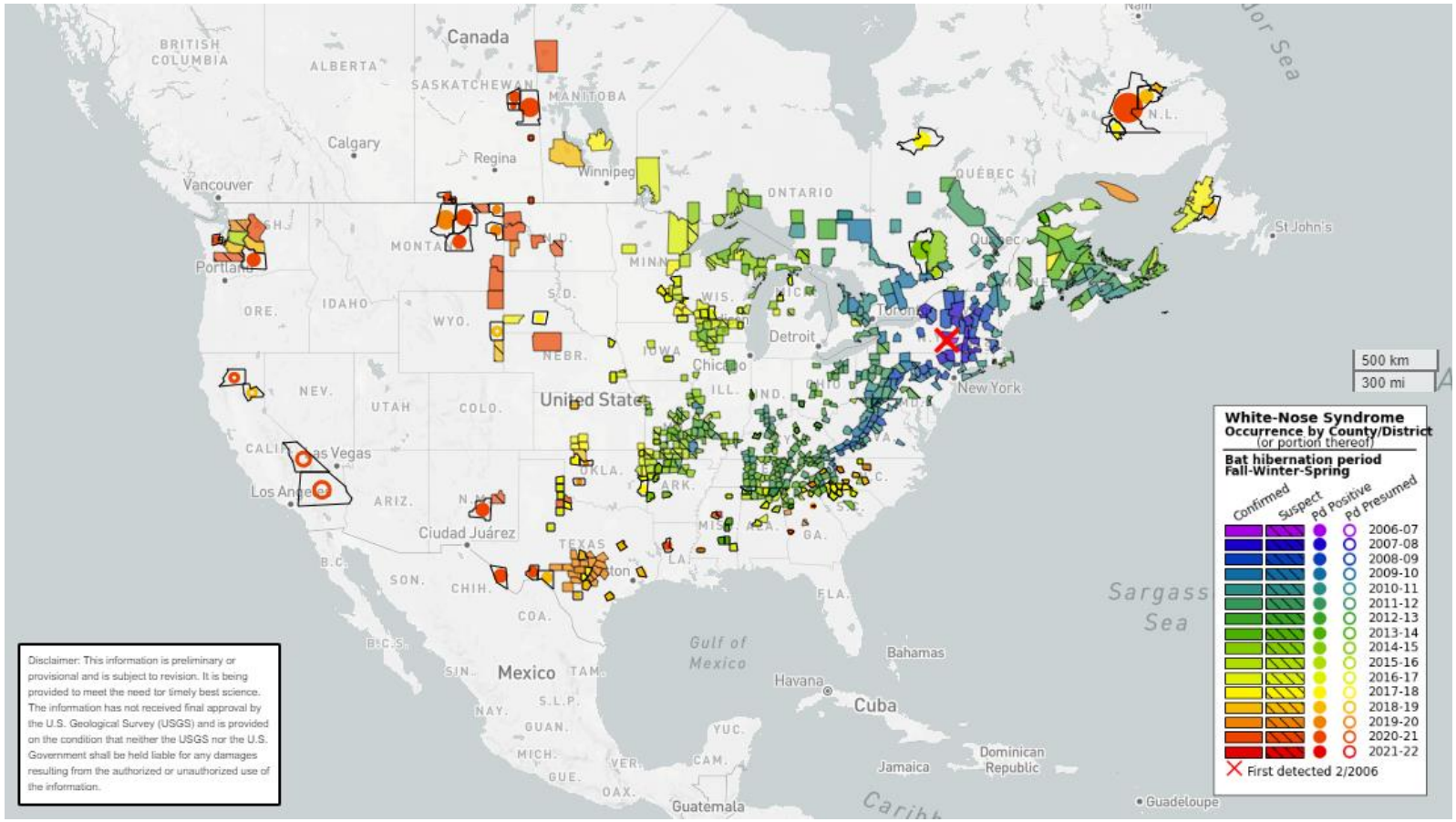

Figure 1.3. Confirmed and suspected occurrence of *Pd* and WNS as of 19 March 2022 (White Nose Syndrome Response Team 2022). Available at http://www.whitenosesyndrome.org/resources/map.

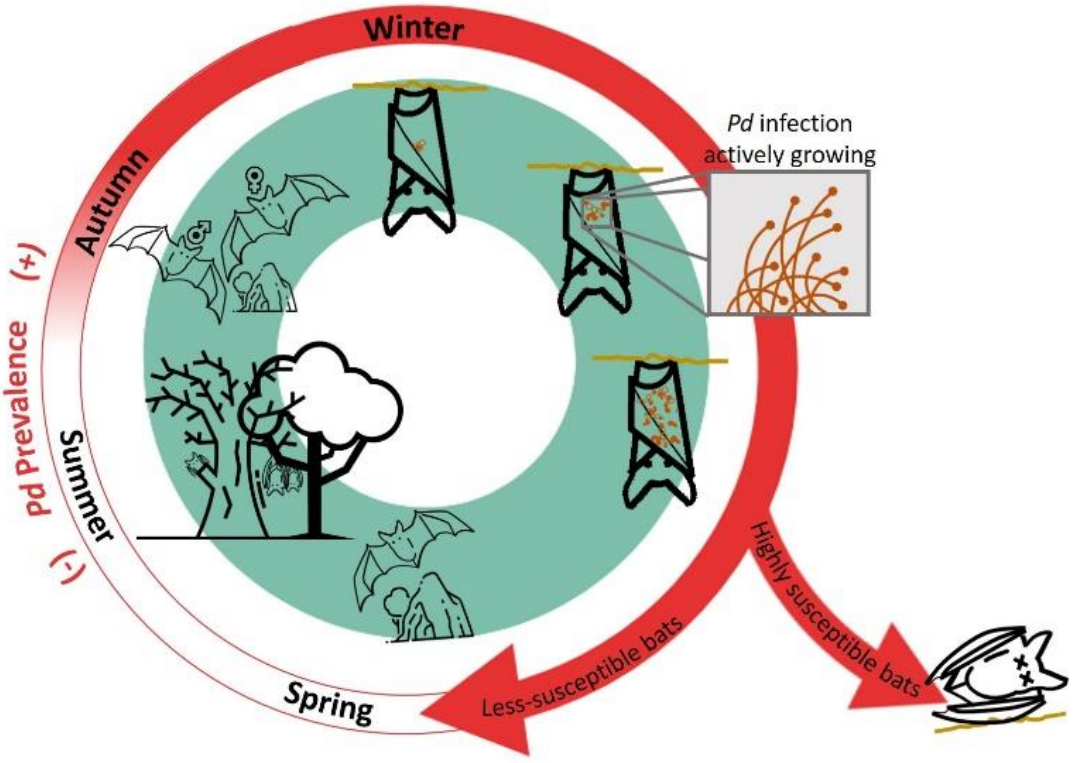

Figure 1.4. Less susceptible bats currently go through their annual life cycle stages in combination with *Pd* interactions.

REFERENCES

Altizer, S., Davis, A.K., Cook, K.C. & Cherry, J.J. (2004). Age, sex, and season affect the risk of mycoplasmal conjunctivitis in a southeastern house finch population. Can. J. Zool., 82, 755–763.

Blehert, D.S., Hicks, A.C., Behr, M., Meteyer, C.U., Berlowski-Zier, B.M., Buckles, E.L., et al. (2009). Bat white-nose syndrome: an emerging fungal pathogen? Science, 323, 227.

Brigham, R.M. (1987). The significance of winter activity by the big brown bat (*Eptesicus fuscus*): the influence of energy reserves. Can. J. Zool., 65, 1240–1242.

Burton, R.S. & Reichman, J. (1999). Does Immune Challenge Affect Torpor Duration. Funct. Ecol., 13, 232–237.

Carroll, S.P. & Corneli, P.S. (1999). The evolution of behavioral reaction norms as a problem in ecological genetics: theory, methods and data. In: The Evolution of Behavioral Phenotypes; Perspectives from the Study of Geographic Variation (eds. Foster, S. & Endler, J.). Oxford University Press, Oxford, pp. 52–68.

Cheng, T.L., Reichard, J.D., Coleman, J.T.H., Weller, T.J., Thogmartin, W.E., Reichert, B., et al. (2021). The scope and severity of White-nose Syndrome on hibernating bats in North America. Conserv. Biol., 35, 1586–1597.

Cortez, M.J. V., Rabajante, J.F., Tubay, J.M. & Babierra, A.L. (2017). From epigenetic landscape to phenotypic fitness landscape: Evolutionary effect of pathogens on host traits. Infect. Genet. Evol., 51, 245–254.

Cryan, P.M., Meteyer, C.U., Blehert, D.S., Lorch, J.M., Reeder, D.M., Turner, G.G., et al. (2013). Electrolyte Depletion in White-nose Syndrome Bats. J. Wildl. Dis., 49, 398–402.

Daszak, P., Cunningham, A.A. & Hyatt, A.D. (2001). Anthropogenic environmental change and the emergence of infectious diseases in wildlife. Acta Trop., 78, 103–116.

Downs, C.J., Schoenle, L.A., Han, B.A., Harrison, J.F. & Martin, L.B. (2019). Scaling of Host Competence. Trends Parasitol., 35, 182–192.

Drees, K., Puechmaille, S., Parise, K.L. & Wibbelt, G. (2017). Phylogenetics of a Fungal Invasion: Origins and Widespread Dispersal of White-Nose Syndrome. MBio, 8, e01941-17.

Frank, C.L., Michalski, A., McDonough, A.A., Rahimian, M., Rudd, R.J. & Herzog, C. (2014). The resistance of a North American bat species (*Eptesicus fuscus*) to White-Nose Syndrome (WNS). PLoS One, 9, 1–14.

Frerichs, K.U., Smith, C.B., Brenner, M., DeGracia, D.J., Krause, G.S., Marrone, L., et al. (1998). Suppression of protein synthesis in brain during hibernation involves inhibition of protein initiation and elongation. PNAS, 95, 14511–14516.

Frick, W.F., Cheng, T.L., Langwig, K.E., Hoyt, J.R., Janicki, A.F., Parise, K.L., et al. (2017). Pathogen dynamics during invasion and establishment of white-nose syndrome explain mechanisms of host persistence. Ecology, 98, 624–631.

Frick, W.F., Pollock, J.F., Hicks, A.C., Langwig, K.E., Reynolds, D.S., Turner, G.G., et al. (2010). An emerging disease causes regional population collapse of a common North American bat species. Science, 329, 679–82.

Frick, W.F., Puechmaille, S.J., Hoyt, J.R., Nickel, B.A., Langwig, K.E., Foster, J.T., et al. (2015). Disease alters macroecological patterns of North American bats. Glob. Ecol. Biogeogr., 24, 741–749.

Fuller, N.W., Mcguire, L.P., Pannkuk, E.L., Blute, T., Haase, C.G., Mayberry, H.W., et al. (2020). Disease recovery in bats affected by white-nose syndrome. J. Exp. Biol., 223, jeb211912.

Geiser, F. (2007). Yearlong hibernation in a marsupial mammal. Naturwissenschaften, 94, 941–944.

Geiser, F. (2013). Hibernation. Curr. Biol., 23, 188–193.

Gervasi, S.S., Civitello, D.J., Kilvitis, H.J. & Martin, L.B. (2015). The context of host competence: A role for plasticity in host-parasite dynamics. Trends Parasitol., 31, 419–425.

Haase, C.G., Fuller, N.W., Dzal, Y.A., Hranac, C.R., Hayman, D.T.S., Lausen, C.L., et al. (2021). Body mass and hibernation microclimate may predict bat susceptibility to white-nose syndrome. Ecol. Evol., 11, 506–515.

Hill, R.W., Wyse, G.A. & Anderson, M. (Eds.). (2016). Animal Physiology. Fourth edition. Sinauer Associates Inc., Sunderland, MA.

Humphries, M.M., Thomas, D.W. & Kramer, D.L. (2003). The role of energy availability in mammalian hibernation: A cost-benefit approach. Physiol. Biochem. Zool., 76, 165–179.

Jonasson, K. & Willis, C.K.R. (2017). Thrifty Females, Frisky Males: Winter Energetics of Hibernating Bats from a Cold Climate. Physiol. Biochem. Zool., 90, 502–511.

Jonasson, K.A. & Willis, C.K.R. (2012). Hibernation energetics of free-ranging little brown bats. J. Exp. Biol., 215, 2141–2149.

Jones, K.E., Patel, N.G., Levy, M.A., Storeygard, A., Balk, D., Gittleman, J.L., et al. (2008). Global trends in emerging infectious diseases. Nature, 44, 319–335.

Kolaeva, S.G., Kramarova, L.I., Ilyasova, E.N. & Ilyasov, F.E. (1980). The kinetics and metabolism of the cells of hibernating animals during hibernation. Int. Rev. Cytol., 66, 147–170.

Leopardi, S., Blake, D. & Puechmaille, S.J. (2015). White-nose syndrome fungus introduced from Europe to North America. Curr. Biol., 25, R217–R219.

Lorch, J.M., Meteyer, C.U., Behr, M.J., Boyles, J.G., Cryan, P.M., Hicks, A.C., et al. (2011). Experimental infection of bats with *Geomyces destructans* causes white-nose syndrome. Nature, 480, 376–378.

Marjanovic, B.Y.M. & Willis, J.S. (1992). ATP dependence of Na+ - K+ pump of cold-sensitive and sold-tolerant mammalian red blood cells. J. Physiol., 456, 575–590.

Mason, P.A. (2016). On the role of host phenotypic plasticity in host shifting by parasites. Ecol. Lett., 19, 121–132.

McGuire, L.P., Mayberry, H.W. & Willis, C.K.R. (2017). White-nose syndrome increases torpid metabolic rate and evaporative water loss in hibernating bats. Am. J. Physiol. - Regul. Integr. Comp. Physiol., 313, R680–R686.

Meierhofer, M.B., Johnson, J.S., Field, K.A., Lumadue, S.S., Kurta, A., Kath, J.A., et al. (2018). Bats recovering from white-nose syndrome elevate metabolic rate during wing healing in Spring. J. Wildl. Dis., 54, 480–490.

Meteyer, C.U., Buckles, E.L., Blehert, D.S., Hicks, A.C., Green, D.E., Shearn-bochsler, V., et al. (2009). Histopathologic criteria to confirm white-nose syndrome in bats. J. Vet. Diagnostic Investig., 21, 411–414.

Moore, M.S., Field, K.A., Behr, M.J., Turner, G.G., Furze, M.E., Stern, D.W.F., et al. (2018). Energy conserving thermoregulatory patterns and lower disease severity in a bat resistant to the impacts of white-nose syndrome. J. Comp. Physiol. B Biochem. Syst. Environ. Physiol., 188, 163–176.

Nedergaard, J., Cannon, B. & Jaenicke, R. (1990). Mammalian Hibernation. Philos. Trans. R. Soc. London. Ser. B, Biol. Sci., 326, 669–686.

Poorten, T.J. & Rosenblum, E.B. (2016). Comparative study of host response to chytridiomycosis in a susceptible and a resistant toad species. Mol. Ecol., 25, 5663–5679.

Prendergast, B.J., Freeman, D.A., Zucker, I. & Nelson, R.J. (2002). Periodic arousal from hibernation is necessary for initiation of immune responses in ground squirrels. Am. J. Physiol. - Regul. Integr. Comp. Physiol., 282, R1054–R1062.

Rabajante, J.F., Tubay, J.M., Uehara, T., Morita, S., Ebert, D. & Yoshimura, J. (2015). Red Queen dynamics in multi-host and multi-parasite interaction system. Sci. Rep., 5, 1–7.

Reeder, D.M., Frank, C.L., Turner, G.G., Meteyer, C.U., Kurta, A., Britzke, E.R., et al. (2012). Frequent Arousal from Hibernation Linked to Severity of Infection and Mortality in Bats with White-Nose Syndrome. PLoS One, 7, e38920.

Ruf, T. & Geiser, F. (2015). Daily torpor and hibernation in birds and mammals. Biol. Rev., 90, 891–926.

Schlaepfer, M.A., Sherman, P.W., Blossey, B. & Runge, M.C. (2005). Introduced species as evolutionary traps. Ecol. Lett., 8, 241–246.

Simonis, M.C., Brown, B.B. & Bahn, V. (2020). Mobile bat acoustic routes indicate cavity-roosting species undergo compensatory changes in community composition following white-nose syndrome. Acta Chiropterologica, 22, 315–326.

Speakman, J.R. & Thomas, T. (2003). Physiological Ecology and Energetic of Bats. In: Bat Ecology (eds. Kunz, T.H. & Fenton, M.B.). The University of Chicago Press, pp. 430–490.

Strauss, S.Y., Lau, J.A. & Carroll, S.P. (2006). Evolutionary responses of natives to introduced species: What do introductions tell us about natural communities? Ecol. Lett., 9, 354–371.

Sulkin, S.E., Allen, R., Sims, R. & Singh, K. V. (1966). Studies of arthropod-borne virus infections in Chiroptera. Am. J. Trop. Med. Hygeine, 15, 418–427.

Turner, G.G., Reeder, D. & Coleman, J.T.H. (2011). A Five-year Assessment of Mortality and Geographic Spread of White-Nose Syndrome in North American Bats, with a look to the future. Bat Res. News, 52, 13–27.

VanderWaal, K.L. & Ezenwa, V.O. (2016). Heterogeneity in pathogen transmission: mechanisms and methodology. Funct. Ecol., 30, 1606–1622.

Verant, M.L., Boyles, J.G., Waldrep, W., Wibbelt, G. & Blehert, D.S. (2012). Temperature-Dependent Growth of *Geomyces destructans*, the Fungus That Causes Bat White-Nose Syndrome. PLoS One, 7, e46280.

Verant, M.L., Meteyer, C.U., Speakman, J.R., Cryan, P.M., Lorch, J.M. & Blehert, D.S. (2014). White-nose syndrome initiates a cascade of physiologic disturbances in the hibernating bat host. BCM Physiol., 14.

Voyles, J., Berger, L., Young, S., Speare, R., Webb, R., Warner, J., et al. (2007). Electrolyte depletion and osmotic imbalance in amphibians with chytridiomycosis. Dis. Aquat. Organ., 77, 113–118.

Wang, L.C.H. & Wolowyk, M.W. (1988). Torpor in mammals and birds. Can. J. Zool., 66, 133–137.

West-Eberhard, M.J. (2003). Developmental Plasticity and Evolution. Oxford University Press.

White Nose Syndrome Response Team. (2022). White-nose syndrome occurrence map by year. Hadley, Massachusetts. https://www.whitenosesyndrome.org/.

Willis, C.K.., Lane, J.E., Liknes, E.T., Swanson, D.L. & Brigham, R.M. (2005). Thermal energetics of female big brown bats (*Eptesicus fuscus*). Can. J. Zool., 83, 871–879.

Willis, C.K.R. (2015). Conservation physiology and conservation pathogens: White-nose syndrome and integrative biology for host-pathogen systems. Integr. Comp. Biol., 55, 631–641.

Willis, J.S. (1982). The mystery of the periodic arousal. In: Hibernation and Torpor in Mammals and Birds (eds. Lyman, C.P., Willis, J.S., Malan, A. & Wang, L.C.H.). Academic, New York, New York, pp. 92–103.

CHAPTER 2

EPTESICUS FUSCUS DECREASES BODY MASS WITH INCREASING LATITUDE AND LONG-TERM EXPOSURE TO AN INVASIVE FUNGAL PATHOGEN

ABSTRACT

Invasive pathogens threaten wildlife health and biodiversity. Physiological responses of species highly susceptible to pathogen infections following invasion are well described. However, the responses of less susceptible species (relative to highly susceptible species) are not well known despite their larger contributions to diversity and pathogen dynamics following pathogen invasion. Latitudinal gradients, which influence body condition and/or reflect the time it takes for an introduced pathogen to spread geographically, add an additional layer for how less susceptible species respond to pathogen exposure. My goal was to understand how hosts less susceptible to pathogen infections respond physiologically to long-term pathogen exposure across a broad latitudinal gradient. I examined changes in body mass throughout pathogen exposure time across the eastern US in *Eptesicus fuscus*, a persisting bat species classified as less susceptible to infection by the invasive fungal pathogen that causes white-nose syndrome, *Pseudogymnoascus destructans* (*Pd*). Using 30 years of capture records, I created linear mixed effects models for female and male bats to determine how mass or mass variation changed across the eastern US from pre-*Pd* invasion years through *Pd* invasion (0-1 years with *Pd*), epidemic (2-4 years with *Pd*) and established years (5+ years

with *Pd*). By *Pd* establishment, all female and male bats decreased body mass with increasing latitude across a spatial threshold at 39.6 °N. Differences in bat mass north and south of the spatial threshold progressively increased over *Pd* exposure time-steps such that, body mass was less in northern latitudes compared to southern latitudes by *Pd* establishment. Additionally, non-reproductive female bat mass variation in northern latitudes decreased by *Pd* establishment and post-lactating bat mass variation increased toward values lower than their average mass by *Pd* establishment. I suggest the progressive effects of *Pd* exposure on *E. fuscus* body mass across the eastern US could be due to increases to intraspecific competition over invasion time as highly susceptible species become rarer. This is because intraspecific competition is theoretically stronger than interspecific competition. Further, lower body mass in northern latitudes compared to southern latitudes could alter thermoregulatory patterns for *E. fuscus* across the eastern US because body mass is positively correlated with energy expenditures. As pathogen introductions and emerging infectious diseases become more prevalent on the landscape, it is imperative we understand how less susceptible species directly and indirectly respond to long-term pathogen exposure in order to maintain population health in surviving species.

INTRODUCTION

Introduced and invasive species change environments and ecosystems globally (Mack *et al.* 2000). Introduced pathogens causing emerging and re-emerging infectious diseases are evolutionary threats to biodiversity (Daszak *et al.* 2000), and induce varied inter- and intraspecific physiological responses in hosts (Poorten & Rosenblum 2016; Moore *et al.* 2018). Species highly susceptible to infection with high mortality rates receive most study (Altizer *et al.* 2004; Voyles *et al.* 2007; McGuire *et al.* 2017). Consequently, we know less about responses of less susceptible hosts although they are also at risk. Ignoring less susceptible host responses overlooks the largest contributors to diversity following pathogen invasions, the mechanisms they deploy that make them less vulnerable to pathogen infection, and ignores potentially innovative and effective treatments for highly susceptible species with infections.

Pathogen exposure elicits energetically expensive host immune responses, so energy-based trait responses may influence species' susceptibility to disease (Schoenle *et al.* 2018). Body condition (mass or fat) contributes to host susceptibility such that susceptibility generally scales negatively with body condition (Downs *et al.* 2019). Host responses to infection can have negative, positive, or null responses (Sánchez *et al.* 2018). For example, several species decrease mass or fat and/or increase energy expenditures while responding to pathogens, while others surviving infections may maintain or increase mass or fat

(Cheng et al., 2019; Luong *et al*. 2017; McGuire *et al*. 2017; Poorten & Rosenblum, 2016).

Environmental, behavioral, and physiological factors may also add to the complexities of host responses to pathogens. For example, climatic and/or land use factors associated with pathogen reproduction, resource availability, and/or nutrition quality can contribute to pathogen emergence, transmission, and epidemics (Descloux *et al.* 2012; Hall 2019). Avoidance of pathogens or parasites by hosts or management interactions by humans can contain the extent of a disease outbreak (Loehle 1995; Ferguson *et al.* 2001). Finally, seasonal movements associated with life history or life cycle stages can create hotspots for disease outbreaks, particularly when hosts are under additional stressors like reproduction and/or migration (Bartel *et al.* 2011; Plowright *et al.* 2014). Thus, spatial gradients add another layer of complexity to how individuals physiologically respond to pathogen emergence.

Species with broad geographic ranges may have greater mass in high latitudes compared to low latitudes to reduce surface area to volume ratios, and thus heat loss, in colder climates as Bergmann's rule suggests (Bergmann 1847). Body mass is also negatively associated with host susceptibility to pathogens such that, as host body mass increases, host susceptibility to pathogen infection decreases due to increased immune functioning (Downs *et al.* 2019). If both tendencies for mass exist, I would then expect mammals to have a decreased susceptibility to pathogen infections as latitude increases. However, these patterns are unlikely when heterothermic mammals undergo periods of suppressed

immune functioning (*e.g.*, torpor or hibernation; Prendergast *et al*. 2002), nor if the pathogen thrives in hibernacula such as caves where heterothermic mammals like bats overwinter.

Pseudogymnoascus destructans (*Pd*) is an invasive fungal pathogen that causes white-nose syndrome (WNS) in North American hibernating bats (Blehert *et al.* 2009; Lorch *et al.* 2011). *Pd* was introduced from Eurasia and discovered in 2006 in New York, USA (Blehert *et al.* 2009; Leopardi *et al.* 2015; Drees *et al.* 2017). *Pd* exhibits optimal growth between 12 °C and 16 °C (Verant *et al.* 2012), allowing it to thrive in bat hibernacula. *Pd* infects epithelial tissues during hibernation which increases evaporative water loss, requires higher metabolic rates to fight infection, and induces a host energy imbalance and consequent starvation (Meteyer *et al.* 2009; McGuire *et al.* 2017). Extreme depletion of energy from *Pd* infection has led to local extinctions of highly susceptible bat species, devastating populations of North American temperate bats (Frick *et al.* 2015; Cheng *et al*. 2021).

Highly susceptible bats surviving winter infections have energy-based trait changes that may impact life history stages outside of hibernation. *Pd* infections in winter increase energy expenditures in spring as bats fight infection upon arousal (Meierhofer *et al.* 2018; Fuller *et al.* 2020). Combined with migration and females becoming pregnant at the same time, available energy for immune functioning is limited. Therefore, additive energy depletions likely have consequences that carry over into all seasons.

Despite estimated population declines of up to 50% from WNS (Turner *et al.* 2011; Simonis *et al.* 2020; Cheng *et al.* 2021), *Eptesicus fuscus* are classified as a less susceptible species with some degree of resistance to *Pd* infection that allows them to persist in greater numbers than highly susceptible species with population losses exceeding 90% (Cheng *et al.* 2021). *E. fuscus* are a large-bodied temperate bat species, so energy-based trait shifts may go unnoticed because their ability to survive *Pd* invasion is predicted to be due, in part, to their greater body mass relative to other bat species (Haase *et al.* 2021). However, *E. fuscus* continue to have repeated *Pd* infections each winter, setting up seasonal shifts in body mass due to additive energy expenditures needed to mount immune responses to fight *Pd* infections during winter hibernation and spring emergence (Field *et al.* 2015; McGuire *et al.* 2017; Meierhofer *et al.* 2018). Here, I quantify changes to *E. fuscus* body mass as a first step to understanding their persistence on the landscape despite chronic *Pd* exposure. I use long-term datasets to understand how *E. fuscus* body mass changed under long-term pathogen pressures, how individual variation in responses contributes to that change, and how these changes occur across a broad spatial scale. I quantify shifts in *E. fuscus* body mass before and after *Pd* introduction across the eastern US using 30 years of capture data. I hypothesized average mass and mass variation would decrease over *Pd* exposure time, with declines in mass and mass variation increasing with latitude. These results illuminate how species less susceptible to pathogen infection are subject to physiological changes under pathogen pressures over exposure time and across a large spatial gradient.

MATERIALS AND METHODS

Data Collection

I collated 40,414 *E. fuscus* capture records collected between March and October 1990–2020 from wildlife agencies and researchers in Georgia, Illinois, Indiana, Kentucky, Mississippi, New York, North Carolina, Ohio, Pennsylvania, Tennessee, and Virginia. These capture records represented individual *E. fuscus* captures but not mark and recaptures; therefore, specific individuals were not tracked. I extracted records that included date of capture, capture site name, sex (male/female), reproductive status (females only: non-reproductive/pregnant/lactating/post-lactating), age (adult/juvenile), and mass (g) at time of capture. I removed records not meeting these minimal requirements from the dataset and 30,496 individual capture records remained. Site description substituted for unnamed sites. If no site description was reported, I further assigned an individual site name based on state and county of capture. Finally, if site names were labeled by capture nets (e.g., "Site 1 Net A", "Site 1 Net B"), I pooled nets under the single site name (e.g., "Site 1 Net A" and "Site 1 Net B" both become "Site 1"). Due to the potential of exposing the location of sensitive species, site was masked for all analyses by labeling each site name by state and a unique identifier. For example, "Site 1" in Ohio became "OH_01".

I subset data for adult *E. fuscus* captures only. Data were further cleaned to remove inconsistencies in the capture records. For example, if an *E. fuscus* was

marked as a pregnant male, it was eliminated from the dataset. I identified outliers based on mass. Mass values outside the range of 8.8 g to 35.2 g were removed since these values are half and two times the average body mass of 17.6 g for adult *E. fuscus* (Kunz & Fenton 2003). In doing so, I was able to account for very small adults and large pregnant females. The resulting *E. fuscus* capture dataset represented 24,129 adults: females (n = 14,162) and males (n = 9,967; Fig. 2.1).

To evaluate *E. fuscus* across the landscape, I incorporated county of capture into the dataset. If county was provided by data contributors, I used the reported county of capture. If latitude and longitude of capture was provided, I linked this spatial point to the county of capture using the *housingData* package in the statistical environment R (Hafen 2016; R Core Team 2021). Once county was identified for each entry, I determined the county centroid point using the *housingData* package (Hafen 2016). Year of *Pd* introduction was determined as the earliest year of confirmed or suspected *Pd* occurrence using data provided by the US Geological Survey for *Pd* surveillance at whitenosesyndrome.org (White Nose Syndrome Response Team 2022). To standardize *Pd* introduction across capture datasets in different states, I set year of confirmed or suspected *Pd* occurrence in each state as the baseline (‘0’) so the number of *Pd* exposure years spanning from before introduction were negative integers and those after introduction were positive integers. From these data, time-steps were created to represent groupings for disease statuses at the time of capture (*sensu* Langwig *et al.*, 2015a): pre-*Pd* invasion (< 0 years), *Pd* invasion (0–1 years), *Pd* epidemic (2–4 years) and *Pd* established (5 + years). I used these time-steps to remain

consistent with pathogen invasion time groupings used within the North American bat / *Pd* disease system (Cheng *et al.* 2021).

Statistical Analyses

I completed statistical analyses in R version 4.0.5 and data visualizations using the package ggplot2 (Wickham 2009; R Core Team 2021). To quantify changes in body mass with increasing *Pd* exposure time, I used a two-step approach (Appendix A Fig. S2.1). First, I created linear mixed effects models using the function *lmer* from the package lme4 (Bates *et al.* 2015). Separate linear mixed effects models were created for male or female bats for mass as a function of an interaction between *Pd* exposure time-steps and county centroid latitude. For adult female models, I included reproductive status at time of capture into the interaction term. I used capture site as a random effect in all linear mixed effects models to account for differences in researcher site visits year-to-year, nightly capture effort and spatial autocorrelation. I also weighted each model by the number of samples in each *Pd* exposure time-step to account for increases and decreases in annual capture effort throughout different regions of the eastern US following *Pd* introduction (U.S. Fish and Wildlife Service 2020). I used a Type III ANOVA with Satterthwaite's method using the function *anova* in base R (R Core Team 2021) to determine a relationship between the interaction terms and mass. To determine how *Pd* exposure time-steps (and reproductive status for females) drove changes to mass across the landscape, I calculated the slopes for mass across latitude for each time-step and reproductive status (females only) using the *emtrends* function in the emmeans package (Lenth 2021).

Second, analyses for mass identified an average latitudinal point at 39.6 °N where changes occurred over time for males and females. This point where the interaction occurred ranged from 37.2 °N to 42.1 °N depending on reproductive status (females only) and *Pd* exposure time-step. To quantify differences across the identified spatial threshold, I created secondary linear mixed effects models similar to initial models, but replaced county centroid latitude with a newly created variable for categories north/south of the full model spatial threshold average at 39.6 °N (Appendix A Fig. S2.1A). These secondary models were weighted by the number of *E. fuscus* captures within each latitudinal category. I used a Type III ANOVA with Satterthwaite's method with the function *anova* in base R (R Core Team 2021) to determine differences in body mass as explained by an interaction between *Pd* exposure time-steps and latitudinal category (north/south) and including capture site as a random effect. I again included reproductive status in female models to better understand how chronic *Pd* exposure may affect mass throughout reproduction. When interactions between *Pd* exposure time-step, latitudinal category and reproductive status (females only) were significant, I restricted *post-hoc* analyses to biologically relevant pairwise contrasts using the *emmeans* and *pairs* functions with a Tukey's p-value adjustment method in the emmeans package (Lenth 2021). For example, I limited contrasts to determine significant differences between bat mass from northern and southern populations within a given reproductive status and/or *Pd* time-step (see Fig. 2.2, 2.4) or to determine significant differences within a given reproductive status across *Pd* time-steps and/or latitudinal category (see Appendix A Fig. S2.3,

S2.6). Finally, differences in northern to southern mass was determined by extracting mass differences and their standard errors from post-hoc analyses and performing two-tailed t-tests on normal distributions between individual *Pd* exposure time-steps.

To quantify changes to variation in *E. fuscus* body mass across space and *Pd* exposure time-steps, I used a hierarchical method (Appendix A Figure S2.1B). I first created male or female linear mixed effects models using the function *lmer* from the package lme4 (Bates *et al.* 2015). The models were created for mass and each sex (male/female) as functions of only random effects (no fixed effects) for capture year, month and site. Using only random effects allowed me to account for natural year to year variation, fluctuations in body mass caused by reproduction and natural history from March through October, and variation in survey effort at capture sites. I then extracted residuals from these models and used them as a proxy for mass variation as the response variable in secondary linear models to determine spatiotemporal changes from pathogen invasion. Using the function *lm* in base R (R Core Team 2021), I subjected mass variation (mass residuals from first model) to an interaction of *Pd* exposure time-steps and north/south of the spatial threshold (Appendix A Figure S2.1). In female models, I also incorporated reproductive status into the interaction term. For these secondary variation models, I used a Type I ANOVA to determine differences in mass variation north/south of the spatial threshold over time using the *anova* function in base R (R Core Team 2021). I calculated *post-hoc* pairwise contrasts with a Tukey's p-value adjustment method using the *emmeans* and *pairs* functions

in the emmeans package (Lenth 2021) in the same way as average body mass comparisons.

RESULTS

Changes in female mass over space and time

I identified a spatial threshold at 39.6 °N where an interaction of *Pd* exposure time-steps and reproductive status occurred ($F_{9, 2646} = 4.010$, $P = 0.0342$, $R^2 = 0.71$; Appendix A Fig. S2.2A). Non-reproductive female mass did not have a significant slope (stable) with latitude in pre-invasion (n = 364) and invasion (n = 346) years, but decreased with latitude in epidemic (n = 599) and establishment years (n = 619; Appendix A Fig. S2.2A). Pregnant bat mass was stable in pre-invasion (n = 298), invasion (n = 341) and epidemic years (n = 745), but decreased with latitude in establishment years (n = 701; Appendix A Fig. S2.2A). Lactating bat mass was stable with latitude in pre-invasion (n = 564) and invasion years (n = 983), but decreased with latitude in epidemic (n = 1677) and establishment years (n = 1,820; Appendix A Fig. S2.2A). Post-lactating bat mass was stable in pre-invasion (n = 614) and invasion years (n = 1,154), but decreased with latitude in epidemic (n = 1,864) and establishment years (n = 1,473; Appendix A Fig. S2.2A).

When splitting latitude into categories north/south of the spatial threshold, female mass was lower in northern latitudes compared to southern latitudes by *Pd* establishment for non-reproductive, pregnant, lactating, and post-lactating bats ($F_{9, 2646} = 2.185$, $P = 0.0201$, $R^2 = 0.53$; Fig. 2.2). Non-reproductive, lactating, and post-lactating bat mass was not different north to south in pre-invasion years but

was lower in the north compared to the south in invasion, epidemic, and establishment years (Fig. 2.2A, 2.2C, 2.2D). Pregnant bat mass was not different north to south in pre-invasion and invasion years but was lower in the north than the south in epidemic and established years (Fig. 2.2B). The mass of female bats significantly varied between northern and southern bats within each reproductive status and across *Pd* time-steps (Appendix A Fig. S2.3). Non-reproductive and post-lactating bat mass in the north decreased from pre-invasion to establishment years while their mass in the south did not change from pre-invasion to establishment years (Appendix A Fig. S2.3A, S2.3D). Pregnant bat mass in the north and the south did not change from pre-invasion to establishment years (Appendix A Fig. S2.3B). Finally, northern lactating bat mass did not change from pre-invasion to establishment years but southern lactating bat mass increased from pre-invasion to establishment years (Appendix A Fig. S2.3C).

Differences in north to south mass from pre-invasion to establishment years increased for all female demographics (Fig. 2.3). The greatest mass difference between northern and southern non-reproductive, pregnant, and lactating bats occurred in *Pd* establishment years, but post-lactating bats had the greatest mass difference during epidemic years (Fig. 2.3)

Changes in female mass variation over space and time

Year, month, and capture site accounted for 53% of variation in mass ($t = 29.22$, $P < 0.0001$, $R^2 = 0.53$; Appendix A Table S2.1). Mass variation also significantly differed between categories north/south of the spatial threshold with *Pd* exposure time-steps and reproductive status, and accounted for an additional

5% of variation ($F_9 = 1.986$, $P = 0.0367$, $R^2 = 0.05$; Appendix A Fig. S2.4). Mass variation for all female demographics was not different north to south in pre-invasion and invasion years (Appendix A Fig. S2.4). In epidemic years, post-lactating bat mass variation in the north was less than the south but non-reproductive, pregnant, and lactating bat mass variation was not different north to south (Appendix A Fig. S2.4). In *Pd* establishment years, non-reproductive and lactating female bats had more mass variation skewed toward values greater than the mean in the north compared to the south, pregnant bats had less mass variation in the north compared to the south, and post-lactating bat mass variation was not different north to south (Appendix A Fig. S2.4).

Mass variation significantly differed by reproductive status, latitudinal category, and *Pd* time-steps (Appendix A Fig. S2.5). Northern non-reproductive female mass variation increased toward values less than the mean from pre-invasion to establishment years while southern non-reproductive mass variation did not change from pre-invasion to establishment years (Appendix A Fig. S2.5). Northern and southern pregnant and lactating bat mass variation did not change over *Pd* time-steps (Appendix A Fig. S2.5). Finally, northern post-lactating bat mass variation decreased from pre-invasion to establishment years while southern post-lactating bat mass variation did not change from pre-invasion to establishment years (Appendix A Fig. S2.5).

Changes in male mass over space and time

Just as with female mass, I identified a spatial threshold at 39.6 °N where an interaction of *Pd* exposure time-steps occurred ($F_{3, 2729} = 5.474$, $P < 0.0001$, R^2

= 0.58; Appendix A Fig. S2.2B). Male mass did not have a significant slope with latitude in pre-invasion (n = 1,542) and invasion years (n = 1,813), but decreased with increasing latitude in epidemic (n = 3,237) and establishment years (n = 3, 375; Appendix A Fig. S2.2B). When using a latitudinal category for north/south of the spatial threshold, male mass significantly differed north to south depending on *Pd* exposure time-steps ($F_{3, 2729} = 6.790$, P = 0.0002, $R^2 = 0.41$; Fig. 2.5A). Male bats weighed less in the north than the south in pre-invasion years, lost that difference north to south during invasion years, but weighed less in the north compared to the south in epidemic and establishment years (Fig. 2.5A). Although northern male mass was less than southern male mass in pre-invasion years, the difference between northern and southern mass more than doubled by *Pd* establishment (Fig. 2.5A). When grouped by latitudinal category, northern male bat mass decreased from pre-invasion to establishment years while southern male bat mass did not change from pre-invasion to establishment (Appendix A Fig. S2.6).

Differences between northern and southern male bat mass increased from pre-invasion to epidemic and *Pd* establishment years (Fig. 2.5B). In epidemic and established years, male bats had the greatest mass differences between latitudinal categories (Fig. 2.5B).

Changes in male mass variation over space and time

Month, year, and site described 61% of male mass variation (t = 23.75, P < 0.0001, $R^2 = 0.61$; Appendix A Table S2.1). Male mass variation significantly differed north to south depending on *Pd* exposure time-steps, and accounted for

less than 1% of additional variation ($F_3 = 3.006$, $P = 0.0291$, $R^2 = 0.003$). However, this secondary male mass variation model failed to converge with a y-intercept that was not statistically different from zero.

DISCUSSION

Emerging infectious disease epidemics threaten biodiversity globally (Daszak *et al.* 2000), and are difficult to assess, many times due to lack of data prior to pathogen emergence. Furthermore, research on species less susceptible to pathogen infections (*e.g. E. fuscus*) is limited and/or typically put in the context of comparisons to highly susceptible species. I focus on understanding how pathogen exposure uniquely changes less susceptible species as they become greater contributors to what remains of diversity as highly susceptible species become rarer (Cortez *et al.* 2017). Using a robust 30-year dataset consisting of 24,129 individual *E. fuscus*, I demonstrate that progressive *Pd* exposure caused *E. fuscus* body mass to decrease with increasing latitude, the effects of which were greater with increasing pathogen exposure time, and were most pronounced at higher latitudes. Additionally, variation in body mass decreased or skewed toward values below average mass with increasing latitude and pathogen exposure time-steps. These results highlight the importance of how introduced pathogens can cause spatially-driven reductions in trait diversity over time.

Anthropogenic changes in the environment which alter insect prey populations, such as climate change and insecticide use, could play a role in altering *E. fuscus* body mass with *Pd* exposure time-steps (Wagner 2020). All female demographics and male bat body mass decreased with latitude by *Pd* establishment, and differences between northern and southern bat mass

progressively increased. This may reflect differences in insect availability. *Eptesicus fuscus* are insectivores and typically prefer to eat beetles even when the relative abundance of beetle prey is low compared to other insect prey species (Whitaker 1995; Wray *et al.* 2021). This is particularly problematic since beetle abundance has decreased globally. In the US, warming winter conditions in the northeastern US have decreased beetle abundance by 39% since the 1970s (Harris *et al.* 2019). These declines in available beetle prey in northern latitudes are also likely due to heavy insecticide use which contributes to global insect declines (Sánchez-Bayo & Wyckhuys 2019). In this dataset, the threshold that delineated changes in body mass (39.6 °N) runs directly through the lower extent of the Corn Belt region in the midwestern US. The Corn Belt region has the largest quantities of insecticide use in the US (Pimentel & Burgess 2014), suggesting beetle availability may be lower in this region compared to other regions. In addition to decreasing beetle availability, ingestion of insecticides can impact *E. fuscus*' physiology. When *E. fuscus* ingests insecticides, insecticide toxicity can cause thermoregulatory irregularities and weight loss (Eidels *et al.* 2016), which could contribute to bat body mass being lower in northern latitudes where the Corn Belt region is, compared to southern latitudes by pathogen establishment. Therefore, the impacts of climate change and insecticide use could have additive effects on *E. fuscus* body mass with increasing latitude and long-term *Pd* exposure.

I would expect broad latitudinal patterns for body mass, like Bergmann's Rule, to be altered by a pathogen because of increased energy expenditures associated with active and healing infections (McGuire *et al.* 2017; Meierhofer *et*

al. 2018). Bergmann's Rule suggests that species have greater mass in higher latitudes compared to lower latitudes to reduce surface area to volume ratios, thereby decreasing heat loss in those colder climates (Bergmann 1847). Latitudinal patterns for *E. fuscus* body mass did change across *Pd* exposure time-steps, but *E. fuscus* did not follow Bergmann's Rule at any *Pd* time-step. There was no difference in body mass north to south in pre-invasion years across *E. fuscus* reproductive statuses, however, lower body masses were found in northern latitudes compared to southern latitudes by *Pd* establishment years. Further, male *E. fuscus* weighed less in northern latitudes compared to southern latitudes in pre-invasion and establishment years. *Eptesicus fuscus* body mass opposed Bergmann's Rule by *Pd* establishment (body mass decreasing with latitude). I also expected patterns for Bergmann's Rule to be present in pre-invasion years (which was not supported) because it would maximize *E. fuscus*' ability to conserve body heat in cooler, northern climates in combination with Allen's Rule (Burnett 1983). *Eptesicus fuscus* are known to follow Allen's Rule prior to *Pd* introduction which states that the length of mammalian extremities should decrease with increasing latitude to reduce surface area to volume ratios (Allen 1877). To provide insight into how latitudinal thermoregulatory patterns are altered with pathogen exposure, research investigating changes in extremities, such as forearm length, for *E. fuscus* is needed.

Latitudinal patterns for *E. fuscus* body mass following *Pd* introduction could be explained by changes in competition. *Eptesicus fuscus* body mass for males and females decreased with increasing latitude by *Pd* establishment years

with differences between northern and southern bat mass increasing with *Pd* exposure time-steps. These effects could support a spatially-driven, unstable coexistence between less susceptible and highly susceptible species. Highly susceptible hosts mortalities from *Pd* infections are greater in northern latitudes compared to southern latitudes in the eastern US, likely due to how individual hosts and *Pd* interact with their environment, and because *Pd* has been in the northeastern US longer (Hayman *et al.* 2016; Frick *et al.* 2017). Interspecific competition with *E. fuscus* should decrease with increasing latitude since there are fewer highly susceptible hosts. This suggests intraspecific competition between *E. fuscus* individuals may increase with latitude throughout spring through summer months because 1) there are proportionally more *E. fuscus* individuals present in northeastern and midwestern states following *Pd* introduction (Francl *et al.* 2012; Pettit & O'Keefe 2017), and 2) *E. fuscus* have strong site fidelity, especially for females during reproduction, suggesting they would still use the same foraging and roosting areas post-*Pd* (Brigham, 1991; Wilkinson & Barclay, 1997). Taken together, progressive effects of *Pd* exposure time on *E. fuscus* body mass mirrors spatial gradients of highly susceptible species mortalities. Increases to intraspecific competition may not benefit populations long-term because theoretically intraspecific competition is stronger than interspecific competition according to the Lotka-Volterra competition model (Gotelli 2008). While *E. fuscus* does attempt to mitigate the cost of intraspecific competition following *Pd* invasion by preferentially foraging at sites where highly susceptible *Myotis lucifugus* are still present in small numbers (Jachowski *et al.* 2014), pressures for

intraspecific competition under *Pd* establishment may be an indirect effect of pathogen invasion, as reflected by decreases to body mass with latitude and *Pd* exposure time-steps.

Eptesicus fuscus have some degree of resistance to *Pd* infection (Frank *et al.* 2014) and are less susceptible to infection compared to the highly susceptible *M. lucifugus* (Moore *et al.* 2018). However, resistance to pathogens comes at an energetic cost. For example, it costs energy to mount immune responses (Hegemann *et al.* 2012), avoid pathogens or parasites (Luong *et al.* 2017), or even just meet increased energy demands (Voigt *et al.* 2010). I found males and non-reproductive and post-lactating females lost mass from pre-invasion to *Pd* establishment in northern latitudes. From pre-invasion to establishment, northern males lost 3 % (0.6 g) mass. Although northern males weighed 2 % (0.4 g) less than southern males in pre-invasion years, that difference was doubled to 5 % (0.8 g) by establishment years. Northern non-reproductive females lost on average 5 % (0.9 g) of their body weight pre-invasion when compared to establishment years. Northern post-lactating bats lost 5 % (1 g) mass in the same time period. Declines to body mass in northern latitudes could be detrimental to *E. fuscus* entering hibernation as surviving hibernation is positively correlated with body mass (Brigham, 1987). In contrast, highly susceptible, non-resistant *M. lucifugus* surviving *Pd* invasion have opposite changes to body mass, with 1.1 g increases in mass on average (Cheng *et al.* 2019). Body mass and fat increases in surviving *M. lucifugu*s could potentially provide enough energy for them to make it through hibernation with *Pd* infections (Cheng *et al.* 2019). Therefore, although highly

susceptible, non-resistant species have widespread mortalities from initial pathogen invasion (Cheng *et al.* 2021), resistant *E. fuscus* may also incur detrimental consequences to dealing with energy demands of chronic pathogen exposure as time goes on.

I expected reproductive female body mass to decrease following *Pd* introduction because winter *Pd* infections increase bat energy expenditures in spring (Meierhofer *et al.* 2018). Prior to *Pd* invasion, female *E. fuscus* needed to consume 99% of their body weight during peak lactation in order to maintain body mass while caring for pups (Kurta *et al.* 1990). Therefore, in order for pregnant and lactating *E. fuscus* to maintain body mass in northern latitudes, or increase body mass in southern latitudes, in the face of additional energy losses from winter *Pd* exposure, bats would either need to eat more or increase torpor to conserve energy. Since *E. fuscus*' preferred food choice of beetles are limited throughout spring and summer months (Menzel *et al.* 2020), I predict that reproductive *E. fuscus* use torpor to reduce caloric use more frequently following *Pd* invasion. Many heterothermic small mammals and birds use torpor during reproduction as a fitness trade-off (McAllan & Geiser 2014; Calder & Booser 2016; Geiser *et al*. 2005). *Eptesicus fuscus* specifically use torpor during pregnancy and lactation (Audet & Fenton 1988). Additionally, *E. fuscus* have lower torpid metabolic rates at warm temperatures in the south than in the north (Dunbar & Brigham 2010). Therefore, it is possible pregnant and lactating *E. fuscus* north/south of the spatial threshold I identified here are maximizing their use of torpor during reproduction to maintain body mass in the north or increase

body mass in the south over *Pd* exposure time-steps. Further research into reproductive energy expenditures is needed to determine how torpor patterns in pregnant and lactating *E. fuscus* change following *Pd* invasion and if changes could affect future populations by limiting reproductive success.

I could not directly measure pathogen pressures on bats (*i.e.*, fungal loads on individual bats); therefore, I used *Pd* exposure time-steps as an index of chronic pathogen exposure. Methods for accounting for *Pd* exposure are adequate for the following two reasons. First, North American bats heal from winter *Pd* infections and *Pd* becomes undetectable in spring months (Langwig *et al.*, 2015b; Fuller *et al.*, 2020). Since pathogen intensity decreases in spring months and becomes largely non-existent, I would likely not see *Pd* on individual bats even if they were swabbed for *Pd* during April through October. Second, body condition for North American bats is less likely to be related to *Pd* infection intensity, but more likely the duration of infection and/or exposure time (Moore *et al.* 2018; Cheng *et al.* 2019). Therefore, while the failure to directly measure pathogen pressure is a limitation in this dataset, *Pd* exposure time-steps are a suitable indirect metric for pathogen pressures within the *Pd* system.

This work represents a crucial first step in quantifying how less susceptible species respond to an introduced pathogen, and how their body mass responds to long-term exposure to that pathogen. I also highlight how the long-term effects of pathogen exposure for less susceptible species are spatially manifested, and suggest these gradient effects reflect losses of highly susceptible competitor hosts. As emerging pathogens become more prominent, it is likely that

less susceptible species will become greater contributors to population dynamics as species richness decreases following pathogen invasion. Thus, making efforts to understand less susceptible species responses to pathogens over time will support wildlife diversity in the future.

ACKNOWLEDGEMENTS

I thank all the researchers, field biologists and technicians who collected *E. fuscus* data over the 30 years of the capture dataset. I gratefully acknowledge data contributors from Georgia (Georgia Department of Natural Resources), Illinois (Tim Carter, Ball State University), Indiana (Indiana US Fish and Wildlife Service), Kentucky (Kentucky Department of Fish and Wildlife Resources), Mississippi (Katelin Cross, Mississippi Museum of Natural Science), New York (New York State Department of Environmental Conservation), North Carolina (North Carolina US Fish and Wildlife Service; North Carolina Wildlife Resources Commission), Ohio (Sarah Stankavich, Ohio Department of Natural Resources' Division of Wildlife; Lisa Cooper, Northeastern Ohio Medical University), Pennsylvania (Pennsylvania Game Commission), Tennessee (Tennessee Wildlife Resource Agency), and Virginia (Virginia Department of Wildlife Resources). Data collection from Virginia for this publication was completed with funds provided by the Virginia Department of Wildlife Resources using resources from the national Wildlife Restoration program provided by the U.S. Fish and Wildlife Service. I thank Yasmeen Samar for her help with early data cleaning and Wright State University Biological Sciences Department's Biology Award for Research Excellence.

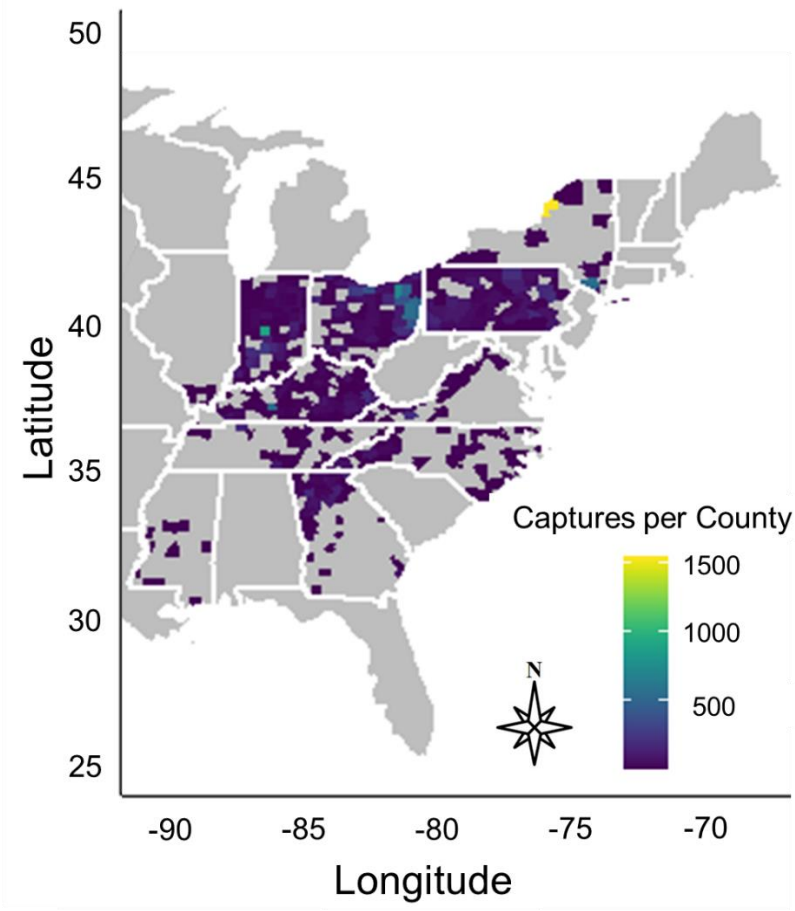

Figure 2.1. Adult (female and male) *E. fuscus* capture counts per county March through October from 1990 to 2020 in this eastern US dataset. Gray shading represents areas where data were either not collected or not contributed.

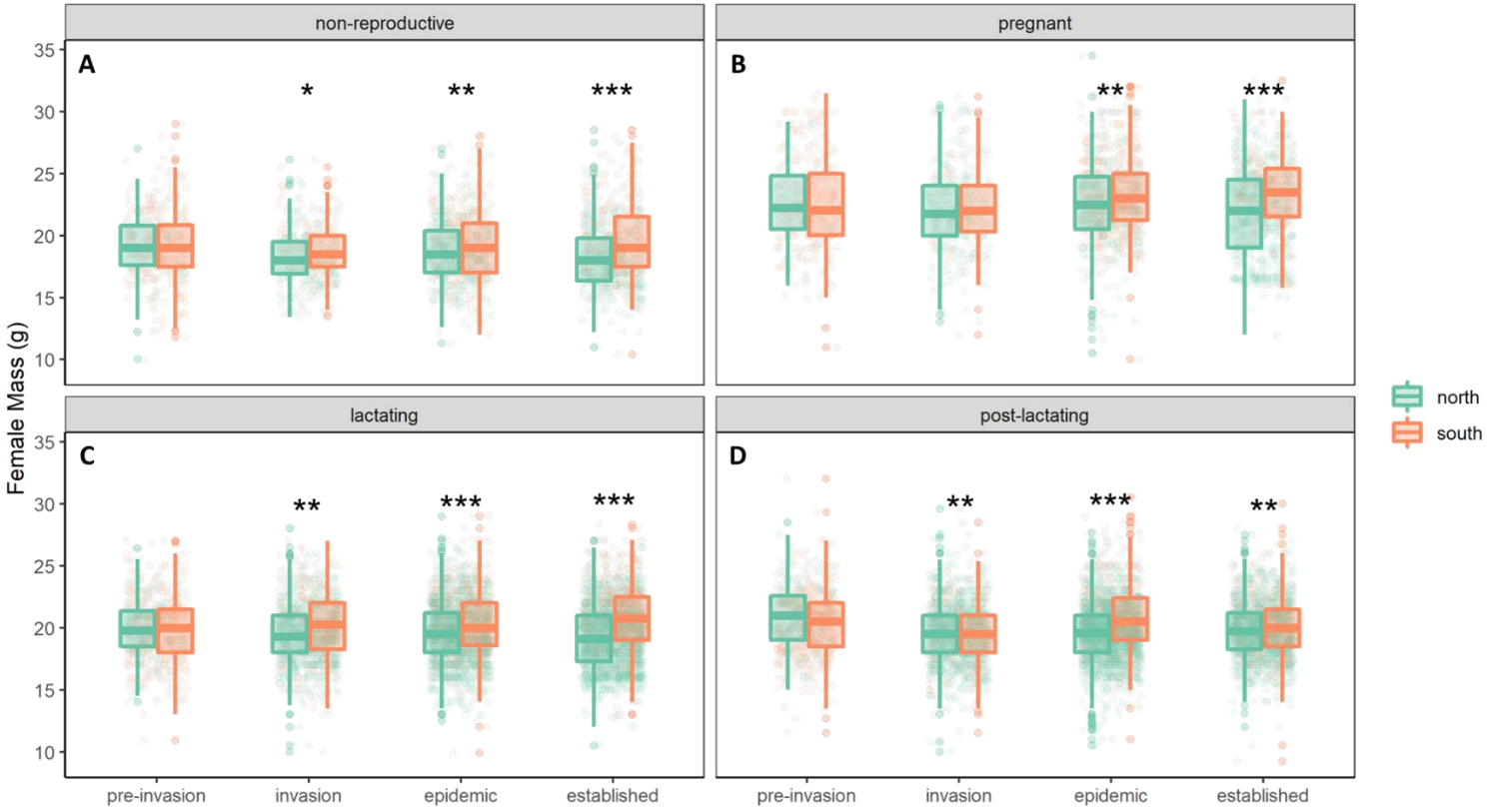

Figure 2.2. Female mass is less in northern latitudes compared to southern latitudes by *Pd* establishment for non-reproductive (A), pregnant (B), lactating (C) and post-lactating (D) *E. fuscus* ($F_{9, 2646} = 2.185$, $P = 0.0201$, $R^2 = 0.53$). Circles represent raw

data. Boxes represent 50% of raw data and thick lines within each box is median mass. Upper and lower whiskers are an additional 25% of data each. *P < 0.05; **P < 0.01; ***P < 0.001.

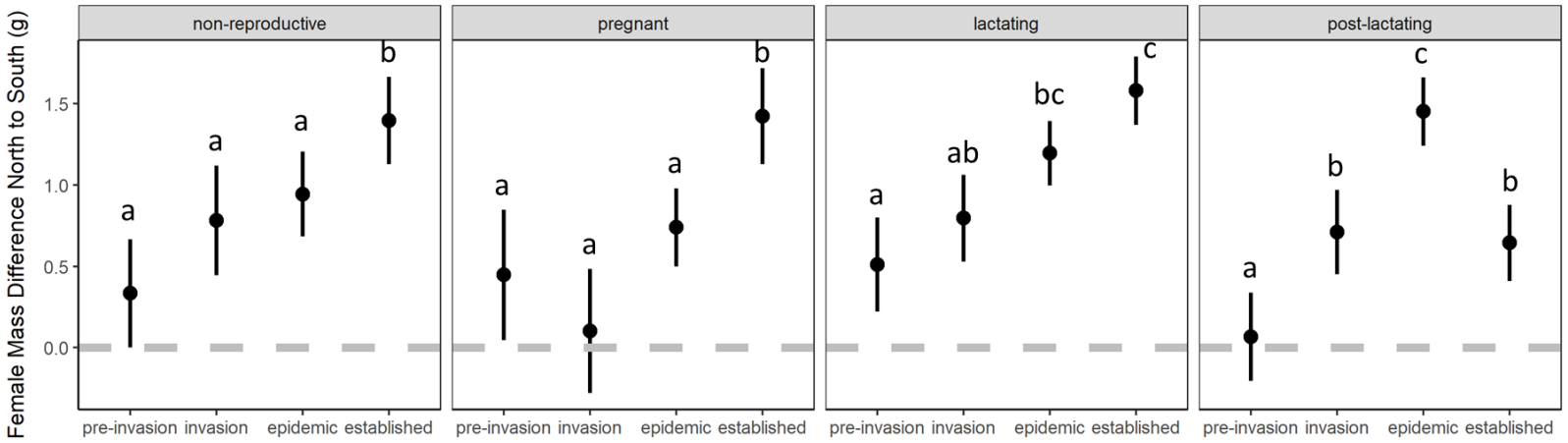

Figure 2.3. The difference in female mass north to south increases from pre-invasion to *Pd* established years. Points are mean differences in mass and error bars are standard errors extracted from *post hoc* results for north/south comparisons across *Pd* time-steps and grouped by reproductive status. Dotted lines at '0' represent the neutral point where there is no difference in body condition north to south. Lowercase letters indicate significant differences based on t-tests between individual comparisons for *Pd* exposure time-steps within groupings for reproductive status.

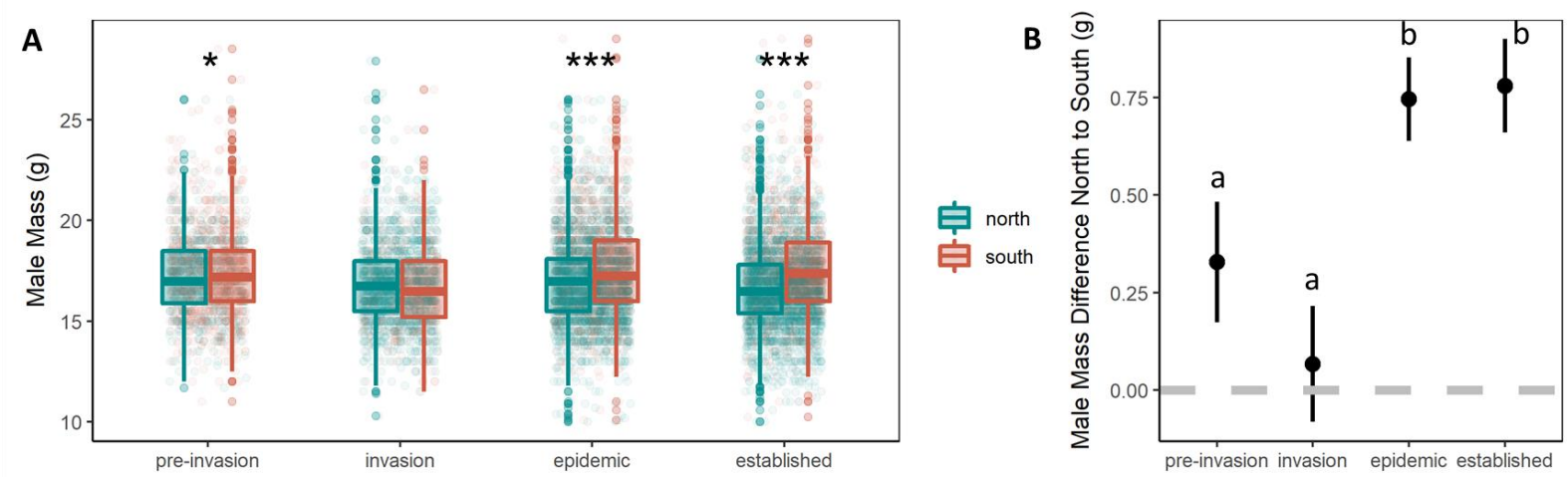

Figure 2.4. Male mass is less in northern latitudes compared to southern latitudes during *Pd* establishment ($F_{3, 2729} = 6.790$, P = 0.0002, $R^2 = 0.41$; **A**), and the north/south difference in mass increases across *Pd* exposure time-steps (**B**). **A**) Circles represent raw data. Boxes represent 50% of raw data and thick lines within each box represents median values. Upper and lower whiskers represent an additional 25% of values. *P < 0.05; **P < 0.01; ***P < 0.001. **B**) Points are mean differences in mass and error bars are standard errors extracted from *post hoc* results for north/south comparisons across *Pd* time-steps. Dotted

lines at ‘0’ represent the neutral point where there is no difference in body condition north to south. Lowercase letters indicate significant differences based on t-tests between individual comparisons for *Pd* exposure time-steps.

REFERENCES

Allen, J.A. (1877). The influence of physical conditions on the genesis of species. Radic. Rev., 1, 108–140.

Altizer, S., Davis, A.K., Cook, K.C. & Cherry, J.J. (2004). Age, sex, and season affect the risk of mycoplasmal conjunctivitis in a southeastern house finch population. Can. J. Zool., 82, 755–763.

Audet, D. & Fenton, M.B. (1988). Heterothermy and the use of torpor by the bat *Eptesicus fuscus* (Chiroptera: Vespertilionidae): A field study. Physiol. Zool., 61, 19.

Bartel, R.A., Oberhauser, K.S., De Roode, J.C. & Altizer, S.M. (2011). Monarch butterfly migration and parasite transmission in eastern North America. Ecology, 92, 342–351.

Bates, D., Maechler, M., Bolker, B. & Walker, S. (2015). Fitting Linear Mixed-Effects Models Using lme4. J. Stat. Softw., 67, 1–48.

Bergmann, C. (1847). Ueber die verhältnisse der wärmeökonomie der thiere zu ihrer grösse. Göttinger Stud., 3, 595–708.

Blehert, D.S., Hicks, A.C., Behr, M., Meteyer, C.U., Berlowski-Zier, B.M., Buckles, E.L., et al. (2009). Bat white-nose syndrome: an emerging fungal pathogen? Science, 323, 227.

Brigham, R.M. (1987). The significance of winter activity by the big brown bat (*Eptesicus fuscus*): the influence of energy reserves. Can. J. Zool., 65, 1240–1242.

Brigham, R.M. (1991). Flexibility in foraging and roosting behaviour by the big brown bat (*Eptesicus fuscus*). Can. J. Zool., 69, 117–121.

Burnett, C.D. (1983). Geographic and Climatic Correlates of Morphological Variation in *Eptesicus fuscus*. J. Mammal., 64, 437–444.

Calder, W.A. & Booser, J. (2016). Hypothermia of Broad-Tailed Hummingbirds during Incubation in Nature with Ecological Correlations. Science, 180, 751–753.

Cheng, T.L., Gerson, A., Moore, M.S., Reichard, J.D., DeSimone, J., Willis, C.K.R., et al. (2019). Higher fat stores contribute to persistence of little brown bat populations with white-nose syndrome. J. Anim. Ecol., 88, 591–600.

Cheng, T.L., Reichard, J.D., Coleman, J.T.H., Weller, T.J., Thogmartin, W.E., Reichert, B., et al. (2021). The scope and severity of White-nose Syndrome on hibernating bats in North America. Conserv. Biol., 35, 1586–1597.

Cortez, M.J. V., Rabajante, J.F., Tubay, J.M. & Babierra, A.L. (2017). From epigenetic landscape to phenotypic fitness landscape: Evolutionary effect of pathogens on host traits. Infect. Genet. Evol., 51, 245–254.

Daszak, P., Cunningham, A. & Hyatt, A. (2000). Emerging Infectious Diseases of Wildlife - Threats to Biodiversity and Human Health. Science, 287, 443–449.

Descloux, E., Mangeas, M., Menkes, C.E., Lengaigne, M., Leroy, A., Tehei, T., et al. (2012). Climate-based models for understanding and forecasting dengue epidemics. PLoS Negl. Trop. Dis., 6, e1470.

Downs, C.J., Schoenle, L.A., Han, B.A., Harrison, J.F. & Martin, L.B. (2019). Scaling of Host Competence. Trends Parasitol., 35, 182–192.

Drees, K., Puechmaille, S., Parise, K.L. & Wibbelt, G. (2017). Phylogenetics of a Fungal Invasion: Origins and Widespread Dispersal of White-Nose Syndrome. MBio, 8, e01941-17.

Dunbar, M.B. & Brigham, R.M. (2010). Thermoregulatory variation among populations of bats along a latitudinal gradient. J. Comp. Physiol. B Biochem. Syst. Environ. Physiol., 180, 885–893.

Eidels, R.R., Sparks, D.W., Whitaker, J.O. & Sprague, C.A. (2016). Sub-lethal Effects of Chlorpyrifos on Big Brown Bats (*Eptesicus fuscus*). Arch. Environ. Contam. Toxicol., 71, 322–335.

Ferguson, N.M., Donnelly, C.A. & Anderson, R.M. (2001). The foot-and-mouth epidemic in Great Britain: Pattern of spread and impact of interventions. Science, 292, 1155–1160.

Field, K.A., Johnson, J.S., Lilley, T.M., Reeder, S.M., Rogers, E.J., Behr, M.J., et al. (2015). The White-Nose Syndrome Transcriptome: Activation of Anti-fungal Host Responses in Wing Tissue of Hibernating Little Brown Myotis. PLoS Pathog., 11, 1–30.

Francl, K.E., Ford, W.M., Sparks, D.W. & Brack, V. (2012). Capture and reproductive trends in summer bat communities in West Virginia: Assessing the impact of white-nose syndrome. J. Fish Wildl. Manag., 3, 33–42.

Frank, C.L., Michalski, A., McDonough, A.A., Rahimian, M., Rudd, R.J. & Herzog, C. (2014). The resistance of a North American bat species (*Eptesicus fuscus*) to White-Nose Syndrome (WNS). PLoS One, 9, 1–14.

Frick, W.F., Cheng, T.L., Langwig, K.E., Hoyt, J.R., Janicki, A.F., Parise, K.L., et al. (2017). Pathogen dynamics during invasion and establishment of white-nose syndrome explain mechanisms of host persistence. Ecology, 98, 624–631.

Frick, W.F., Puechmaille, S.J., Hoyt, J.R., Nickel, B.A., Langwig, K.E., Foster, J.T., et al. (2015). Disease alters macroecological patterns of North American bats. Glob. Ecol. Biogeogr., 24, 741–749.

Fuller, N.W., Mcguire, L.P., Pannkuk, E.L., Blute, T., Haase, C.G., Mayberry, H.W., et al. (2020). Disease recovery in bats affected by white-nose syndrome. J. Exp. Biol., 223, jeb211912.

Geiser, F., Mcallan, B.M. & Brigham, R.M. (2005). Daily torpor in a pregnant dunnart (*Sminthopsis macroura* Dasyuridae: Marsupialia). Mamm. Biol., 70, 117–121.

Gotelli, N.J. (2008). A Primer of Ecology. Fourth Edition. Sinauer Associates Inc., Sunderland, MA.

Haase, C.G., Fuller, N.W., Dzal, Y.A., Hranac, C.R., Hayman, D.T.S., Lausen, C.L., et al. (2021). Body mass and hibernation microclimate may predict bat susceptibility to white-nose syndrome. Ecol. Evol., 11, 506–515.

Hafen, R. (2016). housingData: U.S. Housing Data from 2008 to 2016. R Package. version 0.3.0.

Hall, R.J. (2019). Modeling the effects of resource-driven immune defense on parasite transmission in heterogeneous host populations. Integr. Comp. Biol., 59, 1253–1263.

Harris, J.E., Rodenhouse, N.L. & Holmes, R.T. (2019). Decline in beetle abundance and diversity in an intact temperate forest linked to climate warming. Biol. Conserv., 240, 108219.

Hayman, D.T.S., Pulliam, J.R.C., Marshall, J.C., Cryan, P.M. & Webb, C.T. (2016). Environment, host, and fungal traits predict continental-scale white-nose syndrome in bats. Sci. Adv., 2, 1–13.

Hegemann, A., Matson, K.D., Versteegh, M.A. & Tieleman, B.I. (2012). Wild skylarks seasonally modulate energy budgets but maintain energetically costly inflammatory immune responses throughout the annual cycle. PLoS One, 7, e36358.

Jachowski, D.S., Dobony, C.A., Coleman, L.S., Ford, W.M., Britzke, E.R. & Rodrigue, J.L. (2014). Disease and community structure: White-nose syndrome alters spatial and temporal niche partitioning in sympatric bat species. Divers. Distrib., 20, 1002–1015.

Kunz, T.H. & Fenton, M.B. (2003). Bat Ecology. The University of Chicago Press, Chicago and London, pp. 107–112.

Kurta, A., Kunz, T.H. & Nagy, K.A. (1990). Energetics and Water Flux of Free-Ranging Big Brown Bats (*Eptesicus fuscus*) during Pregnancy and Lactation. J. Mammal., 71, 59–65.

Langwig, K.E., Voyles, J., Wilber, M.Q., Frick, W.F., Murray, K.A., Bolker, B.M., et al. (2015a). Context-dependent conservation responses to emerging wildlife diseases. Front. Ecol. Environ., 13, 195–202.

Langwig, K.E., Frick, W.F., Reynolds, R., Parise, K.L., Drees, K.P., Hoyt, J.R., et al. (2015b). Host and pathogen ecology drive the seasonal dynamics of a fungal disease, white-nose syndrome. Proc. R. Soc. B Biol. Sci., 282, 10–12.

Lello, J., Boag, B. & Hudson, P.J. (2005). The effect of single and concomitant pathogen infections on condition and fecundity of the wild rabbit (Oryctolagus cuniculus). Int. J. Parasitol., 35, 1509–1515.

Lenth, R. (2021). emmeans: Estimated Marginal Means, aka Least-Squares Means.

Leopardi, S., Blake, D. & Puechmaille, S.J. (2015). White-nose syndrome fungus introduced from Europe to North America. Curr. Biol., 25, R217–R219.

Loehle, C. (1995). Social Barriers to Pathogen Transmission in Wild Animal Populations. Ecology, 76, 326–335.

Lorch, J.M., Meteyer, C.U., Behr, M.J., Boyles, J.G., Cryan, P.M., Hicks, A.C., et al. (2011). Experimental infection of bats with *Geomyces destructans* causes white-nose syndrome. Nature, 480, 376–378.

Luong, L.T., Horn, C.J. & Brophy, T. (2017). Mitey costly: Energetic costs of parasite avoidance and infection. Physiol. Biochem. Zool., 90, 471–477.

Mack, R.N., Simberloff, D., Lonsdale, W.M., Evans, H., Clout, M. & Bazzaz, F.A. (2000). Biotic invasions: Causes, epidemiology, global consequences and control. Ecol. Appl., 10, 689–710.

McAllan, B.M. & Geiser, F. (2014). Torpor during reproduction in mammals and birds: Dealing with an energetic conundrum. Integr. Comp. Biol., 54, 516–532.

McGuire, L.P., Mayberry, H.W. & Willis, C.K.R. (2017). White-nose syndrome increases torpid metabolic rate and evaporative water loss in hibernating bats. Am. J. Physiol. - Regul. Integr. Comp. Physiol., 313, R680–R686.

Meierhofer, M.B., Johnson, J.S., Field, K.A., Lumadue, S.S., Kurta, A., Kath, J.A., et al. (2018). Bats recovering from white-nose syndrome elevate metabolic rate during wing healing in Spring. J. Wildl. Dis., 54, 480–490.

Menzel, M.A., Carter, T.C., Mitchell, B.L., Jablonowski, L.R., Chapman, B.R. & Laerm, J. (2020). Prey selection by a maternity colony of big brown bats (*Eptesicus fuscus*) in the southeastern United States. Florida Sci., 63, 232–241.

Meteyer, C.U., Buckles, E.L., Blehert, D.S., Hicks, A.C., Green, D.E., Shearn-bochsler, V., et al. (2009). Histopathologic criteria to confirm white-nose syndrome in bats. J. Vet. Diagnostic Investig., 21, 411–414.

Moore, M.S., Field, K.A., Behr, M.J., Turner, G.G., Furze, M.E., Stern, D.W.F., et al. (2018). Energy conserving thermoregulatory patterns and lower disease severity in a bat resistant to the impacts of white-nose syndrome. J. Comp. Physiol. B Biochem. Syst. Environ. Physiol., 188, 163–176.

Pettit, J.L. & O'Keefe, J.M. (2017). Impacts of White-Nose Syndrome Observed During Long-Term Monitoring of a Midwestern Bat Community. J. Fish Wildl. Manag., 8, 69–78.

Pimentel, D. & Burgess, M. (2014). Environmental and Economic Costs of the Application of Pesticides Primarily in the United States. In: Integrated Pest Management: Pesticides Problems Vol. 3 (eds. Pimentel, D. & Peshin, R.). Springer Science + Business Media, New York, pp. 47–71.

Plowright, R.K., Eby, P., Hudson, P.J., Smith, I.L., Westcott, D., Bryden, W.L., et al. (2014). Ecological dynamics of emerging bat virus spillover. Proc. R. Soc. B Biol. Sci., 282.

Poorten, T.J. & Rosenblum, E.B. (2016). Comparative study of host response to chytridiomycosis in a susceptible and a resistant toad species. Mol. Ecol., 25, 5663–5679.

Prendergast, B.J., Freeman, D.A., Zucker, I. & Nelson, R.J. (2002). Periodic arousal from hibernation is necessary for initiation of immune responses in ground squirrels. Am. J. Physiol. - Regul. Integr. Comp. Physiol., 282, R1054–R1062.

R Core Team. (2021). R: A language and environment for statistical computing.

Sánchez-Bayo, F. & Wyckhuys, K.A.G. (2019). Worldwide decline of the entomofauna: A review of its drivers. Biol. Conserv., 232, 8–27.

Sánchez, C.A., Becker, D.J., Teitelbaum, C.S., Barriga, P., Brown, L.M., Majewska, A.A., et al. (2018). On the relationship between body condition and parasite infection in wildlife: a review and meta-analysis. Ecol. Lett., 21, 1869–1884.

Schoenle, L.A., Downs, C.J. & Martin, L.B. (2018). An Introduction to Ecoimmunology. In: Advances in Comparative Immunology (ed. Cooper, E.L.). Springer International Publishing AG, Cham, Switzerland, pp. 901–932.

Simonis, M.C., Brown, B.B. & Bahn, V. (2020). Mobile bat acoustic routes indicate cavity-roosting species undergo compensatory changes in community composition following white-nose syndrome. Acta Chiropterologica, 22, 315–326.

Turner, G.G., Reeder, D. & Coleman, J.T.H. (2011). A Five-year Assessment of Mortality and Geographic Spread of White-Nose Syndrome in North American Bats, with a look to the future. Bat Res. News, 52, 13–27.

U.S. Fish and Wildlife Service. (2020). 2020 Range-wide Indiana Bat Survey Guidelines. Available at https://www.fws.gov/library/collections/range-wide-indiana-bat-and-northern-long-eared-bat-survey-guidelines.

Verant, M.L., Boyles, J.G., Waldrep, W., Wibbelt, G. & Blehert, D.S. (2012). Temperature-Dependent Growth of *Geomyces destructans*, the Fungus That Causes Bat White-Nose Syndrome. PLoS One, 7, e46280.

Voigt, C.C., Sörgel, K. & Dechmann, D.K.N. (2010). Refueling while flying: Foraging bats combust food rapidly and directly to power flight. Ecology, 91, 2908–2917.

Voyles, J., Berger, L., Young, S., Speare, R., Webb, R., Warner, J., et al. (2007). Electrolyte depletion and osmotic imbalance in amphibians with chytridiomycosis. Dis. Aquat. Organ., 77, 113–118.

Wagner, D.L. (2020). Insect declines in the Anthropocene. Annu. Rev. Entomol., 65, 457–480.

Whitaker, J.O. (1995). Food of the Big Brown Bat *Eptesicus fuscus* from Maternity Colonies in Indiana and Illinois. Am. Midl. Nat., 134, 346–360.

White Nose Syndrome Response Team. (2022). White-nose syndrome occurrence map by year. Hadley, Massachusetts. https://www.whitenosesyndrome.org/.

Wickham, H. (2009). ggplot2: Elegant Graphics for Data Analysis. Springer-Verlag New York.

Wilkinson, L.C. & Barclay, R.M.R. (1997). Differences in the foraging behaviour of male and female big brown bats (*Eptesicus fuscus*) during the reproductive period. Ecoscience, 4, 279–285.

Wray, A.K., Peery, M.Z., Jusino, M.A., Kochanski, J.M., Banik, M.T., Palmer, J.M., et al. (2021). Predator preferences shape the diets of arthropodivorous bats more than quantitative local prey abundance. Mol. Ecol., 30, 855–873.

CHAPTER 3

TORPID METABOLIC RATES OF RESISTANT *EPTESICUS FUSCUS* MAY INCREASE OR NOT CHANGE WITH LONG-TERM *PSEUDOGYMNOASCUS DESTRUCTANS* EXPOSURE

ABSTRACT

Resistance to pathogens can cost energy. For small mammals that hibernate, offsetting additional energy expenditures can be challenging when food is scarce in winter months. To determine if pathogen resistance increases torpid metabolic rates, I measured torpid metabolic rates across a wide range of ambient temperatures from *Eptesicus fuscus*, a North American temperate bat species that has less susceptibility and some degree of resistance to the invasive fungal pathogen, *Pseudogymnoascus destructans* (*Pd*). I collected *E. fuscus* nine and ten years following the introduction of *Pd*, suggesting long-term exposure to the pathogen. I compared data I collected (post-*Pd*) to data in the literature collected prior to *Pd* introduction (pre-*Pd*) and found conflicting results. When comparing torpid metabolic rates post-*Pd* to pre-*Pd* using data from Herreid and Schmidt-Nielsen (1966) and Willis et al. (2005), I found there was no difference in torpid metabolic rates across ambient temperatures. When using pre-*Pd* data from Szewczak and Jackson (1992), I found *E. fuscus* had greater torpid metabolic rates post-*Pd* compared to pre-*Pd*. I strongly encourage additional research for *E. fuscus* measuring field and lab torpor patterns to determine to what degree *E. fuscus* energy expenditures change or do not change with long-term *Pd* exposure.

INTRODUCTION

Like other small mammals, *Eptesicus fuscus* (big brown bats; Kurta & Baker 1990) use torpor to save energy during periods of high energy demand or low energy availability. Small endotherms require high metabolic rates relative to their body size to be euthermic (Hill *et al.* 2016). These energy costs are met by consuming large amounts of food relative to their body size. When food availability is scarce (*e.g.*, during winter months), many endotherms, including *E. fuscus*, reduce their energy expenditures by dropping body temperature (T_b) as they enter torpor.

During hibernation (seasonal bouts of extended torpor) there is a general risk for starvation since survival is dependent on balancing energy expenditures with available fat stores (Brigham 1987; Speakman & Thomas 2003; Willis *et al.* 2005; Jonasson & Willis 2017). Periodic arousals (*i.e.*, returning to euthermia from torpor) can account for over half, and even up to 85%, of energy expenditures throughout hibernation (Geiser 2007; Jonasson & Willis 2012). These arousals are necessary for mounting immune responses and adjusting metabolic imbalances such as excreting waste, stabilizing electrolyte imbalances, accommodating sleep deprivation, restoring neural and synaptic activity, and/or restoring blood glucose (Fisher 1964; Galster & Morrison 1970; Willis 1971; Daan *et al.* 1991; Prendergast *et al.* 2002; Dave *et al.* 2012; Ruf & Geiser 2015). Disturbances in a hibernaculum can increase the number of periodic arousals and thus, increase the amount of energy expended during hibernation. Disturbances in a hibernacula may be anthropogenic such as lights and sounds from human activity

(Speakman *et al.* 1991), abiotic such as temperature or humidity changes, or they may be biotic such as disease-causing pathogens.

In North America, temperate cave-hibernating bats are disturbed during hibernation by the introduced fungal pathogen *Pseudogymnoascus destructans* (*Pd*) that causes white-nose syndrome (WNS; Blehert *et al.*, 2008; Lorch *et al.*, 2011). *Pd* was introduced from Eurasia to New York, USA and first detected in winter 2006 (Blehert *et al.* 2009; Leopardi *et al.* 2015; Drees *et al.* 2017). *Pd* exhibits optimal growth between 12 °C and 16 °C (Verant *et al.* 2012), making hibernacula, like caves, the perfect environment for *Pd* to thrive. Within hibernacula where *Pd* is present, *Pd* infects the epithelial tissue of bats wings and muzzles via direct contact with *Pd* on hibernacula walls and/or other infected bats (Blehert *et al.* 2009; Meteyer *et al.* 2009; Lorch *et al.* 2011). In species highly susceptible to infection, *Pd* infection causes increases in periodic arousals, decreases in torpor bout durations, respiratory acidosis, hypotonic dehydration, and increased metabolic rates while bats are hibernating, ultimately leading to death from energy depletion during hibernation (Lorch *et al.* 2011; Reeder *et al.* 2012; Cryan *et al.* 2013; Verant *et al.* 2014; McGuire *et al.* 2017). Such extreme negative physiological effects have led to local extinctions of highly susceptible bat species and devastated populations of highly susceptible North American temperate bats, with losses estimated to be over 90% (Frick *et al.* 2015; Cheng *et al.* 2021).

Eptesicus fuscus are considered less susceptible to *Pd* infection relative to other highly susceptible species and may exhibit some degree of resistance (Frank *et al.* 2014; Moore *et al.* 2018). Unlike highly susceptible species, *E. fuscus* increase or do not change their torpor bout durations while infected with *Pd* which may decrease the risk of

starvation from rapidly depleted fat stores throughout hibernation (Frank *et al.* 2014; Moore *et al.* 2018). Winter populations of *E. fuscus* are estimated to have declines of up to 41% following the introduction of *Pd* (Turner *et al.* 2011; Cheng *et al.* 2021). This suggests that *E. fuscus* torpor is still disrupted by *Pd* exposure due to either annual infections and/or the energetic cost of resistance.

To determine if *E. fuscus* increase their torpid energy expenditures with long-term pathogen exposure, I quantified torpid metabolic rates of *E. fuscus* across a wide range of ambient temperatures (T_a) nine and ten years following *Pd* introduction to southwestern Ohio. I compared torpid metabolic rates of *E. fuscus* post-*Pd* to torpid metabolic rates prior to *Pd* introduction (Herreid & Schmidt-Nielsen 1966; Szewczak & Jackson 1992b; Willis *et al.* 2005), and hypothesized that torpid metabolic rates post-*Pd* would be greater than torpid metabolic rates before *Pd* introduction. I highlight how *E. fuscus* may suffer negative energetic effects from long-term term pathogen exposure even though they are less susceptible to *Pd* infection and have some resistance.

MATERIALS AND METHODS

Animal Collection and Housing

I opportunistically collected 19 *E. fuscus* from Brukner Nature Center's Wildlife Rehabilitation Unit in Troy, OH, during the winters (January through March) of 2020 (n = 7) and 2021 (n = 12). Over the two-year period, I collected 10 male and 9 female *E. fuscus* (average mass ± SD = 18.77 ± 3.06 g; Appendix B Table 3.1). Each bat was suspected to have *Pd* upon collection due to the presence of orange/yellow UV fluorescence on wings and/or muzzles of bats when they were admitted into the rehabilitation unit (Turner *et al.* 2014). Previous work has shown that 98.8% of bats with UV fluorescence have histologic diagnosis of *Pd* infection and thus, white-nose syndrome (Turner *et al.* 2014). Further, at Brukner Nature Center in winter 2016, the presence of *Pd* was confirmed using culturing methods for bats that presented with UV fluorescence on wings and muzzles (Simonis *et al.* 2018). Finally, *Pd* was first confirmed in 2011 in Ohio (Ohio Department of Natural Resources 2011) and is considered to be an established pathogen (Langwig *et al.* 2015); therefore, because *Pd* prevalence is suggested to be stable across the state, I would expect bats to present with *Pd* infection in winter.

Bats considered healthy releasable candidates with suspected *Pd* were transported via car from Brukner Nature Center to Wright State University in Dayton, OH, under state permits for scientific collections and sub permits for wildlife rehabilitation under Brukner Nature Center (permits for Simonis, #21-154 and #55501). All animal care and

experimental procedures were approved and compliant with Wright State University's Institutional Animal Care and Use Committee (AUP# 1141). I housed bats individually at Wright State University in 62.5 L plastic enclosures with pillowcases draped over the interiors of the enclosure (Appendix B Fig. S3.1A), under which they typically hid (Appendix B Fig. S3.1B) or hung vertically (Appendix B Fig. S3.1C). Upon arrival at WSU, bats acclimated to laboratory conditions for 72 hours in a walk-in environmental chamber set to room temperature (20 °C - 22 °C) with light:dark cycles set to match daylengths at time of acclimation (typically 10 hours:14 hours). Bats were offered ~ 3 g - 4 g mealworms once per day in the evenings and fresh water *ad libitum*. After a maximum of eight days (three days for acclimation and up to five days for data collection), I transported bats from Wright State University back to Brukner Nature Center.

Confirmation of Pd

To confirm *Pd* infection, I swabbed bat wings and muzzles when they arrived at Wright State University. Swabs were frozen at -80 °C until data collection was complete for all 19 bats (~ two years). Swabs were then sent to the Colorado State University Veterinary Diagnostic Laboratories for qPCR detection of *Pd* (presence/absence; Appendix B Table S3.1).

Respirometry

I used standard methods for open-flow respirometry to quantify post-*Pd* metabolic rates ($\dot{V}_{O_2}$). Bats were placed in a 0.09 L metabolic chamber made of clear PVC piping (Appendix B Fig. S3.2). Copper mesh hardware fabric adhered to a flattened foam panel insert allowed bats to comfortably roost in a sternal (Appendix B Fig. S3.2A, S3.2B) or

vertical position (Appendix B Fig. S3.2C), depending on individual bat preference. A suction pump pulled air through the metabolic chamber at flow rates adjusted to prevent hypercarbia and hypoxia in the metabolic chambers (typically 0.1 – 0.3 $L*min^{-1}$; O_2 differential mean = 0.0016 mL min^{-1}, SD = 0.0013 mL min^{-1}; airflow pathway diagrammed in Fig. 1). A drying column (12 mL) filled with DM Desiccant Media (Perma Pure LLC, Toms River, NJ) inline between the metabolic chamber and the oxygen analyzer removed water vapor. The fraction of O_2 was measured with a S-3A/I O_2 Analyzer (AEI Technologies, Inc., Pittsburgh, PA; sensitivity ± 0.001% O_2; Fig. 1). I measured air flow rates and barometric pressure in-line with a TSI® 4100 Series flowmeter (TSI Incorporated, Shoreview, Minnesota). Bats were weighed to the nearest hundredth of a gram prior to and immediately after data collection.

To determine $\dot{V}_{O_2}$ across a wide range of T_a, I collected fractions of expired O_2 from *E. fuscus* at T_a setpoints of 0 °C, 5 °C, 10 °C, 15 °C, 20 °C, 25 °C, 30 °C, 35 °C, 37 °C, and 37.5 °C over a two-day period. For one bat in 2020, three days were needed for data collection. For another bat in 2020, data were not collected at 0 °C, 5 °C and 15 °C. To prevent bats from experiencing extreme temperature changes in relatively short periods of time, I exposed bats to T_a of 20 °C and below on the first day of data collection, and 20 °C and above on the second day. The order of temperature setpoints to which the bats were exposed was randomly chosen using the function *sample* in base R prior to any data collection, and that order was repeated for each individual bat (R Core Team 2021). During the first day of data collection, bats started at 20 °C and moved to 15 °C, 5 °C, 0 °C and then 10°C. One bat in 2020 did not have data collected at 20 °C in the first day of data collection. On the second day of data collection, bats started at 20 °C

again, but moved to 35 °C, 37 °C or 37.5 °C, 30 °C and then to 25 °C. I regulated T_a within the environmental chamber itself in 2020 or by using a Polystat heated immersion circulating water bath (Cole-Parmer ®, Vernon Hills, IL) in 2021. I used the water bath in 2021 to gain precision in ambient temperature regulation. There was no difference between years of data collection across T_a ($\chi^2_1 = 0.0574$; $P = 0.8107$, $R^2 = 0.0003$). At the highest T_a setpoints, bats were exposed to 37 °C in 2020 and 37.5 °C in 2021. This adjustment in setpoint was made in 2021 in attempts to push *E. fuscus* outside of their thermoneutral zone. In 2020, three of six bats sampled had data collected at 37 °C, and all 13 bats sampled in 2021 had data collected at 37.5 °C. MLT422/A Temperature Probes (ADInstruments, Sydney, Australia) connected to an ML309 Thermistor Pod (ADInstruments, Sydney, Australia) collected T_a in the metabolic chamber in 2020, and iButtons (Maxim Integrated®, San Jose, California) logged T_a in the metabolic chamber in 2021.

I collected skin temperature (T_{sk}) continuously for each individual bat during data collection together with $\dot{V}_{O_2}$ to distinguish when bats were torpid. To collect T_{sk}, two temperature probes were placed between the abdomen of each bat and the copper mesh covered foam panel inside the metabolic chamber. I measured T_{sk} with temperature probes instead of T_b surgical implants or rectal thermistors because this method 1) it is an appropriate proxy for T_b in the field and the lab and does not disturb resting bats (Hirshfeld & O'Farrell 1976; Audet & Fenton 1988; Szewczak & Jackson 1992b), and 2) it eliminated the need for additional recovery days in the lab for surgical implant removal after data collection. I chose the warmest temperature between the two T_{sk} recordings in case a bat moved one of the temperature probes off of its abdomen. Bats' T_{sk} settled at

each T_a within one to four hours, scaling with the magnitude of change from one T_a setpoint to the next. Once a bat settled at a T_a setpoint, I collected continuous T_a, T_{sk} and expired O_2 data using the LabChart8 software (ADInstruments, Sydney, Australia). Two-point O_2 calibrations correlated the fraction of O_2 with voltage output before and after 15 – 30 min data collection periods using room air (20.94% O_2) and 16.1 ± 0.02% O_2. I calibrated temperature probes and iButtons before and after data collection each day by correlating voltage output to known temperatures measured with an immersion thermometer (Fisher Scientific, Hampton, New Hampshire).

I performed a two-point calibration using bat mass from before and after data collection and estimated bat mass throughout data collection using linear regression. I assumed a linear decline in bat body mass during each day of data collection. Two-point calibration curves were created for before and after data collection periods for recorded fractions of expired O_2 and for T_a and T_{sk} each day using linear regression. Using the regressions for before and after data collection periods, I performed linear interpolation to account for instrument drift of the O_2 analyzer, temperature probes and iButtons during data collection.

To calculate mass-specific metabolic rates of each bat, I first calculated metabolic rates at ambient temperature and pressure dry using the equation

$$\dot{V}O_2 = FR_i(F_iO_2) - FR_e\ (F_eO_2)$$

where $\dot{V}_{O_2}$ is the metabolic rate, FR_i and FR_e are the flow rate, and F_{iO_2} is the fraction of inspired O_2 and F_{eO_2} is the fraction of expired O_2 (difference between O_2 in room air and O_2 in the metabolic chamber; Equation 9.4, Lighton, 2008). This value was then converted to standard temperature and pressure dry (STPD) by accounting for T_a and

barometric pressure. I divided $\dot{V}_{O_2}$ STPD by bat mass derived from linear interpolation of initial to final bat mass to determine average mass-specific $\dot{V}_{O_2}$ across 15-30 min data collection periods for each bat at each T_a set point.

A fan regulating temperature in the walk-in environmental chamber decreased the signal to noise ratio during data collection for some bats at cold T_as. Therefore, I removed average $\dot{V}_{O_2}$ values for two bats at 5 °C, one bat at 10 °C, four bats from 15 °C, two bats from 20 °C in the first day of data collection and one bat from 20 °C in the second day of data collection from statistical analyses.

Pre-Pd Metabolic Data Collection

As a baseline for *E. fuscus* torpid $\dot{V}_{O_2}$, I used published data for *E. fuscus* $\dot{V}_{O_2}$, T_a and T_b or T_{sk} collected before *Pd* introduction. Craig Willis provided average torpid $\dot{V}_{O_2}$, T_a and T_b for individual *E. fuscus* that were originally summarized and published in Willis et al. (2005). Additionally, I extracted average torpid $\dot{V}_{O_2}$, T_a and T_b from individual *E. fuscus* from Herreid and Schmidt-Nielsen (1966) using GetData Graph Digitizer version 2.26.0.20 (http://getdata-graph-digitizer.com/index.php). Finally, I used average torpid $\dot{V}_{O_2}$ and T_a and T_{sk} setpoints from Table 1 in Szewczak and Jackson (1992).

Statistical Analyses

To compare torpid energy expenditures of *E. fuscus* before and after *Pd* introduction, I compared torpid $\dot{V}_{O_2}$ values I collected post-*Pd* to pre-*Pd* values in each of

the previous studies (Herreid & Schmidt-Nielsen 1966; Szewczak & Jackson 1992b; Willis *et al.* 2005). Using T_a as a continuous variable, I created a linear mixed effects model for torpid $\dot{V}_{O_2}$ as a function of an interaction between recorded T_a and a categorical variable for data collection pre- and post-*Pd* (pre-*Pd* Herreid and Schmidt-Nielsen / pre-*Pd* Willis et al. / post-*Pd*) using the function *lmer* in the package lme4 in R version 4.0.5 (Bates *et al.* 2015; R Core Team 2021). I included a random effect for individual bat ID to account for multiple measures of each bat within my data and Willis et al. (2005) data. Within the Herreid and Schmidt-Nielsen (1966) data, I assumed that each bat was only measured once and therefore, each individual measure had its own unique ID. I tested this model using an ANOVA with a Type II Wald Chi-squared test using the function *Anova* from the car package in R to determine how the linear relationship of torpid $\dot{V}_{O_2}$ with T_a differed before and after *Pd* introduction for *E. fuscus* (Fox & Wesberg 2019; R Core Team 2021).

To determine how torpid $\dot{V}_{O_2}$ changed across categorical temperature setpoints before and after *Pd* introduction, I compared post-*Pd* torpid $\dot{V}_{O_2}$ at T_a setpoints of 5 ℃, 10 ℃, 20 ℃, 30 ℃ and 37 ℃ and 37.5 ℃ combined, to pre-*Pd* $\dot{V}_{O_2}$ at T_{sk} setpoints of 5 ℃, 10 ℃, 20 ℃, 30 ℃ and 37 ℃ (Szewczak & Jackson 1992b). Setpoints for T_{sk} pre-*Pd* were reported to typically be within 0.5 ℃ of T_a (Szewczak & Jackson 1992a, b). I determined differences between pre- and post-*Pd* $\dot{V}_{O_2}$ at categorical temperature setpoints using mean $\dot{V}_{O_2}$ and standard errors and performed two-tailed t-tests on normal

distributions between pre- and post-*Pd* $\dot{V}_{O_2}$ at each temperature setpoint. Therefore, these analyses drew comparisons for across groupings of $\dot{V}_{O_2}$ for T_{sk} or T_a at categorized temperature setpoints and did not use T_{sk} or T_a as continuous variables.

RESULTS

All *E. fuscus* collected in 2020 and 2021 tested negative for *Pd* DNA by PCR (Appendix B Table S3.2). I considered all *E. fuscus* collected in 2020 and 2021 torpid at all T_a with absolute temperature differentials between T_{sk} and T_a averaging 1.29 ± 1.46 ℃ (Fig. 3.2). 95% of T_{sk} averages fell within 4 ℃ of T_a averages (Fig. 3.2), 4% of T_{sk} averages were >4, but < 7 ℃ of T_a averages and one bat had a T_{sk} 11.5 ℃ above T_a (Fig. 3.2). In cases where measured T_{sk} fell below measured T_a, I suspect temperature probe or iButton sensitivity may have been less than reported by the manufacturer or had non-linear drift over time. Therefore, I suggest our temperature measurement error was more likely ±2.66 ℃, which was the greatest temperature differential when T_{sk} fell below T_a (Fig. 3.2).

Torpid $\dot{V}_{O_2}$ post-*Pd* did not differ significantly between pre-*Pd* $\dot{V}_{O_2}$ from Willis et al. (2005) or Herreid and Schmidt-Nielsen (1966) across T_a, as indicated by a Type II ANOVA ($\chi^2_2 = 0.1050$; $P = 0.9489$; $R^2 = 0.24$). However, torpid $\dot{V}_{O_2}$ did increase with T_a alone ($\chi^2_1 = 12.97$ $P = 0.0003$; Fig. 3.3). When comparing pre- and post-*Pd* torpid $\dot{V}_{O_2}$ at categorical temperature setpoints with data from Szewczak & Jackson (1992) using individual t-tests, torpid $\dot{V}_{O_2}$ was greater post-*Pd* compared to pre-*Pd* at 5 ℃ ($P = 0.0060$; Fig. 3.4A), 10 ℃ ($P = 0.0016$; Fig. 3.4B), 20 ℃ ($P = 0.0066$; Fig. 3.4C), 30 ℃ ($P < 0.0001$; Fig. 3.4D), and 37 ℃ combined with 37.5 ℃ ($P < 0.0001$; Fig. 3.4E).

DISCUSSION

Eptesicus fuscus' resistance to *Pd* infections (Frank *et al.* 2014) may cost additional energy as evidenced by greater torpid $\dot{V}_{O_2}$ post-*Pd* (Fig. 3.4), or may not incur additional cost as implied by the lack of significant increases in *E. fuscus* torpid $\dot{V}_{O_2}$ post-*Pd* when comparing to pre-*Pd* data from Herreid and Schmidt-Nielsen (1966) and Willis et al. (2005; Fig. 3.3). While pathogen resistance benefits the immediate survival of a host in the face of disease, there are physiological and life history trade-offs associated with pathogen resistance. Resistance can cost additional energy for mounting immune responses to reduce pathogen fitness (Purrington 2000; Bonneaud *et al.* 2003; Martin *et al.* 2010; Schoenle *et al.* 2018), or hosts can allocate the energy needed for resistance by trading energetically costly life history processes like host reproduction for immune functioning (Lee 2006). Therefore, long-term host fitness can weaken due to pathogen resistance if there are not enough resources to accommodate its costs (Martin *et al.* 2003).

Maintaining the ability to torpor to the same extent pre- and post-*Pd* is likely one of the physiological mechanisms underlying *E. fuscus*' resistance to *Pd* (Frank *et al.* 2014). All *E. fuscus* collected in winters of 2020 and 2021 (nine and ten years following *Pd* introduction) were torpid throughout data collection, as evidenced by having T_{sk} values within 1.29 ± 1.46 ℃ of T_a on average (Fig. 3.2). Further, when comparing the data collected here to data from Herreid and Schmidt-Nielsen (1966) and Willis et al. (2005; Fig. 3.3), *E. fuscus* torpid $\dot{V}_{O_2}$ post-*Pd* were not different from torpid $\dot{V}_{O_2}$ pre-*Pd*

across a wide range of T_a. This suggests that *E. fuscus* do not expend additional energy during torpor due to resistance after *Pd* introduction. However, it is unclear how no changes to torpid $\dot{V}_{O_2}$ across a wide range of T_a may impact *E. fuscus* reproduction, particularly if the cost of resistance manifests itself by decreasing fecundity, which cannot be determined with these data. *Eptesicus fuscus* use torpor in warmer T_a during pregnancy and lactation, likely as a fitness trade-off when food and other resources are limited (Audet & Fenton 1988; McAllan & Geiser 2014). It is possible pregnant and lactating *E. fuscus* in warm spring and summer months could use torpor more frequently to offset the energy cost of mounting immune responses to continue to fight *Pd* infections obtained in winter. However, if torpid $\dot{V}_{O_2}$ at warmer T_a does not change post-*Pd*, increased frequency of torpor could limit reproductive success by trading off energy needed for gestation and/or pup rearing for immune functions. Further research into how female reproductive energy expenditures, fecundity and pup survival changes with long-term *Pd* exposure is needed to determine if resistance to *Pd* has long-term fitness trade-offs for *E. fuscus*.

Small mammals have an endogenous circannual cycle for torpor patterns and hibernation (Pengelley & Kelly 1966; Press 1990). During winter, small mammals undergo their deepest and longest torpor bouts, while in spring and fall, these patterns a shallower and shorter (Körtner & Geiser 2000). There was no difference in torpid $\dot{V}_{O_2}$ in relation to T_a post-*Pd* compared to pre-*Pd* data from Herreid and Schmidt-Nielsen (1966) and Willis et al. (2005). All post-*Pd E. fuscus* torpid $\dot{V}_{O_2}$ were collected during winter months (January through March), suggesting bats should have been in relatively deep

torpor. Prior to *Pd* introduction, *E. fuscus* torpid $\dot{V}_{O_2}$ were collected in September through January (Herreid & Schmidt-Nielsen 1966), September and May (Willis *et al.* 2005), or lab acclimated at 25 ℃ with season of data collection unknown (Szewczak & Jackson 1992b, a). This suggests that pre-*Pd* bats may not have been in as deep of torpor as post-*Pd* bats. Thus, this seasonal difference in data collection could have confounded any differences in torpid $\dot{V}_{O_2}$ due to long-term *Pd* exposure because pre-*Pd* bats were not within the same circannual period as post-*Pd* bats. If there are seasonal differences in torpid $\dot{V}_{O_2}$ of *E. fuscus*, these results could be interpreted that *E. fuscus* post-*Pd* have torpid energy expenditures in late winter that are no different than pre-*Pd* torpid energy expenditures in spring or fall through early winter. This interpretation would suggest that with long-term pathogen exposure, resistance to *Pd* may cause *E. fuscus* to have shallower torpid periods in winter than they did prior to *Pd* introduction and thus, have greater torpid energy expenditures across T_a post-*Pd* compared to pre-*Pd* in winter months.

Eptesicus fuscus' resistance to *Pd* infections may increase torpid $\dot{V}_{O_2}$ post-*Pd*, suggesting a long-term additional energetic cost for mounting immune responses to reduce *Pd* infections. When I averaged post-*Pd* $\dot{V}_{O_2}$ by the T_a setpoint of the environmental chamber (2020) or water bath (2021) and compared to pre-*Pd* data presented in Szewczak & Jackson (1992), presented as averages at T_{sk} setpoints, *E. fuscus* had greater overall torpid $\dot{V}_{O_2}$ post-*Pd* compared to pre-*Pd* across all temperature setpoints (Fig. 3.4). This suggests that *E. fuscus* resistance *does* cost additional energy to

maintain and, therefore, *E. fuscus* must be able to accommodate the energetic cost of resistance in order to survive. To put this into perspective at hibernating temperatures, using the average mass for bats I collected for this study (18.78 g), a standard conversion factor of 1.96 L O_2 g^{-1} to convert rates of O_2 consumption into grams of fat burned (Brown & Brengelmann 1966), *E. fuscus* post-*Pd* would burn 18.33 or 8.75 times more fat during torpor bouts each day than they did pre-*Pd* at 5 ℃ or 10 ℃ (Appendix B). For pre-*Pd E. fuscus* at T_{sk} setpoints of 5 ℃ and 10 ℃, *E. fuscus* weighing 18.78 g would burn 0.006 g or 0.008 g of fat each day while hibernating (Appendix B). In comparison, post-*Pd E. fuscus* weighing 18.78 g would burn 0.11 g or 0.07 g of fat each day at T_a setpoints of 5 ℃ or 10 ℃ (Appendix B). Although I would not expect *E. fuscus* to hibernate at temperature setpoints 20 ℃ and above, *E. fuscus* would still need enough food to accommodate those additional energy expenditures above 20 ℃. For female *E. fuscus* in T_a greater than 20 ℃, they would also need enough food to support reproduction while fighting off infections in spring and summer. At temperature setpoints of 5 ℃ and 10 ℃, the amount of fat burned post-*Pd* for an 18.78 g *E. fuscus* during torpor bouts would not allow for *E. fuscus* survival in winter months without access to food. Therefore, although the number of periodic arousals and torpor bout durations are not different for *E. fuscus* after *Pd* introduction (Frank *et al.* 2014), *E. fuscus* may yet incur greater energy costs during torpor bouts post-*Pd* compared to pre-*Pd* in order to mount immune responses to *Pd* infections. This, in combination with the lack of *Pd* detection on all *E. fuscus* collected, supports the phenomenon that resistance to pathogen infections is energetically costly for bats that are considered less susceptible (Purrington 2000; Bonneaud *et al.* 2003; Martin *et al.* 2010; Schoenle *et al.* 2018).

If *E. fuscus* increase torpid metabolic rates post-*Pd*, they must be able to accommodate the energetic cost of resistance. At temperature setpoints of 20 ℃ and above, *E. fuscus* are likely able to make up for the majority of these additional energy costs because 1) insect prey are available, 2) declines to *E. fuscus* body mass with long-term *Pd* exposure in spring through fall months are about 1 g on average (see Chapter 1), and 3) capture rates of *E. fuscus* in spring through fall months almost double across the eastern US after *Pd* introduction (see Chapter 3). At temperature setpoints of 5 ℃ and 10 ℃, the potential increases to torpid $\dot{V}_{O_2}$ post-*Pd* could reflect winter population declines of 35 – 41% for *E. fuscus* due to WNS if some *E fuscus* are unable to accommodate additional energy expenditures (Turner *et al.* 2011; Cheng *et al.* 2021). *Eptesicus fuscus* may be able to replenish energy stores between torpor bouts by foraging during periodic arousals, but the degree to which they are able to balance additional energy losses in doing so is unknown. *Eptesicus fuscus* are known to leave caves throughout hibernation and change hibernacula (Swanson & Evans 1936; Rysgaard 1942), and have been found with evidence of recent predation on moths, beetles and flies in the winter (Dunbar *et al.* 2007). *Eptesicus fuscus* are also highly active throughout hibernation on warm winter nights post-*Pd* relative to other North American hibernating bat species (Reynolds *et al.* 2017). This winter foraging activity by *E. fuscus* to accommodate for increased torpid energy expenditures could also contribute to estimated winter population declines if they become a more frequent prey item to birds of prey (Negro *et al.* 1992). The potential increased energetic cost of torpor post-*Pd* compared to pre-*Pd* (Fig. 3.4) suggests foraging behaviors of *E. fuscus* and insect availability of their insect prey need to be monitored, particularly in winter months when food availability is minimal, to better

understand the mechanism linking increased metabolic costs of *E fuscus* post-*Pd* with seasonal increases or decreases in the abundance of *E. fuscus*.

If the decrease in torpid metabolic rates passively follows declining body temperatures with deeper torpor at lower T_a, then using a linear mixed effects model to compare *E. fuscus* torpid $\dot{V}_{O_2}$ pre- and post-*Pd* when using Herreid and Schmidt-Nielsen (1966) and Willis et al. (2005) data is the best comparison. Temperature-dependence of torpid $\dot{V}_{O_2}$ has been tested linearly across many species throughout North America, including *E. fuscus* (McGuire *et al.* 2021). It is possible, though, that a non-linear relationship between torpid $\dot{V}_{O_2}$ and T_a may be more accurate for several reasons. Increased torpid metabolic rates to prevent freezing at very low T_a and metabolic depression independent of T_b are two such possibilities. Many North American temperate bats have a minimum T_a while torpid below which torpid energy expenditures can increase in order to avoid freezing body temperatures, although this minimum temperature has not yet been identified for *E. fuscus* (Hock 1951; Dunbar & Tomasi 2006; Humphries *et al.* 2006; Boyles *et al.* 2020; McGuire *et al.* 2021). Prior to *Pd* introduction, a potential increase in torpid $\dot{V}_{O_2}$ appears to occur at 5 ℃ or below for Herreid and Schmidt-Nielsen (1966) and Willis et al. (2005) data (Fig. 3.3). Post-*Pd*, it appears this increase in torpid $\dot{V}_{O_2}$ to avoid freezing body temperatures may also occur around a minimum T_a 5 ℃ (Fig. 3.3). A minimum T_a of 5 ℃ at which *E. fuscus* may initiate freeze-avoidance mechanisms and increase torpid $\dot{V}_{O_2}$ post-*Pd* is also supported

in comparisons to Szewczak & Jackson (1992) pre-*Pd* data. When averaging torpid $\dot{V}_{O_2}$ at T_a setpoints, *E. fuscus* post-*Pd* seems to decrease torpid $\dot{V}_{O_2}$ between 5 ℃ and 10 ℃ and then being increasing torpid $\dot{V}_{O_2}$ between 10 ℃ and 20 ℃, and may continue to increase as temperature setpoints increase (Fig. 3.4). Therefore, it is possible that the amplitude of torpid energy costs below a minimum T_a has increased post-*Pd*. Further research investigating non-linear relationships of torpid $\dot{V}_{O_2}$ is needed to determine if *E. fuscus*' minimum T_a, and associated torpid energy expenditures below that minimum T_a, change with long-term pathogen exposure.

The relationship between torpid $\dot{V}_{O_2}$ and T_a may also be non-linear if passive chemical properties of the temperature-dependence of metabolic rate are altered by regulatory pathways. Thyroid regulation can alter temperature-dependent torpid $\dot{V}_{O_2}$ (Frare *et al.* 2021). Replenishment of ATP can cost energy and increase temperature-dependent torpid $\dot{V}_{O_2}$ (Abnous & Storey 2021). Season adjustments to circannual and circadian rhythms can change torpid $\dot{V}_{O_2}$ relationships with T_a (Hut *et al.* 2014). Finally, the temperature dependence of neural-immune responses can cause torpid $\dot{V}_{O_2}$ to vary with T_a (Madden 2017). If the data presented here have additive effects, it would imply that the temperature-dependence of torpid $\dot{V}_{O_2}$ is variable for *E. fuscus*. Therefore, the temperature-dependence of *E. fuscus* of torpid $\dot{V}_{O_2}$ is possibly regulated by other mechansims that could change within *E. fuscus* before and after *Pd* introduction. Further

research and/or analysis is needed to determine if *E. fuscus* torpid $\dot{V}_{O_2}$ have additive (non-linear) effects with T_a and if patterns of variable energy expenditures with T_a differ before and after *Pd* introduction.

Results for changes in *E. fuscus* torpid $\dot{V}_{O_2}$ before and after *Pd* introduction differed based on the data available in the literature for comparison. When testing torpid $\dot{V}_{O_2}$ across continuous values for measured T_a, there was no change in torpid $\dot{V}_{O_2}$ pre- to post-*Pd* (Fig. 3.3) assuming a linear relationship between torpid $\dot{V}_{O_2}$ and T_a. In contrast, when averaging torpid $\dot{V}_{O_2}$ around T_{sk} (pre-*Pd*) or T_a (post-*Pd*) categorical setpoints and comparing pre- and post-*Pd* torpid $\dot{V}_{O_2}$ at each setpoint, there were significant increases to torpid $\dot{V}_{O_2}$ across all temperature setpoints (Fig. 3.4). These conflicting results may be reflective of how I was able to test my hypothesis based on the data provided in the literature. Ideally, if all pre-*Pd* torpid $\dot{V}_{O_2}$ data (Herreid & Schmidt-Nielsen 1966; Szewczak & Jackson 1992b; Willis *et al.* 2005) were paired with their measured T_a for each individual bat, I would have a single, and more rigorous statistical analysis due to the inclusion of all pre-*Pd* data. Instead, data from Szewczak & Jackson (1992) were presented as torpid $\dot{V}_{O_2}$ averages and standard errors for at specific T_{sk} setpoints and an additional analysis was needed. Comparisons pre- to post-*Pd* in this additional analysis using t-tests at each categorical temperature setpoint may be responsible for different results than the continuous comparison using Herreid and Schmidt-Nielsen (1966) and Willis et al. (2005) data, due to a loss of individual variability and statistical power

(Royston *et al.* 2006). An additional option for including all pre-*Pd* data could be to categorize Herreid and Schmidt-Nielsen (1966) and Willis et al. (2005) data by binning torpid $\dot{V}_{O_2}$ values around temperature setpoints and completing individual t-tests against each pre- or post-*Pd* data collector. However, this option would lose the individual variability across all pre-*Pd* data collectors. Therefore, I chose to maintain the structure of the pre-*Pd* data available in the literature by completing two separate robust analyses (*i.e.* ANOVA or t-tests). Differing results highlight the importance of individual data availability in order to make holistic before and after comparisons, particularly in instances where obtaining animals that have never been exposed to a pathogen may not be possible.

Results a decade after the introduction of *Pd* indicate a need for further investigations for *E. fuscus* torpor patterns in the lab and in the field. These investigations should focus on our ability to draw more holistic comparisons between *E. fuscus* with and without long-term *Pd* exposure. Future research in the lab should use *Pd* inoculation experiments to investigate *E. fuscus* torpor patterns holistically (periodic arousals, torpor bout durations and torpid $\dot{V}_{O_2}$) at multiple different hibernating temperatures to better understand the energetic consequences *E. fuscus* may face fighting annual *Pd* exposure. In the field, I suggest additional research for periodic arousals and torpor bout durations of *E. fuscus* during hibernation be conducted following establishment of *Pd* on the landscape (five or more years post-*Pd*; Langwig *et al.* 2015; Cheng *et al.* 2021). I would also suggest that measurements for torpid $\dot{V}_{O_2}$ be conducted in the field at hibernating T_a across multiple time points during hibernation to understand *E. fuscus*' depth of torpor

throughout circannual cycles. This additional research will provide clearer comparisons for how *E. fuscus* respond to *Pd* exposure at varying T_a, varying seasons and over long-term *Pd* exposure via their torpid energy expenditures.

ACKNOWLEDGEMENTS

I am extremely grateful for Cassie Poeppelman's help with raw data calculations. I also thank Craig Willis for providing data from his 2005 publication with colleagues, and Ayşe Şahin for her guidance on how to calculate linear interpolations. I would also like to thank Pete Simonis for his help with calculating linear interpolations. Finally, I thank Brukner Nature Center for providing bats to conduct this research and Wright State University's Laboratory Animal Resources staff for their help and guidance.

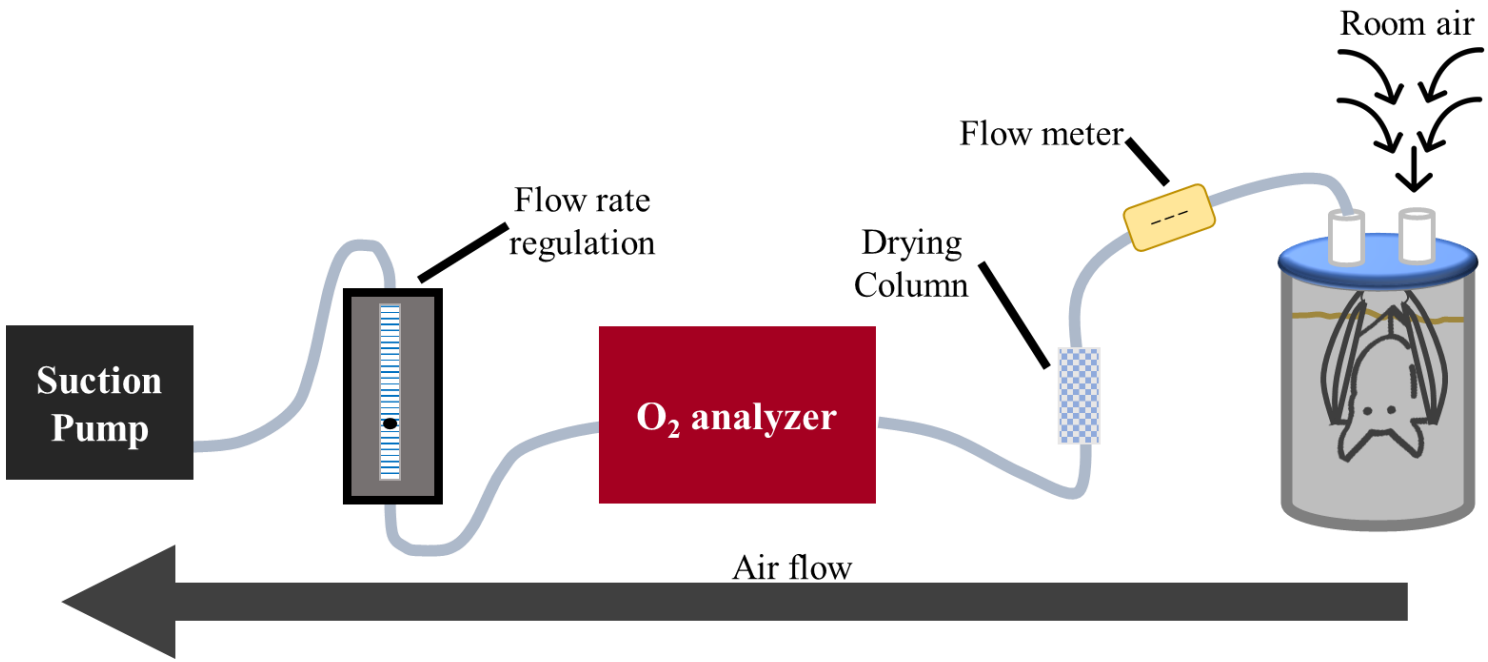

Figure 3.1. Lines of airflow during respirometry experiments with *E. fuscus*. I pulled room air from a 0.9 L metabolic chamber where bats rested through a flow meter and drying column before reaching an oxygen analyzer.

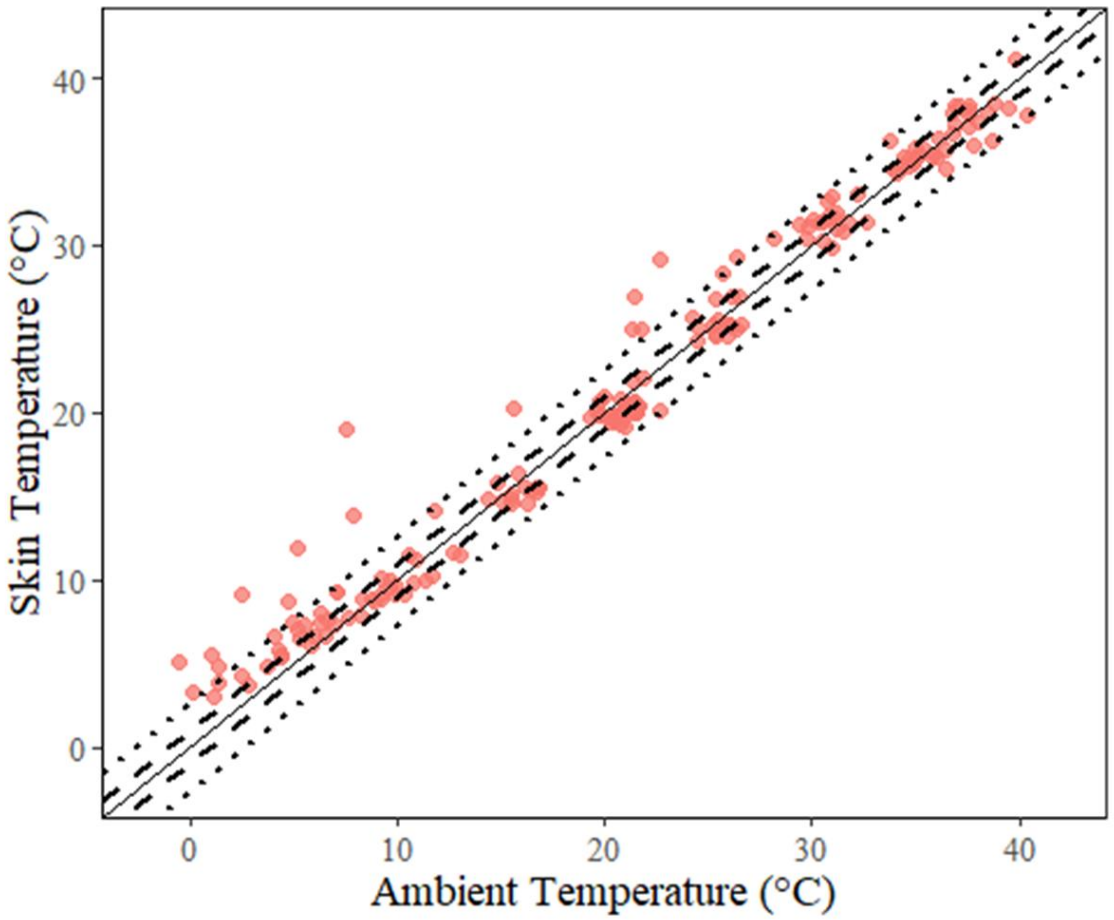

Figure 3.2. I considered all *E. fuscus* torpid across the range of ambient temperatures used for data collection because the average temperature differential between skin and ambient temperatures was 1.29 ± 1.46 ℃. Circles represent average *E. fuscus* skin temperatures in relation to average ambient temperatures collected from 19 bats during respirometry experiments in the winters of 2020 and 2021 (post-*Pd*). The solid black line is the identity line (1:1) showing where skin temperatures would be equal to ambient temperatures. Dashed black lines are 1 ℃ error bars around the 1:1 line representing

iButton sensitivity, which was the least sensitive equipment used to measure temperature. Dotted black lines are 2.66 ℃ error bars around the 1:1 line representing actual estimated temperature measurement sensitivity based on the largest temperature differential when skin temperature was lower than ambient temperature.

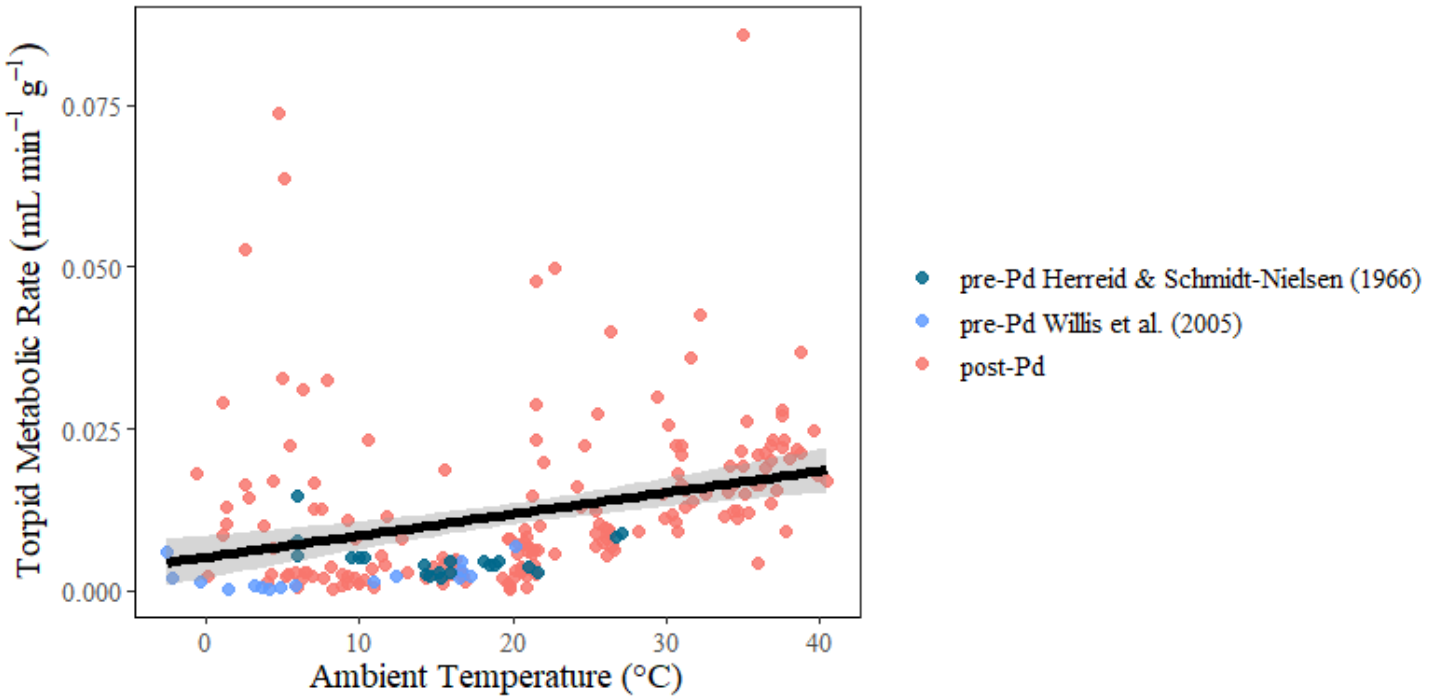

Figure 3.3. Torpid metabolic rates increase with ambient temperature regardless of pre- or post-*Pd* status (χ^2_1 = 14.4 P = 0.0002). Gray shaded area around regression line represents 95% confidence intervals. Circles in blue hues are data collected pre-*Pd* (Herreid & Schmidt-Nielsen 1966; Willis *et al.* 2005) and circles in red are data collected in this study post-*Pd*.

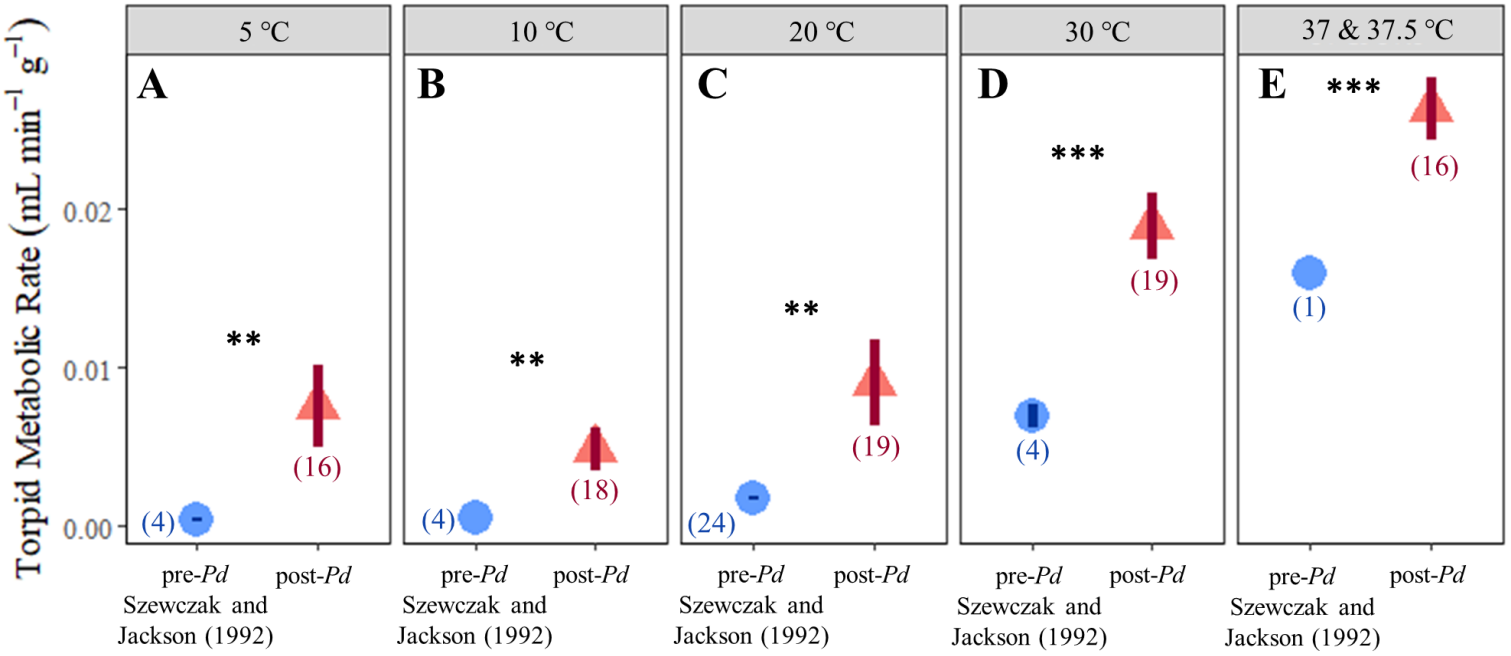

Figure 3.4. Torpid metabolic rates post-*Pd* are greater than torpid metabolic rates pre-*Pd* at T_a and T_{sk} setpoints of **A)** 5 °C, **B)** 10 °C, **C)** 20 °C, **D)** 30 °C, and **E)** 37 °C and 37.5 °C. Temperature setpoints for pre-*Pd* data from Szewczak and Jackson (1992) are for T_{sk} while temperature setpoints for post-*Pd* data were for T_a. Points represent average torpid metabolic rates at each temperature setpoint and error bars are standard errors of the mean. Sample sizes are indicated in parentheses with each corresponding point. Points, error bars and sample sizes are colored by data collectors before and after *Pd* introduction.

Significance values were obtained using two-tailed t-tests on normal distributions at each temperature setpoint. *P < 0.05; **P < 0.01; ***P < 0.001.

REFERENCES

Abnous, K. & Storey, K.B. (2021). 5′-Adenosine monophosphate deaminase regulation in ground squirrels during hibernation. Comp. Biochem. Physiol. Part B, 253, 110543.

Audet, D. & Fenton, M.B. (1988). Heterothermy and the use of torpor by the bat *Eptesicus fuscus* (Chiroptera: Vespertilionidae): A field study. Physiological Zool., 61, 197–204.

Bates, D., Maechler, M., Bolker, B. & Walker, S. (2015). Fitting Linear Mixed-Effects Models Using lme4. J. Stat. Softw., 67, 1–48.

Blehert, D.S., Hicks, A.C., Behr, M., Meteyer, C.U., Berlowski-Zier, B.M., Buckles, E.L., et al. (2009). Bat white-nose syndrome: an emerging fungal pathogen? Science, 323, 227.

Bonneaud, C., Mazuc, J., Gonzalez, G., Haussy, C., Chastel, O., Faivre, B., et al. (2003). Assessing the cost of mounting an immune response. Am. Nat., 161, 367–379.

Boyles, J.G., Johnson, J.S. & Lilley, T.M. (2020). Optimal hibernation theory. Mamm. Rev., 50, 91–100.

Brigham, R.M. (1987). The significance of winter activity by the big brown bat (*Eptesicus fuscus*): the influence of energy reserves. Can. J. Zool., 65, 1240–1242.

Brown, A.C. & Brengelmann, G. (1966). Energy Metabolism. In: Physiology and Biophysics (eds. Ruch, T.C. & Patton, H.D.). W.B. Saunders, Philadelphia.

Cheng, T.L., Reichard, J.D., Coleman, J.T.H., Weller, T.J., Thogmartin, W.E., Reichert, B., et al. (2021). The scope and severity of White-nose Syndrome on hibernating bats in North America. Conserv. Biol., 35, 1586–1597.

Cryan, P.M., Meteyer, C.U., Blehert, D.S., Lorch, J.M., Reeder, D.M., Turner, G.G., et al. (2013). Electrolyte Depletion in White-nose Syndrome Bats. J. Wildl. Dis., 49, 398–402.

Daan, S., Barnes, B. & Strijkstra, A. (1991). Warming up for sleep? Ground squirrels sleep during arousals from hibernation. Neurosci. Lett., 128, 265–268.

Dave, K.R., Christian, S.L., Perez-pinzon, M.A. & Drew, K.L. (2012). Neuroprotection: Lessons from hibernators. Comp. Biochem. Physiol. Part B, 162, 1–9.

Drees, K., Puechmaille, S., Parise, K.L. & Wibbelt, G. (2017). Phylogenetics of a Fungal Invasion: Origins and Widespread Dispersal of White-Nose Syndrome. MBio, 8, e01941-17.

Dunbar, M.B., Whitaker, J.O. & Robbins, L.W. (2007). Winter feeding by bats in Missouri. Acta Chiropterologica, 9, 305–322.

Dunbar, M.B. & Tomasi, T.E. (2006). Arousal patterns, metabolic rate, and an energy budget of Eastern red bats (*Lasiurus borealis*) in winter. J. Mammal., 87, 1096–1102.

Fisher, K. (1964). On the mechanism of periodic arousal in the hibernating ground squirrel. Ann. Acad. Sci. Fenn. Ser A IV Biol., 74, 141–156.

Fox, J. & Wesberg, S. (2019). An R Companion to Applied Regression. Third Edition. Sage, Thousand Oaks, CA.

Frank, C.L., Michalski, A., McDonough, A.A., Rahimian, M., Rudd, R.J. & Herzog, C. (2014). The resistance of a North American bat species (*Eptesicus fuscus*) to White-Nose Syndrome (WNS). PLoS One, 9, 1–14.

Frare, C., Williams, C.T. & Drew, K.L. (2021). Molecular and Cellular Endocrinology Thermoregulation in hibernating mammals: The role of the “thyroid hormones system”. Mol. Cell. Endocrinol., 519, 111054.

Frick, W.F., Puechmaille, S.J., Hoyt, J.R., Nickel, B.A., Langwig, K.E., Foster, J.T., et al. (2015). Disease alters macroecological patterns of North American bats. Glob. Ecol. Biogeogr., 24, 741–749.

Galster, W.A. & Morrison, P. (1970). Cyclic changes in carbohydrate concentrations during hibernation in the arctic ground squirrel. Am. J. Physiol., 218, 1228–1232.

Geiser, F. (2007). Yearlong hibernation in a marsupial mammal. Naturwissenschaften, 94, 941–944.

Herreid, F. & Schmidt-Nielsen, K. (1966). Oxygen consumption, temperature, and water loss in bats from different environments. Am. J. Physiol., 211, 1108–1112.

Hill, R.W., Wyse, G.A. & Anderson, M. (Eds.). (2016). Animal Physiology. Fourth. Sinauer Associates Inc., Sunderland, MA.

Hirshfeld, J.R. & O'Farrell, M.J. (1976). Comparisons of differential warming rates and tissue temperatures in some species of desert bats. Comp. Biochem. Physiol. -- Part A Physiol., 55, 83–87.

Hock, R.J. (1951). The Metabolic Rates and Body Temperatures of Bats. Biol. Bull., 101, 289–299.

Humphries, M., Speakman, J. & Thomas, D. (2006). Hibernation Energetics of *Myotis Lucifugus*. In: Functional and Evolutionary Ecology of Bats (eds. Zubaid, A., McCracken, G. &
Kunz, T.). Oxford University Press, Inc., New York, New York, pp. 23–37.

Hut, R.A., Dardente, H. & Riede, S.J. (2014). Seasonal Timing: How Does a Hibernator Know When to Stop Hibernating? Curr. Biol., 24, R602–R605.

Jonasson, K. & Willis, C.K.R. (2017). Thrifty Females, Frisky Males: Winter Energetics of Hibernating Bats from a Cold Climate. Physiol. Biochem. Zool., 90, 502–511.

Jonasson, K.A. & Willis, C.K.R. (2012). Hibernation energetics of free-ranging little brown bats. J. Exp. Biol., 215, 2141–2149.

Körtner, G. & Geiser, F. (2000). The temporal organization of daily torpor and hibernation: circadian and circannual rhythms. Chronobiol. Int., 17, 103–128.

Kurta, A. & Baker, R.H. (1990). *Eptesicus fuscus*. Mamm. Species, 356, 1–10.

Langwig, K.E., Voyles, J., Wilber, M.Q., Frick, W.F., Murray, K.A., Bolker, B.M., et al. (2015). Context-dependent conservation responses to emerging wildlife diseases. Front. Ecol. Environ., 13, 195–202.

Lee, K.A. (2006). Linking immune defenses and life history at the levels of the individual and the species, 46, 1000–1015.

Leopardi, S., Blake, D. & Puechmaille, S.J. (2015). White-nose syndrome fungus introduced from Europe to North America. Curr. Biol., 25, R217–R219.

Lighton, J.R.B. (2008). Measuring Metabolic Rates: A Manual for Scientists. Oxford University Press, Inc., New York.

Lorch, J.M., Meteyer, C.U., Behr, M.J., Boyles, J.G., Cryan, P.M., Hicks, A.C., et al. (2011). Experimental infection of bats with *Geomyces destructans* causes white-nose syndrome. Nature, 480, 376–378.

Madden, K.S. (2017). Sympathetic neural-immune interactions regulate hematopoiesis, thermoregulation and inflammation in mammals. Dev. Comp. Immunol., 66, 92–97.

Martin, L.B., Hopkins, W.A., Mydlarz, L.D. & Rohr, J.R. (2010). The effects of anthropogenic global changes on immune functions and disease resistance. Ann. N. Y. Acad. Sci., 1195, 129–148.

Martin, L.B., Scheuerlein, A. & Wikelski, M. (2003). Immune activity elevates energy expenditure of house sparrows: a link between direct and indirect costs? Proc. R. Soc. B Biol. Sci., 270, 153–158.

McAllan, B.M. & Geiser, F. (2014). Torpor during reproduction in mammals and birds: Dealing with an energetic conundrum. Integr. Comp. Biol., 54, 516–532.

McGuire, L.P., Fuller, N.W., Dzal, Y.A., Haase, C.G., Baerwald, B.J.K., Silas, K.A., et al. (2021). Interspecific variation in evaporative water loss and temperature response, but not metabolic rate, among hibernating bats. Sci. Rep., 1–9.

McGuire, L.P., Mayberry, H.W. & Willis, C.K.R. (2017). White-nose syndrome increases torpid metabolic rate and evaporative water loss in hibernating bats. Am. J. Physiol. - Regul. Integr. Comp. Physiol., 313, R680–R686.

Meteyer, C.U., Buckles, E.L., Blehert, D.S., Hicks, A.C., Green, D.E., Shearn-bochsler, V., et al. (2009). Histopathologic criteria to confirm white-nose syndrome in bats. J. Vet. Diagnostic Investig., 21, 411–414.

Moore, M.S., Field, K.A., Behr, M.J., Turner, G.G., Furze, M.E., Stern, D.W.F., et al. (2018). Energy conserving thermoregulatory patterns and lower disease severity in a bat resistant to the impacts of white-nose syndrome. J. Comp. Physiol. B Biochem. Syst. Environ. Physiol., 188, 163–176.

Negro, J.J., Ibánez, C., Pérez Jord, J.L. & Dela Riva, M.J. (1992). Winter predation by common kestrel falco tinnunculus on pipistrelle bats *Pipistrellus pipistrellus* in southern Spain. Bird Study, 39, 195–199.

Ohio Department of Natural Resources. (2011). White-nose Syndrome Detected in Ohio: News Release.

Pengelley, E. & Kelly, K. (1966). A “Circannian’’ rhythm in hibernating species of the genus *Citellus* with observations on their physiological evolution. Comp. Biochem. Physiol., 19, 603–617.

Prendergast, B.J., Freeman, D.A., Zucker, I. & Nelson, R.J. (2002). Periodic arousal from hibernation is necessary for initiation of immune responses in ground squirrels. Am. J. Physiol. - Regul. Integr. Comp. Physiol., 282, R1054–R1062.

Geiser, F., Hiebert, S. & Kenagy, G.J. (1990). Torpor Bout Duration during the Hibernation Season of Two Sciurid Rodents: Interrelations with Temperature and Metabolism. Physiol. Zool., 63, 489–503.

Purrington, C.B. (2000). Costs of resistance. Curr. Opin. Plant Biol., 3, 305–308.

R Core Team. (2021). R: A language and environment for statistical computing.

Reeder, D.M., Frank, C.L., Turner, G.G., Meteyer, C.U., Kurta, A., Britzke, E.R., et al. (2012). Frequent Arousal from Hibernation Linked to Severity of Infection and Mortality in Bats with White-Nose Syndrome. PLoS One, 7, e38920.

Reynolds, D.S., Shoemaker, K., Von Oettingen, S. & Najjar, S. (2017). High Rates of Winter Activity and Arousals in Two New England Bat Species: Implications for a Reduced White-Nose Syndrome Impact? Northeast. Nat., 24, B188–B208.

Royston, P., Altman, D.G. & Sauerbrei, W. (2006). Dichotomizing continuous predictors in multiple regression: A bad idea. Stat. Med., 25, 127–141.

Ruf, T. & Geiser, F. (2015). Daily torpor and hibernation in birds and mammals. Biol. Rev., 90, 891–926.

Rysgaard, G.N. (1942). A Study of the Cave Bats of Minnesota with Especial Reference to the Large Brown Bat, *Eptesicus fuscus fuscus* (Beauvois). Am. Midl. Nat., 28, 245–267.

Schoenle, L.A., Downs, C.J. & Martin, L.B. (2018). An Introduction to Ecoimmunology. In: Advances in Comparative Immunology (ed. Cooper, E.L.). Springer International Publishing AG, Cham, Switzerland, pp. 901–932.

Simonis, M.C., Crow, R.A. & Rúa, M.A. (2018). Case study: methods and observations of overwintering Eptesicus fuscus with White-nose Syndrome in Ohio, USA. J. Wildl. Rehabil., 38, 11–16.

Speakman, J., Webb, P. & Racey, P. (1991). Effects of Disturbance on the Energy Expenditure of Hibernating Bats. J. Appl. Ecol., 28, 1087–1104.

Speakman, J.R. & Thomas, T. (2003). Physiological Ecology and Energetic of Bats. In: Bat Ecology (eds. Kunz, T.H. & Fenton, M.B.). The University of Chicago Press, pp. 430–490.

Swanson, G. & Evans, C. (1936). The Hibernation of Certain Bats in Southern Minnesota. J. Mammal., 17, 39–43.

Szewczak, J.M. & Jackson, D.C. (1992a). Acid-base state and intermittent breathing in the torpid bat, Eptesicus fuscus. Respir. Physiol., 88, 205–215.

Szewczak, J.M. & Jackson, D.C. (1992b). Ventilatory response to hypoxia and hypercapnia in the torpid bat, Eptesicus fuscus. Respir. Physiol., 88, 217–32.

Turner, G.G., Meteyer, C.U., Barton, H., Gumbs, J.F., Reeder, D.M., Overton, B., et al. (2014). Nonlethal Screening of Bat-Wing Skin With the Use of Ultraviolet Fluorescence To Detect Lesions Indicative of White-Nose Syndrome. J. Wildl. Dis., 50, 566–573.

Turner, G.G., Reeder, D. & Coleman, J.T.H. (2011). A Five-year Assessment of Mortality and Geographic Spread of White-Nose Syndrome in North American Bats, with a look to the future. Bat Res. News, 52, 13–27.

Verant, M.L., Boyles, J.G., Waldrep, W., Wibbelt, G. & Blehert, D.S. (2012). Temperature-Dependent Growth of *Geomyces destructans*, the Fungus That Causes Bat White-Nose Syndrome. PLoS One, 7, e46280.

Verant, M.L., Meteyer, C.U., Speakman, J.R., Cryan, P.M., Lorch, J.M. & Blehert, D.S. (2014). White-nose syndrome initiates a cascade of physiologic disturbances in the hibernating bat host. BCM Physiol., 14.

Willis, C.K.., Lane, J.E., Liknes, E.T., Swanson, D.L. & Brigham, R.M. (2005). Thermal energetics of female big brown bats (*Eptesicus fuscus*). Can. J. Zool., 83, 871–879.

Willis, J. (1971). Tissue K concentration in relation to the role of the kidney in hibernation and the cause of periodic arousal. Comp. Biochem. Physiol. - A Comp. Physiol., 39, 437–445.

CHAPTER 4

CAPTURE RATES OF *EPTESICUS FUSCUS* INCREASE FOLLOWING FUNGAL PATHOGEN INVASION ACROSS THE EASTERN US

ABSTRACT

Emerging infectious diseases threaten biodiversity globally. While the effects of infectious diseases on highly susceptible species often receive considerable attention, effects of less susceptible hosts are less frequently studied despite their biological importance. To understand how populations of less susceptible hosts and their population structures change in the face of disease, I quantified changes to capture rates of *Eptesicus fuscus* (big brown bats), a species less susceptible to the introduced fungal pathogen *Pseudogymnoascus destructans* (*Pd*; causative agent for white-nose syndrome) across the eastern US. I hypothesized that capture rates of adult male and female *E. fuscus* would increase over time since *Pd* invasion due to a release from interspecific competition from highly susceptible species. I also hypothesized increases to the capture rates of *E. fuscus* would be greater in northern latitudes compared to southern latitudes, mirroring spatial gradients for highly susceptible species mortalities. Using 30 years of capture records, I created Bayesian generalized linear models to determine how the capture rates of adult *E. fuscus* (male and female) or of reproductive bats (females only) changed across the eastern US from pre-*Pd* invasion years through *Pd* invasion, epidemic and established years. Overall, capture rates of male and female *E. fuscus* increased from pre-invasion to established years, with greater increases to the capture rates of females than males.

Further, capture rates of lactating and post-lactating female bats increased with latitude by established years. Taken together, results suggest that 1) *E. fuscus* have undergone a release from competition from highly susceptible species, and 2) increases in the capture rates of lactating and post-lactating female *E. fuscus* with latitude may create spatial gradients for intraspecific pressures due to their greater need for food compared to other *E. fuscus* demographics. Therefore, *E. fuscus* likely undergo a combination of ecological and pathogen pressures following pathogen introduction. This work highlights the importance of understanding how less susceptible host populations and structures change with long-term pathogen exposure across a broad spatial scale. Understanding the persistence of less susceptible wildlife hosts is critical for predicting future host populations and their structures under continued threats of emerging infectious disease.

INTRODUCTION

Introduced pathogens and emerging infectious diseases are currently one of the largest threats to biodiversity and wildlife populations (Daszak *et al.* 2000; Gurevitch & Padilla 2004; Young *et al.* 2017), decimating wildlife populations at alarming rates (Dhondt *et al.* 1998; Hochachka & Dhondt 2000; Yaremych *et al.* 2004; Voyles *et al.* 2009; Cheng *et al.* 2019, 2021). Furthermore, decreases to biodiversity and wildlife populations can exacerbate the prevalence of emerging infectious diseases on the landscape due to a dilution effect (Civitello *et al.* 2015). Major biodiversity losses from emerging infectious diseases are typically due to high mortality rates and population declines from species highly susceptible to pathogen infections (Hochachka & Dhondt 2000; Skerratt *et al.* 2007; Frick *et al.* 2015). As biodiversity decreases from devastating population losses of highly susceptible species, how an emerging infectious disease maintains itself on the landscape becomes dependent upon host species populations that persist despite infections (Holt & Dobson 2006). Therefore, as pathogens devastate populations of species that are highly susceptible to infection, persisting host populations less susceptible to infection become greater contributors to diversity and thus, critical contributors to community, population, and ecosystems dynamics (Gervasi *et al.* 2015; VanderWaal & Ezenwa 2016; Cortez *et al.* 2017). Evaluating changes to the abundance of persisting host species is critical for understanding current and future dynamics of introduced pathogens.

Once an introduced pathogen becomes established, the abundance of less susceptible hosts can respond in one of three ways (Fig. 4.1). First, the abundance of less susceptible hosts can decrease due to pathogen infection. Despite their status as a less susceptible species, decreases to the abundance of less susceptible hosts could still occur, just slower than species highly susceptible to infection over time, simply because their rate of infection is lower (Moore et al. 2018; Cheng et al. 2021; Fig. 4.1). This lower rate of infection for less susceptible host species can mean that decreases to their abundance can go unnoticed and/or are of least concern because their losses in abundance are less than that of highly susceptible species. Another way the abundance of less susceptible hosts may decrease following disease emergence could be due to increased predation (Fig. 4.1). Since infection rates often correlate with mortality rates, less susceptible hosts may become the only available prey to predators after the extinction of highly susceptible hosts; therefore, less susceptible hosts may increase in frequency as a prey item and their populations would decline, as suggested by the prey-switching hypothesis (Kiørboe *et al.* 1996; Kjellander & Nordström 2003; Siddon & Witman 2004; Moleón *et al.* 2009; Murdoch 2014). Secondly, the abundance of less susceptible hosts can increase due to the emergence of an introduced pathogen (Fig. 4.1). Because less susceptible hosts often have lower mortality rates compared to highly susceptible species, a release from competition with highly susceptible species could increase the abundance of less susceptible hosts, as theoretically suggested from the Lotka-Volterra competition model (Gotelli 2008; Fig. 4.1). Further, if less susceptible hosts are able to expand their niche space following a release from competition, their abundance may be able to increase in greater numbers than what occurs from competitive release alone (Wilson 1961;

MacArthur et al. 1972; Herrmann et al. 2021; Fig. 1). Third, the abundance of less susceptible hosts could not change with the introduction of a pathogen. This could be due to minimal mortalities associated with pathogen infections, or a balance of decreases and increases in abundance. For example, the abundance of less susceptible hosts may initially decrease due to pathogen infection early in disease emergence time, but subsequently rebound due to increases in the amount of resources available once highly susceptible competitors die. Alternatively, if less susceptible host populations initially increase and expand their niche space, they may experience increases to predation since they are the only prey item left on the landscape which would in turn, level out the abundance over time. Consequently, even though the dynamics of less susceptible host species are rarely studied or only studied in context with highly susceptible species (Frick *et al.* 2015; Russell *et al.* 2019; Cheng *et al.* 2021), understanding their responses is important for predicting future pathogen dynamics and population structures.

Emerging infectious diseases can also drive changes to population structures by directly altering sex ratios and/or the number of reproductive hosts within a population. For example, when female survival is greater than male survival, host populations can become female-biased. This has been documented for multiple frog species infected with *Batrachochytrium dendrobatidis* and for *Apis mellifera* (honey bees) infected with *Nosema ceranae* parasites for which female survival is greater than male survival in inoculation experiments (Retschnig *et al.* 2014; Russell *et al.* 2019). This can possibly lead to fewer males than females in the wild and become problematic because when female-biased sex ratios become extreme (greater than 90%), female fecundity decreases (Milner-Gulland *et al.* 2003; Dyson & Hurst 2004; J. Rankin & Kokko 2007), possibly

due to fewer available mates for females. On the other hand, non-extreme female-biased populations can theoretically provide optimal population growth (Vlad 1989), which would be helpful following mortality from disease emergence. Pathogen infections can also alter sex ratios through changes in host reproduction. For example, female *Sarcophilus harrisii* (Tasmanian devils) with devil facial tumor disease give birth to more females than males when infected and thus, may have more female-biased future populations (Jones *et al.* 2008b). The number of hosts that reproduce within a population can also change in response to pathogen infections. Decreases to the age of first reproduction under pathogen infections would increase the abundance of reproductive females, as seen in *S. harrisii* with devil facial tumor disease and *Myotis lucifugus* (little brown bats) with white-nose syndrome (Jones *et al.* 2008b; Ineson 2020). After disease emergence, the number of breeding one-year-old *S. harrissii* increased by 13% - 83%, and the reproductive rates of *M. lucifugus* in their first year increased 40% (Jones *et al.* 2008b; Ineson 2020). Depending on how pathogen infections and emerging infectious diseases alter the balance of sex ratios and reproductive demographics, as pathogen exposure and infections become chronic, population recovery could become increasingly challenging.

North American bat populations are currently threatened by *Pseudogymnoascus destructans* (*Pd*), an introduced and invasive fungal pathogen from Eurasia that causes the symptoms manifesting as white-nose syndrome (Blehert *et al.* 2009; Lorch *et al.* 2011; Leopardi *et al.* 2015; Drees *et al.* 2017). *Pd* was first introduced and detected in New York, USA, in 2006 and has since spread across North America (Blehert *et al.* 2009; White Nose Syndrome Response Team 2022). *Pd* infects wings and muzzles of

hibernating North American bats which disrupts their ability to torpor (Meteyer *et al.* 2009). Under *Pd* infections, bats have increased torpor arousals, increased torpid energy expenditures and decreased torpor bouts, all of which deplete their fat stores faster than without infection during hibernation (Reeder *et al.* 2012; McGuire *et al.* 2017; Moore *et al.* 2018). This has resulted in mortality rates in the eastern US of more than 90% in species that are highly susceptible to infection. (Frick *et al.* 2010b, 2015; Cheng *et al.* 2021). For the small portion of bats that do survive winter infections and emerge from hibernation in the spring, the additional energy required to heal winter infections is suggested to decrease reproductive success as females typically become pregnant within a few days following emergence (Wimsatt 1945; Meierhofer *et al.* 2018; Fuller *et al.* 2020). Therefore, the impacts of *Pd* on North American bat populations are not only dependent upon winter exposure and infections, but also dependent upon how winter infections impact the reproductive success of persisting hosts outside of hibernating months. While bats leave hibernacula in the spring and heal infections, *Pd* remains in hibernacula throughout the year, setting up repeated annual exposure and infections for hosts that survive.

In the *Pd* / hibernating bat system, host survival and persistence are impacted by how *Pd* interacts with its bat hosts and its environment at different locations over time. In *Pd*'s native range throughout Eurasia, where *Pd* and hibernating bats have coevolved together (Wibbelt *et al.* 2010; Puechmaille *et al.* 2011; Hoyt *et al.* 2016; Drees *et al.* 2017), *Pd* decays in summer months within hibernacula (Hoyt *et al.* 2020). Therefore, when bats re-enter hibernacula in the winter, the prevalence of *Pd* within the hibernacula has decreased since they left hibernacula in the spring. This leads to reduced host

infection intensity throughout hibernation, and thus increased chances of survival (Hoyt 2020). In contrast, in North America where *Pd* is invasive, *Pd* prevalence is stable in hibernacula throughout summer months (Hoyt *et al.* 2020). Its overall prevalence within hibernacula in North America is also greater throughout the year than in its native range (Hoyt *et al.* 2020). Coupled together, this causes hibernating bats in *Pd*'s invasive range to have earlier onsets of host infection when bats enter the hibernacula in winter, bats to incur greater infection intensities throughout hibernation and thus, suffer greater mortalities from infection compared to hosts in *Pd*'s native range (Hoyt 2020). The prevalence of *Pd* in the environment and on hosts is undoubtedly important for understanding how overall bat populations respond to infections globally over time and space. However, this work examines multiple species in *Pd*'s invasive range their responses together. To fully understand the role *Pd* plays in altering bat populations in its invasive range, North American bats that are less susceptible to *Pd* infections may provide greater insights into future pathogen dynamics and host population structures compared to highly susceptible species.

Eptesicus fuscus (big brown bats) are a North American bat species considered less susceptible to *Pd* infections compared to highly susceptible species and have some degree of resistance to infection (Frank *et al.* 2014; Moore *et al.* 2018). As such, *E. fuscus* maintains lower *Pd* prevalence, infection rates and infection intensities compared to highly susceptible species during hibernation (Langwig *et al.* 2015; Frick *et al.* 2017; Moore *et al.* 2018). This lowered susceptibility and resistance to *Pd* causes *E. fuscus* to have pathogen prevalence and intensities throughout hibernation that are closer to, and possibly over time more reflective of, hibernating bat species in *Pd*'s native range, when

compared to North American bats that are highly susceptible to *Pd* infection (Hoyt *et al.* 2016, 2020). Therefore, to understand the full extent of *Pd* impacts on North American bat populations over time, more knowledge into how less susceptible, resistant *E. fuscus* populations are changing is critical.

How the abundance and population structures of *E. fuscus* change in the face of *Pd* are unclear. Estimates for winter populations of *E. fuscus* in the eastern US indicate 35-41% declines since the introduction of *Pd* (Turner *et al.* 2011; Cheng *et al.* 2021). However, because *E. fuscus* are known to frequently move hibernacula in winter and/or hibernate in man-made structures that are not regularly surveyed (Swanson & Evans 1936; Rysgaard 1942; Whitaker & Gummer 1992, 2000; Boyles *et al.* 2007; Mills *et al.* 2019), estimates for how their populations change due to *Pd* may not be best represented through winter hibernacula surveys. Further, winter hibernacula surveys are not able to account for changes in the abundance of female reproductive demographics, which is important for estimating the future success of persisting populations. Therefore, capture surveys outside of winter months may provide better estimates for *E. fuscus* populations before and after pathogen invasion. Contrary to estimates for winter *E. fuscus* declines, multiple sites in the eastern and midwestern US have seen increases following *Pd* introduction and invasion to *E. fuscus* capture rates in spring through fall months (Francl *et al.* 2012; Pettit & O'Keefe 2017; O'Keefe *et al.* 2019). Further, it's been suggested that these increases in captures may reflect increases to intraspecific pressures for *E. fuscus* (see Chapter 2).

Eptesicus fuscus also have variable responses for changes to population structures following *Pd* introduction. Post-lactating female *E. fuscus* captures increase after *Pd*

introduction in Appalachia US (O'Keefe *et al.* 2019), and non-reproductive female bat capture rates increase in the midwestern US (Pettit & O'Keefe 2017), suggesting decreases to reproductive success. Alternatively, the capture rates of reproductive *E. fuscus* did not change between pre- and post-*Pd* in West Virginia, US, and suggests that reproductive success is not impacted by annual pathogen infections (Francl *et al.* 2012). Taken together, there are uncertainties for how *E. fuscus* populations are broadly impacted and structured due to *Pd* invasion, despite their greater potential to inform how pathogen dynamics and population structures may be shaped over time under pathogen pressures compared to highly susceptible species. Therefore, in order to understand how *E. fuscus* populations are responding and persisting under long-term *Pd* exposure, we need to examine broad spatial patterns for changes in their abundance before and after *Pd* invasion.

To determine how the abundance of *E. fuscus* changes across a broad spatial scale and over time since pathogen introduction, I quantified changes to capture rates (as a proxy for abundance) using a 30-year dataset of individual *E. fuscus* captures in spring through fall months across the eastern US (see Chapter 2). I hypothesized that the capture rates of adult male and female *E. fuscus* would increase over time since *Pd* invasion due to a release from interspecific competition from highly susceptible species. Further, I hypothesized that increases in the capture rates of adult *E. fuscus* after *Pd* introduction would become greater as latitude increased, following spatial patterns for suggested increases to intraspecific competitive pressures with increasing latitude in the eastern US (see Chapter 2). Here, I highlight the importance of understanding how pathogen introductions change the abundance of a less susceptible species and alter their

population structures as pathogen exposure time increases across space. Understanding how the abundance of less susceptible species changes with pathogen exposure is an important step toward better evaluating future host population structures and host-pathogen dynamics at a broad scale.

METHODS

I used a large dataset of adult *E. fuscus* capture records spanning 30 years across 11 US states (GA, IL, IN, KY, MS, NY, NC, OH, PA, TN and VA) as described in Chapter 2. Briefly, this dataset consists of 24,129 adult *E. fuscus* (females n = 14,162; males n = 9,967) captured across 3,797 sites outside of hibernating months in April through October from 1990 to 2020. Variables within the dataset used for this paper were date of capture, masked capture site name, county latitude centroid of capture site, sex (male/female) and reproductive status (females only: non-reproductive/pregnant/lactating/post-lactating).

The number of captures per site per year was used as a proxy for adult bat abundance. To obtain this proxy, I summarized individual capture records for adult *E. fuscus* within the dataset by the number of individuals captured per site within each state and county of capture, year of capture, sex and reproductive status using the package *dplyr* in R (R Core Team 2021; Wickham *et al.* 2021). To determine how time since *Pd* invasion changed the capture rates of adult *E. fuscus* by sex and reproductive status (female only) across space, I used a full dataset to compare female and male capture rates and a female-only dataset to compare changes in capture rates by reproductive demographics. Analyses only considered reproductive status for female *E. fuscus* because females move through reproductive life stages in spring through fall months which coincides with the collection of the capture records used here, while male reproduction does not occur until fall or winter which is outside the collection period of this data.

Finally, for the separate adult and female-only *E. fuscus* datasets, I standardized *Pd* invasion across each state and year of capture by classifying them into *Pd* exposure time-steps (see Chapter 2; White Nose Syndrome Response Team 2022). Pre-invasion years were those before suspect or confirmed *Pd* introduction (< 0 years), invasion years occurred 0-1 years within *Pd* introduction, epidemic years were designated as those 2-4 years following *Pd* introduction, and established years occurred 5+ years after the introduction of *Pd*.

Statistical Analyses

I completed all statistical analyses in R version 4.0.5 and data visualizations were made using the packages *ggplot2*, *tidybayes*, and *patchwork* (Wickham 2009b; Kay 2020; Pedersen 2020). To determine how *E. fuscus* capture rates changed across the eastern US over invasion time-steps, I used a two-step modelling approach with Bayesian statistics (Fig. S1). I created separate Bayesian generalized linear mixed models for all adult (males and females combined) *E. fuscus* and only female *E. fuscus* at both model creation steps. All models were created using the STAN computational framework R interface (*rstan* package) with the brm function in the *brms* package (Bürkner 2017; Stan Development Team 2020).

Initial models were created to describe how the capture rates of *E. fuscus* sex or female reproductive statuses changed with latitude over disease time-steps (Appendix C Fig. S4.1). I created Bayesian generalized linear mixed models with Poisson distributions for bat capture rates. To determine how adult *E. fuscus* capture rates changed by sex with latitude and *Pd* exposure time-steps, I created an initial model for adult (males and females combined) bat capture rates as a function of a conditional effects interaction for

sex, latitude of capture county centroid and *Pd* exposure time-steps (Appendix C Fig. S4.1A). To determine how female *E. fuscus* capture rates changed by reproductive status due to latitude and *Pd* exposure time-steps, I created an initial model for the capture rates of female bats as a function of a conditional effects interaction for latitude of capture county centroid, *Pd* exposure time-steps and reproductive status (Appendix C Fig. S4.1B). I included capture site as a group level effect in these initial models to account for varying effort in site visits (Appendix C Fig. S4.1).

I determined a prior distribution for adult and female-only models separately using the function get_prior in the *brms* package (Bürkner 2017). Prior distributions for both initial adult and female-only models were the same and set on a student-t distribution with a mean of 0.7, a standard deviation of 2.5 and degrees of freedom at 3. Both adult and initial female-only models were each run on four Markov chains at 10,000 iterations with a burn-in period of 5,000 iterations. Both adult and female-only models converged with $\hat{R}$ values at 1.00 or 1.01 and resulted in 160,000 posterior samples for adult models and 320,000 posterior samples for female-only models. The larger posterior samples for the adult model compared to the female-only model reflects the number of levels within the conditional effects interaction. Specifically, in the adult model (Appendix C Figure S4.1A), sex has two levels (male/female) while in the female-only model (Appendix C Figure S4.1B), reproductive status has four levels (non-reproductive/pregnant/lactating/post-lactating). Thus, posterior samples for female-only models were doubled to include posterior values for the four levels within the reproductive status variable, as opposed to the two levels within the sex variable in adult models. Finally, in order to determine how *Pd* exposure time-steps altered *E. fuscus*

abundance across space, I calculated the slopes for abundance across latitude for each time-step by sex for adult models (Figure S1A) or reproductive status for female models (Appendix C Figure S4.1B) using the emtrends function in the *emmeans* package (Lenth 2021).

Initial models for both adults (Appendix C Figure S4.1A: Model 1) and females-only (Figure S1B: Model 1) indicated a spatial threshold at 36.3 °N where the interaction of capture county centroid latitude, *Pd* exposure time-steps and sex (adult model, Appendix C Figure S4.1A) or reproductive status (female-only model, Appendix C Figure S4.1B) occurred (Appendix C Fig. S4.2). Therefore, I created a second model for adults or females-only to better understand how capture rates changed above and below the identified spatial threshold over *Pd* exposure time-steps. To do so, I created a latitudinal category variable within the full adult and female-only datasets for 'north' and 'south' of 36.3 °N. The second Bayesian generalized linear mixed models were then created in the same way as initial models, but I replaced county centroid latitude with the newly created latitudinal category variable for 'north' and 'south' of the identified spatial threshold (Appendix C Fig. S4.1: Model 2). Like in initial models, capture site was used as a group level effect for both adult and female-only models (Appendix C Fig. S4.1: Model 2).

The second adult and female-only model prior distributions were also determined by the function get_prior in the *brms* package (Bürkner 2017). Both models were set on the same distribution as first set of models: a student-t distribution with a mean of 0.7, a standard deviation of 2.5 and degrees of freedom at 3. Like initial models, the second adult and female-only models were each run on four Markov chains at 10,000 iterations

with a burn-in period of 5,000 iterations. Adult and female-only models converged with $\hat{R}$ values at 1.00 or 1.01 and resulted in 320,000 posterior samples for adults and 640,000 posterior samples for females. The larger posterior samples for the second model compared to the first model reflects the replacement of the continuous variable for county centroid latitude for the categorical variable with levels for 'north' and 'south' of the spatial thresholds. Thus, posterior samples doubled to include posterior values for both levels.

To understand how the capture rates of adult *E. fuscus* changed by sex (Appendix C Figure S4.1A) and how the capture rates of female *E. fuscus* changed by reproductive status (Appendix C Figure S4.1B) over invasion time-steps and latitudinal category, I extracted posterior means and credible intervals using emmeans function in the package *emmeans* (Lenth 2021), and made comparisons for *Pd* exposure time-steps and latitudinal category. For these models (Appendix C Figure S4.1: Model 2), I compared posterior means and credible intervals in four ways. First, I compared *E. fuscus* capture rates across each *Pd* time-step. Second, I compared *E. fuscus* capture rates at each individual time-step to the capture rates of *E. fuscus* in each latitudinal category separately (northern or southern populations) within the same time-step. Third, I compared the capture rates of *E. fuscus* between northern and southern populations within each *Pd* time-step. Finally, I compared the capture rates of *E. fuscus* within each latitudinal category (northern or southern populations) across *Pd* time-steps. All comparisons in adult models were grouped by sex and all comparisons in female-only models were grouped by reproductive status.

RESULTS

Changes to adult E. fuscus capture rates by sex

Changes in the capture rates of adult *E. fuscus* varied across a spatial threshold at 36.3 °N over *Pd* exposure time-steps and depended on sex [mean (95% credible intervals): R^2 = 0.36 (0.34, 0.37); Appendix C Fig. S4.2A]. The capture rates of adult female bats were stable with increasing latitude in pre-invasion years, increased in invasion years, but was stable again with latitude in epidemic and establishment years (Appendix C Fig. S4.2A). The capture rates of adult male *E. fuscus* increased with increasing latitude in pre-invasion and invasion years, was stable with latitude in epidemic years, but increased again with latitude by *Pd* establishment (Appendix C Fig. S4.2A).

The capture rates of adult *E. fuscus* varied north to south of 39.3 °N by sex over *Pd* exposure time-steps [R^2 = 0.35 (0.34, 0.37); Fig. 4.2]. However, the capture rates of male *E. fuscus* only differed between northern and southern latitudes in invasion years such that, the capture rates of northern male bats were about two times greater than southern male bats [invasion male north: 5.21 (4.45, 6.15), invasion male south: 2.85 (2.18, 3.69); Fig. 4.2B]. There were no other significant differences between northern and southern populations of *E. fuscus* for males or females; however, there were significant differences in bat capture rates over invasion time-steps. Overall, the capture rates of bats increased from pre-invasion to established years [pre-invasion: 3.91 (3.44, 4.48), established: 6.13 (5.51, 6.77)], and this pattern held for both sexes [pre-invasion female:

4.42 (3.76, 5.14), established female: 7.77 (6.89, 8.70); pre-invasion male: 3.47 (2.95, 4.08), established male: 4.83 (4.27, 5.45); Fig. 4.2A, 4.2D]. The capture rates of female *E. fuscus* increased during invasion years [invasion: 5.59 (4.96, 6.34), invasion female: 8.11 (7.06, 9.32); Fig. 4.2B], but the capture rates of male or female *E. fuscus* was never different than the average capture rates for each individual time-step at any other time (Fig. 4.2A, 4.2C, 4.2D).

While the capture rates of all *E. fuscus* increased from pre-invasion to establishment years, the capture rates of female *E. fuscus* increased more than the capture rates of male *E. fuscus* by *Pd* exposure time-steps (Fig. 4.2). In pre-invasion years, the capture rates of male and female *E. fuscus* were not significantly different from one another [pre-invasion female: 4.42 (3.76, 5.14), pre-invasion male: 3.47 (2.95, 4.08); Fig. 4.2A]. However, by *Pd* establishment, the capture rates of female *E. fuscus* were greater than the capture rates of male *E. fuscus* by three bats per site per year [established female: 7.77 (6.89, 8.70), established male: 4.83 (4.27, 5.45); Fig. 4.2D].

Changes to female E. fuscus capture rates by reproductive status

Changes to female *E. fuscus* capture rates varied across a spatial threshold at 36.3 °N over *Pd* exposure time-steps and depended on reproductive status [R^2 = 0.44 (0.41, 0.47); Appendix C Fig. S4.2B]. While the capture rates of non-reproductive female bats were stable with latitude in pre-invasion years, they decreased with latitude during invasion, epidemic and establishment years (Appendix C Fig. S4.2B). The capture rates of pregnant *E. fuscus* decreased with latitude in pre-invasion years, stabilized in invasion years, but decreased with latitude in epidemic and establishment years (Appendix C Fig. S4.2B). The capture rates of lactating bats increased with latitude in pre-invasion years,

stabilized in invasion and epidemic years, but increased with latitude during *Pd* establishment (Appendix C Fig. S4.2B). Finally, the capture rates of post-lactating bats were stable with increasing latitude in pre-invasion years, but increased with latitude during invasion, epidemic and establishment years (Appendix C Fig. S4.2B).

The capture rates of female *E. fuscus* varied north and south of the latitudinal threshold by *Pd* exposure time-steps and reproductive status [R^2 = 0.47 (0.44, 0.49); Fig. 4.3]. The capture rates of non-reproductive female bats did not change significantly across *Pd* time-steps (Fig 4.3A-4.3D), but there were distinctive shifts between the capture rates of northern and southern non-reproductive female bats. Specifically, the capture rates of non-reproductive female *E. fuscus* was not different in the north or south in pre-invasion years, but northern capture rates were less than southern capture rates during invasion, epidemic and establishment years [non-reproductive invasion north: 1.19 (0.83, 1.73), non-reproductive invasion south: 2.84 (1.75, 4.55); non-reproductive epidemic north: 0.85 (0.64, 1.12), non-reproductive epidemic south: 2.17 (1.49, 3.13); and non-reproductive established north: 1.28 (0.96, 1.70), non-reproductive established south: 2.87 (1.98, 4.22); Fig. 4.3B-4.3D].

Pregnant bat capture rates more than doubled from pre-invasion to established years [pregnant pre-invasion: 2.97 (2.02, 4.37), pregnant established: 6.83 (5.33, 8.78); Fig. 4.3E, 4.3H], and the capture rates of pregnant bats also shifted north to south across *Pd* time-steps (Fig. 4.3E-4.3H). The capture rates of pregnant *E. fuscus* was not significantly different between northern and southern latitudes in pre-invasion, invasion and establishment years (Fig. 4.3E, 4.3F, 4.3H), but was less in the north compared to the

south in epidemic years [pregnant epidemic north: 2.86 (2.13, 3.92), pregnant epidemic south: 8.73 (6.42, 11.98); (Fig. 4.3G)].

The capture rates of lactating bats increased by four bats per site per year from pre-invasion years to *Pd* establishment [lactating pre-invasion: 7.06 (5.41, 9.20), lactating established: 11.27 (9.44, 13.59); Fig. 4.3I, 4.3L]. The capture rates of lactating bats were greater in the north than the south in pre-invasion years [lactating pre-invasion north: 10.82 (7.13, 16.46), lactating pre-invasion south: 4.60 (3.35, 6.49); Fig. 4.3I], but was not significantly different in any other *Pd* time-step (Fig. 4.3J-4.3L).

Capture rates of post-lactating bats had the largest increases across *Pd* exposure time-steps. Capture rates of post-lactating bats more than doubled from pre-invasion to invasion years [post-lactating pre-invasion: 4.49 (3.44, 5.79), post-lactating invasion: 10.68 (8.51, 13.29); Fig. 4.3M-4.3N], and almost tripled by *Pd* establishment [post-lactating established: 11.70 (9.58, 14.26); Fig. 4.3P]. The capture rates of post-lactating *E. fuscus* were indistinguishable between northern and southern latitudes in pre-invasion and invasion years (Fig. 4.3M-4.3N**)**, but were greater in northern latitudes than southern latitudes in epidemic years [post-lactating epidemic north: 10.39 (8.78, 12.36), post-lactating epidemic south: 3.94 (2.82, 5.44); Fig. 4.3O]. Further, capture rates of northern post-lactating bats were greater than the posterior mean in epidemic years [post-lactating epidemic: 6.40 (5.27, 7.69), post-lactating epidemic north: 10.39 (8.78, 12.36); Fig. 4.3O]. However, the significant differences between northern and southern post-lactating bats and northern post-lactating bats and the posterior mean disappeared by *Pd* establishment (Fig. 4.3P). Finally, the capture rates of northern and southern post-lactating bats both increased from pre-invasion to establishment years, but increased

more in the north than the south [post-lactating north pre-invasion: 4.70 (3.04, 7.05), post-lactating north established: 15.38 (12.45, 18.99); post-lactating south pre-invasion: 4.29 (3.11, 5.79), post-lactating south established: 8.90 (6.36, 12.52); Fig. 4.3M, 4.3P].

When latitude was used as a continuous variable, capture rates of pregnant bats significantly decreased with increasing latitude, and capture rates of lactating and post-lactating bats significantly increased with latitude in established years. However, when using a latitudinal category, the differences in capture rates between northern and southern reproductive bats were not statistically distinguishable. Instead, capture rates of northern and southern reproductive bats were different within smaller, but notable, credible intervals. The capture rates of northern pregnant *E. fuscus* were less than southern pregnant *E. fuscus* in established years within an 85% credible interval [mean (85% credible intervals): pregnant established north: 5.14 (4.21, 6.28), pregnant established south: 9.09 (6.62, 12.36); Fig. 4.3H]. In contrast, the capture rates of northern lactating bats were greater than the capture rates of southern lactating bats in established years within an 80% credible interval [mean (80% credible intervals): lactating established north: 13.27 (11.76, 15.13), lactating established south: 9.57 (7.81, 11.71); Fig. 4.3L]. Finally, the capture rates of northern post-lactating *E. fuscus* were greater than southern post-lactating *E. fuscus* in established years within a 90% credible interval [mean (90% credible intervals): post-lactating established north: 15.40 (13.39, 17.63), post-lactating established south: 8.90 (7.12, 11.08); Fig. 4.3P].

DISCUSSION

Over 250 species are extinct or critically endangered due to emerging infectious diseases, with even more species populations in danger from disease in combination with other threats(Smith *et al.* 2006; Pedersen *et al.* 2007; Heard *et al.* 2013). Wildlife mortalities induced by introduced pathogens change species diversity such that, as species highly susceptible to infection become more rare, less susceptible species become proportionally more common (Francl *et al.* 2012; Frick *et al.* 2015; Cortez *et al.* 2017; Pettit & O'Keefe 2017; O'Keefe *et al.* 2019; Simonis *et al.* 2020). However, even though less susceptible species become more common, their populations are also likely changing due to chronic pathogen exposure. Here, the overall capture rates of adult *E. fuscus*, a species less susceptible to the fungal pathogen that causes white-nose syndrome, increased from pre-invasion to *Pd* establishment years across the eastern US (Fig. 4.2. Increases to the capture rates of female bats were greater than increases in the capture rates of male bats (Fig. 4.2). There were also increases to lactating and post-lactating female *E. fuscus* capture rates with increasing latitude (Fig. 4.3L, 4.3P, Appendix C S4.3B). These results provide a crucial first step to understanding the changes in the intraspecific population structure of less susceptible hosts across a broad spatial scale following pathogen invasion and potentially inform predictions for how other persisting host populations will be impacted in the future.

I found increases in the capture rates of a species less susceptible to infection (*E. fuscus*) across the eastern US after a pathogen (*Pd*) invaded the landscape, possibly due

to competitive release. In the wake of high mortality due to an introduced pathogen, less susceptible species may undergo an ecological release from competition from highly susceptible species, leading to an increase in their abundance. Competitive release can occur when a species that overlaps niche space with another species is removed; the species that remains exploits more of that niche space and in turn, increases their abundance within that niche space (Wilson 1961). Competitive release is supported throughout the plant and animal kingdom (Wilson 1961; Trewby *et al.* 2008; Bolnick *et al.* 2010; Püttker *et al.* 2019), and across larger geographical scales (Anderson *et al.* 2002). However, the degree to which less susceptible species are released from competition following the introduction of a pathogen which drives highly susceptible species near extinction is unclear. In the *Pd* system, there are several highly susceptible species whose mortality rates and population declines from *Pd* are above 90% including *M. lucifugus*, *Myotis septentrionalis* (Northern long-eared bat) and *Perimyotis subflavus* (tri-colored bat) (Frick *et al.* 2010a, 2015; Ingersoll *et al.* 2013; Cheng *et al.* 2021). These species coexist with *E. fuscus* and overlap their range in the eastern US. Therefore, I predict such high mortality rates in species which share similar niche space as *E. fuscus* have resulted in an ecological release from competition for *E. fuscus* in spring through fall months.

Competitive release can also lead to increases in intraspecific competition (Chesson 2000; Francl *et al.* 2012; Jachowski *et al.* 2014; Pettit & O'Keefe 2017). This could eventually lead to decreases in the abundance of less susceptible species because competitive pressures for intraspecific competition are theoretically greater than for interspecific competition according to the Lotka-Volterra competition model (Gotelli

2008). For *E. fuscus*, this would suggest that the competition for food between *E. fuscus* is greater than the competition for food between *E. fuscus* and highly susceptible species when they are active in spring through fall months. Capture rates of adult *E. fuscus* increased from pre-invasion to established years, suggesting increases in their overall abundance. While capture rates of adult *E. fuscus* did not differ north to south, capture rates of lactating and post-lactating female bats increased with latitude in establishment years (Appendix C Fig. S4.2B) and their capture rates were higher in northern latitudes compared to southern latitudes within 80% and 90% credible intervals (Fig. 4.3L, 4.3P). Higher capture rates for lactating and post-lactating female *E. fuscus* in the north compared to the south could drive latitudinal gradients for intraspecific pressures on their own. This is due to their increased need for insect prey compared to males and other female reproductive stages. Lactating bats must consume their body weight in insects each night to survive and account for additional energy needed to produce milk to feed pups when food is limited, whereas males and non-reproductive and pregnant female bats may only eat about a third of their body weight (Gould 1955; Kurta *et al.* 1990; Grinevitch *et al.* 1995; Menzel *et al.* 2020). Even still, lactating *E. fuscus* lose about 14% of their body mass (Burnett & Kunz 1982), so post-lactating bats must also increase food intake to gain back mass and fat stores prior to winter hibernation (Richardson *et al.* 2018). Body mass for all male and female reproductive stages of *E. fuscus* progressively decreased with increasing latitude by *Pd* exposure time-steps, supporting increased pressures from intraspecific competition with increasing latitude following *Pd* introduction (see Chapter 2). Therefore, changes to *E. fuscus* body mass following *Pd*

introduction could reflect consequences of intraspecific competitive pressures increasing with latitude led by increases to the capture rates of lactating and post-lactating *E. fuscus*.

While overall adult *E. fuscus* capture rates increased from pre-invasion to establishment years, male:female sex ratios decreased over *Pd* exposure time-steps because increases to female capture rates outpaced associated increases in male capture rates. In pre-invasion years, the capture rates of male and female bats per site per year was indistinguishable (Fig. 4.2A). However, by *Pd* establishment, male bat capture rates were 23% lower on average than female bat capture rates, with the difference between the capture rates of male and female bats in the eastern US being over 11,000 bats per year. There are two possible scenarios that would cause a decrease in male:female sex ratios following *Pd* introduction. First, female *E. fuscus* could facultatively adjust sex ratios of their offspring (Cameron 2004). This has been demonstrated in other species following the emergence of a pathogen. For example, female *Sarcophilus harrisii* (Tasmanian devils) infected with devil facial tumor disease have two times as many daughters as non-infected females, possibly due to changes in maternal condition (Lachish *et al.* 2009). Secondly, male bats, particularly those less than a year old, may not survive hibernation when also confronted with *Pd*. Male *E. fuscus* become sexually mature by their first hibernation following birth and mate with females from the fall throughout the winter (Christian 1956; Mumford 1958; Phillips 1966; Kurta & Baker 1990). The increased testosterone necessary to reproduce during this time may suppress innate immunity, which would be critical as a first line of defense against *Pd* infections for newly reproductive male *E. fuscus* going into their first *Pd* exposure in winter hibernacula (Duffy *et al.* 2000; Boonstra *et al.* 2001; Foo *et al.* 2017; Ruoss *et al.* 2019).

This is because they would not have acquired adaptive immune responses to *Pd* yet prior to their first entry into winter hibernacula where they are likely to be exposed to *Pd* since it persists in hibernacula in the absence of bats (Lorch *et al.* 2013). Further, because immune functioning is suppressed during hibernation (Burton & Reichman 1999), additional suppression of innate immune responses while male bats are active throughout winter months would keep them from intermittently fighting *Pd* infections and thus, decrease their chance for survival. Therefore, although the capture rates of male *E. fuscus* increased in spring through fall months from pre-invasion to established years, decreased chances for survival in winter months could keep them from having increasing capture rates as quickly as females. Further research, in this system and others, is needed to determine the mechanisms which underpin how the sex ratios of less susceptible species change with long-term *Pd* exposure.

The terminal investment hypothesis states that animals that reproduce multiple times in their lifespan should increase reproductive investment in the event that they are less likely to survive (Williams 1966). In many disease systems, the terminal investment hypothesis is supported via increases in the number of offspring produced and/or decreases in age of first reproduction (Bonneaud *et al.* 2004; Jones *et al.* 2008b; Lachish *et al.* 2009; Giehr *et al.* 2017; Ineson 2020). Overall capture rates of reproductive female *E. fuscus* (pregnant, lactating and post-lactating) increased in the eastern US from pre-invasion to establishment years (Fig. 4.2). It is possible these increases reflect decreases to the average age of first reproduction. While some female *E. fuscus* are able to reproduce in their first adult year, this is not the standard (Schowalter & Gunson 1979). However, annual *Pd* exposure over many years could increase the number of

reproductive one-year-old female *E. fuscus*. We see this in other bat species that are highly susceptible to *Pd* infections and white-nose syndrome. One-year-old *M. lucifigus*, which are highly susceptible to *Pd* infections and white-nose syndrome, increased yearling reproductive rates by nearly 74% following *Pd* introduction (Moore *et al.* 2018; Ineson 2020). Therefore, if *E. fuscus* follow a similar pattern and are also reproducing by their first year as mature adults following *Pd* introduction, the overall increases to the capture rates of reproductive female *E. fuscus* found here could support the terminal investment hypothesis. Further research examining known colonies of *E. fuscus* need to be performed to determine if one-year-old reproductive rates have increased as a response to pathogen invasion.

The timing of reproductive investment can also change when an animal's environment is disrupted (Todd *et al.* 2011; Francl *et al.* 2012; Roznik *et al.* 2015; Ineson 2020; Zurowski *et al.* 2020). For North American temperate bats, earlier pregnancy and pup births are thought to provide young of the year with more time to prepare for hibernation and thus, increase survival (Frick *et al.* 2010b). Highly susceptible *M. lucifugus* become pregnant earlier following *Pd* introduction and give birth to pups earlier (Francl *et al.* 2012; Ineson 2020), and similar shifts in reproductive timing could contribute to results for increases in the capture rates of reproductive *E. fuscus*. However, if reproductive timing for female *E. fuscus* was shifting to earlier dates, I would expect differences in the capture rates of northern and southern pregnant bats to align with spatial patterns for lactating and post-lactating bats. Instead, data here demonstrate that by *Pd* establishment years, pregnant bat capture rates were lower in the north compared to the south while lactating and post-lactating bat capture rates were higher in the north

than the south (Fig. 4.3H, 4.3L, 4.3P). Further investigation is needed to determine whether changes in *E. fuscus* reproductive timing occur across a broad spatial scale with long-term *Pd* exposure, and if those changes are parsimonious across female reproductive statuses.

It is also possible that other reproductive investment factors may contribute to the spatial complexities of less susceptible reproductive female capture rates demonstrated here. Pathogens can also decrease parental care to offspring due to host energy trade-offs between mounting immune responses to fight off infections versus investing in reproduction (Bonneaud *et al.* 2003; Ratz *et al.* 2021). The difference in spatial patterns between the capture rates of pregnant, lactating and post-lactating bats could also reflect changes in the time investment of *E. fuscus* maternal care. *E. fuscus* post-natal growth is up to two weeks longer than highly susceptible *M. lucifugus* (Fenton & Barclay 1980; Burnett & Kunz 1982; Kurta & Baker 1990), suggesting a greater investment in parental care by *E. fuscus* prior to *Pd* invasion. The capture rates of post-lactating *E. fuscus* more than doubled from pre-invasion to establishment years, with both northern and southern post-lactating capture rates increasing from pre-invasion to establishment (Fig. 4.3M, 4.3P). These findings are also supported by increases in post-lactating *E. fuscus* capture rates in Appalachia, USA, following *Pd* introduction (O'Keefe *et al.* 2019). *Eptesicus fuscus* post-lactating body condition was also poorer in northern latitudes compared to southern latitudes by *Pd* establishment (see Chapter 2). Further, by *Pd* establishment years, northern post-lactating bats weighed the same as northern lactating bats and southern post-lactating bats weighed less than southern lactating bats (see Chapter 2). Taken together, increases to the capture rates of post-lactating *E. fuscus* is concerning

because it suggests *E. fuscus* may not have enough energy to care for pups, and may transition into post-lactation earlier in the maternal season. This brings into question overall reproductive success and if 1) *E. fuscus* are abandoning pups (Pettit & O'Keefe 2017), and/or 2) if newly flighted pups have enough maternal care in summer to be successful in their first winter hibernation in combination with *Pd*. If female *E. fuscus* are transitioning into post-lactation earlier, and pups are surviving but aren't getting the full extent of needed maternal care, mortalities of young adult bats in their first hibernation could reflect why we continue to see declines in *E. fuscus* populations due to white-nose syndrome in winter months (Cheng *et al.* 2021). In order to determine if *E. fuscus* are providing sufficient parental care with long-term pathogen exposure, research quantifying reproductive success with juvenile *E. fuscus* survivorship, capture rates, body condition and growth is needed across a broader spatial scale over invasion time-steps. Finally, year-round estimates of less susceptible host populations are needed to truly quantify population persistence and fecundity.

In conclusion, this work highlights the need to better understand how less susceptible host populations change across broad spatial scales with continued pathogen exposure. Broadly, less susceptible host populations shift demographically and spatially with chronic pathogen exposure. Consequently, those spatial and demographic shifts could impact the persistence of less susceptible hosts like *E. fuscus* in the future by way of intraspecific competition and/or reproductive investment pressures. Future efforts for understanding the degree of persistence of less susceptible wildlife host populations are critical for predicting population structures following emerging infectious disease outbreaks and epidemics.

ACKNOWLEDGEMENTS

I thank all the researchers, field biologists and technicians who collected *E. fuscus* data over the 30 years of the capture dataset. I gratefully acknowledge data contributors from Georgia (Georgia Department of Natural Resources), Illinois (Tim Carter, Ball State University), Indiana (Indiana US Fish and Wildlife Service), Kentucky (Kentucky Department of Fish and Wildlife Resources), Mississippi (Katelin Cross, Mississippi Museum of Natural Science), New York (New York State Department of Environmental Conservation), North Carolina (North Carolina US Fish and Wildlife Service; North Carolina Wildlife Resources Commission), Ohio (Sarah Stankavich, Ohio Department of Natural Resources' Division of Wildlife; Lisa Cooper, Northeastern Ohio Medical University), Pennsylvania (Pennsylvania Game Commission), Tennessee (Tennessee Wildlife Resource Agency), and Virginia (Virginia Department of Wildlife Resources). Data collection from Virginia for this publication was completed with funds provided by the Virginia Department of Wildlife Resources using resources from the national Wildlife Restoration program provided by the U.S. Fish and Wildlife Service. I thank Yasmeen Samar for her help with early data cleaning and Wright State University Biological Sciences Department's Biology Award for Research Excellence.

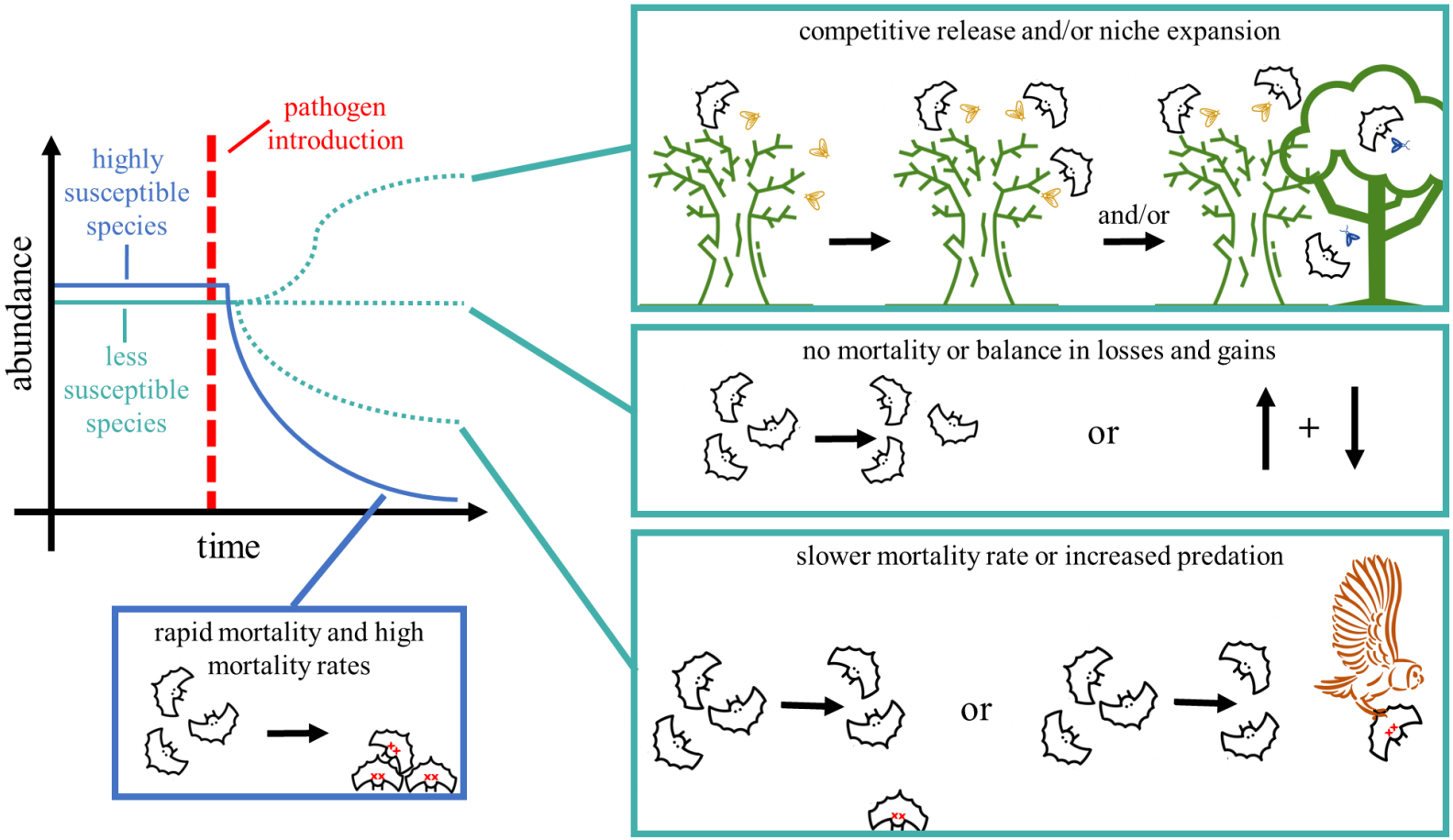

Figure 4.1. The abundance of hosts less susceptible to pathogen infections can increase, not change or decrease following pathogen introduction. The abundance of less susceptible hosts can increase due to a release in competition from highly

susceptible hosts and/or niche expansion. There can be no change to less susceptible host abundance if they do not die from pathogen infections or have a balance of losses and gains in abundance. Finally, less susceptible host abundance can decrease but at slower rates compared to highly susceptible species, or due to increases in predation from prey-switching by predators. Icons were downloaded from the Noun Project (thenounproject.com) and created by the following artists: blue moth, Ben Davis; yellow moth, Georgiana Ionescu; bat, Bernar Novalyi; owl, Alice Noir; dead tree, ProSymbols; live tree, kareemovic3000.

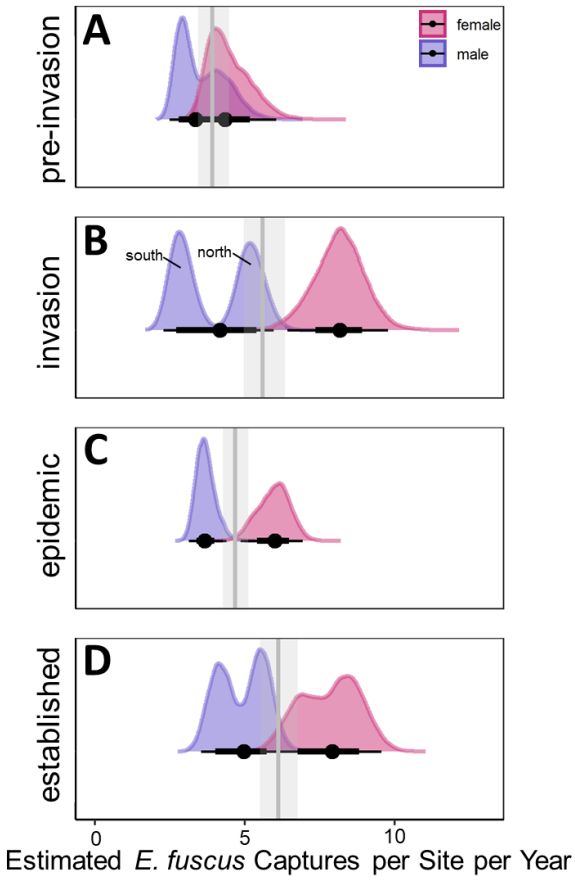

Figure 4.2. The abundance of adult *E. fuscus* increased from pre-invasion years (A) to invasion (B), epidemic (C) and establishment years [D; R^2 = 0.35 (0.34, 0.37)]. Male bat abundance is represented in purple and female bat abundance in pink. B) The only time-step where there were significant differences between the abundance of northern and southern *E. fuscus* was during invasion years such that, there were more male *E. fuscus* in northern latitudes compared to southern latitudes. Black points represent the posterior mean for the abundance of male or female *E. fuscus*, thick black bars represent 66%

credible intervals, and thin black bars are 95% credible intervals. Vertical gray lines are the posterior mean for each *Pd* time-step. Gray transparent rectangles represent 95% credible intervals around the posterior mean for each *Pd* time-step. Significant differences are where there is no overlap in 95% credible intervals.

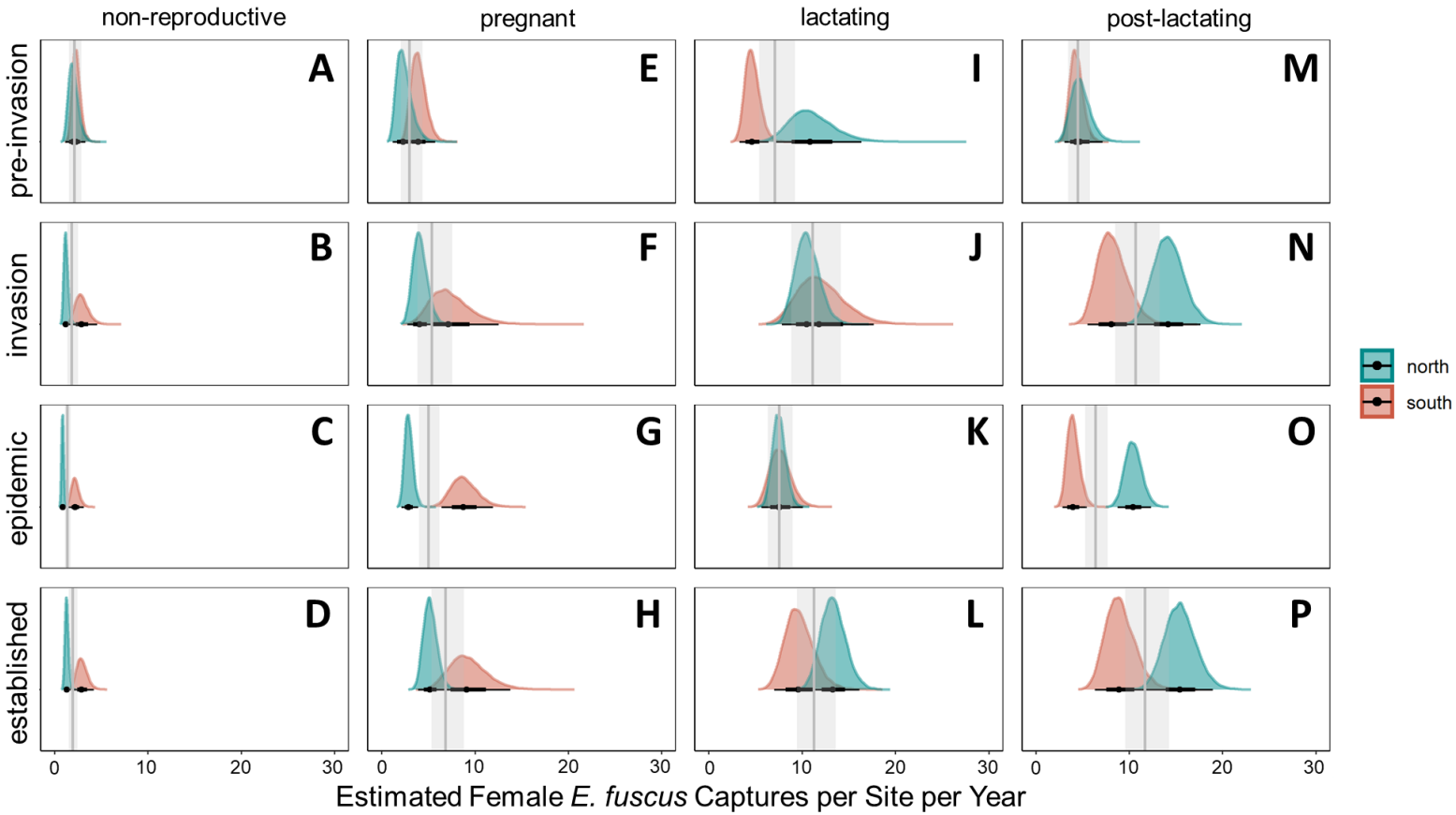

Figure 4.3. Abundance varied for non-reproductive (A-D), pregnant (E-H), lactating (I-L) and post-lactating *E. fuscus* females (M-P) with *Pd* exposure time-steps and latitudinal category [north/south; R^2 = 0.47 (0.44, 0.49)]. Northern female bat

abundance is represented in blue and southern female bat abundance in red. Black points represent the posterior mean for northern or southern *E. fuscus* abundance, thick black bars represent 66% credible intervals, and thin black bars are 95% credible intervals. Vertical gray lines are the posterior mean for each *Pd* time-step within a given reproductive status. Gray transparent rectangles represent credible intervals around the posterior mean for each *Pd* time-step within a given reproductive status. Significant differences are where there is no overlap in 95% credible intervals.

REFERENCES

Anderson, R.P., Peterson, A.T. & Go, M. (2002). Using niche-based GIS modeling to test geographic predictions of competitive exclusion and competitive release in South American pocket mice. OIKOS, 98, 3–16.

Blehert, D.S., Hicks, A.C., Behr, M., Meteyer, C.U., Berlowski-Zier, B.M., Buckles, E.L., et al. (2009). Bat white-nose syndrome: an emerging fungal pathogen? Science, 323, 227.

Bolnick, D.I., Ingram, T., Stutz, W.E., Snowberg, L.K., Lau, O.L. & Pauli, J.S. (2010). Ecological release from interspecific competition leads to decoupled changes in population and individual niche width. Proc. R. Soc. B Biol. Sci., 277, 1789–1797.

Bonneaud, C., Mazuc, J., Chastel, O., Westerdahl, H. & Sorci, G. (2004). Terminal investment induced by immune challenge and fitness traits associated with major histocompatibility complex in the house sparrow. Evolution, 58, 2823–2830.

Bonneaud, C., Mazuc, J., Gonzalez, G., Haussy, C., Chastel, O., Faivre, B., et al. (2003). Assessing the cost of mounting an immune response. Am. Nat., 161, 367–379.

Boonstra, R., McColl, C.J. & Karels, T.J. (2001). Reproduction at all costs: The adaptive stress response of male arctic ground squirrels. Ecology, 82, 1930–1946.

Boyles, J.G., Dunbar, M.B., Storm, J.J. & Brack, V. (2007). Energy availability influences microclimate selection of hibernating bats. J. Exp. Biol., 210, 4345–4350.

Bürkner, P.-C. (2017). brms: An R Package for Bayesian Multilevel Models Using Stan. J. Stat. Softw., 80, 1–28.

Burnett, C.D. & Kunz, T.H. (1982). Growth Rates and Age Estimation in *Eptesicus fuscus* and Comparison with *Myotis lucifugus*. J. Mammal., 63, 33–41.

Burton, R.S. & Reichman, J. (1999). Does Immune Challenge Affect Torpor Duration. Funct. Ecol., 13, 232–237.

Cameron, E.Z. (2004). Facultative adjustment of mammalian sex ratios in support of the Trivers-Willard hypothesis: Evidence for a mechanism. Proc. R. Soc. B Biol. Sci., 271, 1723–1728.

Cheng, T.L., Gerson, A., Moore, M.S., Reichard, J.D., DeSimone, J., Willis, C.K.R., et al. (2019). Higher fat stores contribute to persistence of little brown bat populations with white-nose syndrome. J. Anim. Ecol., 88, 591–600.

Cheng, T.L., Reichard, J.D., Coleman, J.T.H., Weller, T.J., Thogmartin, W.E., Reichert, B., et al. (2021). The scope and severity of White-nose Syndrome on hibernating bats in North America. Conserv. Biol., 35, 1586–1597.

Chesson, P. (2000). General theory of competitive coexistence in spatially-varying environments. Theor. Popul. Biol., 58, 211–237.

Christian, J.J. (1956). The Natural History of a Summer Aggregation of the Big Brown Bat, *Eptesicus fuscus fuscus*. Amer. Midl. Nat. 55, 66–95.

Civitello, D.J., Cohen, J., Fatima, H., Halstead, N.T., Liriano, J., McMahon, T.A., et al. (2015). Biodiversity inhibits parasites: Broad evidence for the dilution effect. PNAS, 112, 8667–8671.

Cortez, M.J. V., Rabajante, J.F., Tubay, J.M. & Babierra, A.L. (2017). From epigenetic landscape to phenotypic fitness landscape: Evolutionary effect of pathogens on host traits. Infect. Genet. Evol., 51, 245–254.

Daszak, P., Cunningham, A. & Hyatt, A. (2000). Emerging Infectious Diseases of Wildlife - Threats to Biodiversity and Human Health. Science, 287, 443–449.

Dhondt, A., Tessaglia, D. & Slothower, R. (1998). Epidemic from conjunctivitis in house finches of Eastern North America. J. Wildl. Dis., 34, 265–280.

Drees, K., Puechmaille, S., Parise, K.L. & Wibbelt, G. (2017). Phylogenetics of a Fungal Invasion: Origins and Widespread Dispersal of White-Nose Syndrome. MBio, 8, e01941-17.

Duffy, D.L., Bentley, G.E., Drazen, D.L. & Ball, G.F. (2000). Effects of testosterone on cell-mediated and humoral immunity in non-breeding adult European starlings. Behav. Ecol., 11, 654–662.

Dyson, E.A. & Hurst, G.D.D. (2004). Persistence of an extreme sex-ratio bias in a natural population. PNAS, 101, 6520–6523.

Fenton, B.M. & Barclay, R.M.R. (1980). *Myotis lucifugus*. Mamm. Species, 142, 1–8.

Foo, Y.Z., Nakagawa, S., Rhodes, G. & Simmons, L.W. (2017). The effects of sex hormones on immune function: a meta-analysis. Biol. Rev., 92, 551–571.

Francl, K.E., Ford, W.M., Sparks, D.W. & Brack, V. (2012). Capture and reproductive trends in summer bat communities in West Virginia: Assessing the impact of white-nose syndrome. J. Fish Wildl. Manag., 3, 33–42.

Frank, C.L., Michalski, A., McDonough, A.A., Rahimian, M., Rudd, R.J. & Herzog, C. (2014). The resistance of a North American bat species (*Eptesicus fuscus*) to White-Nose Syndrome (WNS). PLoS One, 9, 1–14.

Frick, W.F., Cheng, T.L., Langwig, K.E., Hoyt, J.R., Janicki, A.F., Parise, K.L., et al. (2017). Pathogen dynamics during invasion and establishment of white-nose syndrome explain mechanisms of host persistence. Ecology, 98, 624–631.

Frick, W.F., Pollock, J.F., Hicks, A.C., Langwig, K.E., Reynolds, D.S., Turner, G.G., et al. (2010a). An emerging disease causes regional population collapse of a common North American bat species. Science, 329, 679–82.

Frick, W.F., Puechmaille, S.J., Hoyt, J.R., Nickel, B.A., Langwig, K.E., Foster, J.T., et al. (2015). Disease alters macroecological patterns of North American bats. Glob. Ecol. Biogeogr., 24, 741–749.

Frick, W.F., Reynolds, D.S. & Kunz, T.H. (2010b). Influence of climate and reproductive timing on demography of little brown myotis Myotis lucifugus. J. Anim. Ecol., 79, 128–136.

Fuller, N.W., Mcguire, L.P., Pannkuk, E.L., Blute, T., Haase, C.G., Mayberry, H.W., et al. (2020). Disease recovery in bats affected by white-nose syndrome. J. Exp. Biol., 223, jeb211912.

Gervasi, S.S., Civitello, D.J., Kilvitis, H.J. & Martin, L.B. (2015). The context of host competence: A role for plasticity in host-parasite dynamics. Trends Parasitol., 31, 419–425.

Giehr, J., Grasse, A. V., Cremer, S., Heinze, J. & Schrempf, A. (2017). Ant queens increase their reproductive efforts after pathogen infection. R. Soc. Open Sci., 4, 1–8.

Gotelli, N.J. (2008). A Primer of Ecology. Fourth Edition. Sinauer Associates Inc., Sunderland, MA.

Gould, E. (1955). The Feeding Efficiency of Insectivorous Bats. J. Mammal., 36, 399–407.

Grinevitch, L., Holroyd, S.L. & Barclay, R.M.R. (1995). Sex differences in the use of daily torpor and foraging time by big brown bats (*Eptesicus fuscus*) during the reproductive season. J. Zool., 235, 301–309.

Gurevitch, J. & Padilla, D.K. (2004). Are invasive species a major cause of extinctions? Trends Ecol. Evol., 19, 470–474.

Heard, M.J., Smith, K.F., Ripp, K.J., Berger, M., Chen, J., Dittmeier, J., et al. (2013). The Threat of Disease Increases as Species Move Toward Extinction. Conserv. Biol., 27, 1378–1388.

Herrmann, N.C., Stroud, J.T. & Losos, J.B. (2021). The Evolution of 'Ecological Release' into the 21st Century. Trends Ecol. Evol., 36, 206–215.

Hochachka, W.M. & Dhondt, A.A. (2000). Density-dependent decline of host abundance resulting from a new infectious disease. PNAS, 97, 5303–5306.

Holt, R.D. & Dobson, A.P. (2006). Extending the principles of community ecology to address the epidemiology of host-pathogen systems. In: Disease Ecology: Community Structure and Pathogen Dynamics (eds. Collinge, S.K. & Ray, C.). Oxford University Press, Inc., New York, pp. 6–27.

Hoyt, J.R., Langwig, K.E., Sun, K., Lu, G., Parise, K.L., Jiang, T., et al. (2016). Host persistence or extinction from emerging infectious disease: Insights from white-nose syndrome in endemic and invading regions. Proc. R. Soc. B Biol. Sci., 283.

Hoyt, J.R., Langwig, K.E., Sun, K., Parise, K.L., Li, A., Wang, Y., et al. (2020). Environmental reservoir dynamics predict global infection patterns and population impacts for the fungal disease white-nose syndrome. PNAS, 117, 7255–7262.

Ineson, K. (2020). Demography of a Recovery: Tracking the Rebound of Little Brown Bat (*Myotis Lucifugus*) Populations. Doctoral Dissertations. 2529. https://scholars.unh.edu/dissertation/2529.

Ingersoll, T.E., Sewall, B.J. & Amelon, S.K. (2013). Improved Analysis of Long-Term Monitoring Data Demonstrates Marked Regional Declines of Bat Populations in the Eastern United States. PLoS One, 8, e65907.

J. Rankin, D. & Kokko, H. (2007). Do males matter? The role of males in population dynamics. Oikos, 116, 335–348.

Jachowski, D.S., Dobony, C.A., Coleman, L.S., Ford, W.M., Britzke, E.R. & Rodrigue, J.L. (2014). Disease and community structure: White-nose syndrome alters spatial and temporal niche partitioning in sympatric bat species. Divers. Distrib., 20, 1002–1015.

Jones, M.E., Cockburn, A., Hamede, R., Hawkins, C., Hesterman, H., Lachish, S., et al. (2008). Life-history change in disease-ravaged Tasmanian devil populations. PNAS, 105, 10023–10027.

Kay, M. (2020). tidybayes: Tidy Data and Geoms for Bayesian Models, R package.

Kiørboe, T., Saiz, E. & Viitasalo, M. (1996). Prey switching behaviour in the planktonic copepod *Acartia tonsa*. Mar. Ecol. Prog. Ser., 143, 65–75.

Kjellander, P. & Nordström, J. (2003). Cyclic voles, prey switching in red fox, and roe deer dynamics - A test of the alternative prey hypothesis. Oikos, 101, 338–344.

Kurta, A. & Baker, R.H. (1990). *Eptesicus fuscus*. Mamm. Species, 356, 1–10.

Kurta, A., Kunz, T.H., Nagy, K.A., Kurta, A., Kunz, T.H. & Nagy, K.A. (1990). Energetics and Water Flux of Free-Ranging Big Brown Bats (*Eptesicus fuscus*) during Pregnancy and Lactation. J. Mammal., 71, 59–65.

Lachish, S., McCallum, H. & Jones, M. (2009). Demography, disease and the devil: Life-history changes in a disease-affected population of Tasmanian devils (*Sarcophilus harrisii*). J. Anim. Ecol., 78, 427–436.

Langwig, K.E., Frick, W.F., Reynolds, R., Parise, K.L., Drees, K.P., Hoyt, J.R., et al. (2015). Host and pathogen ecology drive the seasonal dynamics of a fungal disease, white-nose syndrome. Proc. R. Soc. B Biol. Sci., 282, 10–12.

Lenth, R. (2021). emmeans: Estimated Marginal Means, aka Least-Squares Means.

Leopardi, S., Blake, D. & Puechmaille, S.J. (2015). White-nose syndrome fungus introduced from Europe to North America. Curr. Biol., 25, R217–R219.

Lorch, J.M., Meteyer, C.U., Behr, M.J., Boyles, J.G., Cryan, P.M., Hicks, A.C., et al. (2011). Experimental infection of bats with *Geomyces destructans* causes white-nose syndrome. Nature, 480, 376–378.

Lorch, J.M., Muller, L.K., Russell, R.E., O'Connor, M., Lindner, D.L. & Blehert, D.S. (2013). Distribution and environmental persistence of the causative agent of white-nose syndrome, *Geomyces destructans*, in bat hibernacula of the eastern United States. Appl. Environ. Microbiol., 79, 1293–1301.

MacArthur, R.H., Diamond, J.M. & Karr, J.R. (1972). Density Compensation in Island Faunas. Ecology, 53, 330–342.

McGuire, L.P., Mayberry, H.W. & Willis, C.K.R. (2017). White-nose syndrome increases torpid metabolic rate and evaporative water loss in hibernating bats. Am. J. Physiol. - Regul. Integr. Comp. Physiol., 313, R680–R686.

Meierhofer, M.B., Johnson, J.S., Field, K.A., Lumadue, S.S., Kurta, A., Kath, J.A., et al. (2018). Bats recovering from white-nose syndrome elevate metabolic rate during wing healing in Spring. J. Wildl. Dis., 54, 480–490.

Menzel, M.A., Carter, T.C., Mitchell, B.L., Jablonowski, L.R., Chapman, B.R. & Laerm, J. (2020). Prey selection by a maternity colony of big brown bats (*Eptesicus fuscus*) in the southeastern United States. Florida Sci., 63, 232–241.

Meteyer, C.U., Buckles, E.L., Blehert, D.S., Hicks, A.C., Green, D.E., Shearn-bochsler, V., et al. (2009). Histopathologic criteria to confirm white-nose syndrome in bats. J. Vet. Diagnostic Investig., 21, 411–414.

Mills, R.S., Barrett, G.W., Farrell, M.P., Mills, R.S., Barrett, G.W. & Farrell, M.P. (2019). Population Dynamics of the Big Brown Bat (*Eptesicus fuscus*) in Southwestern Ohio. J. Mammal., 56, 591–604.

Milner-Gulland, E.J., Bukreeva, O.M., Coulson, T., Lushchekina, A.A., Kholodova, M. V., Bekenovil, A.B., et al. (2003). Reproductive collapse in saiga antelope harems. Nature, 422, 135.

Moleón, M., Sánchez-Zapata, J.A., Real, J., García-Charton, J.A., Gil-Sánchez, J.M., Palma, L., et al. (2009). Large-scale spatio-temporal shifts in the diet of a predator mediated by an emerging infectious disease of its main prey. J. Biogeogr., 36, 1502–1515.

Moore, M.S., Field, K.A., Behr, M.J., Turner, G.G., Furze, M.E., Stern, D.W.F., et al. (2018). Energy conserving thermoregulatory patterns and lower disease severity in a bat resistant to the impacts of white-nose syndrome. J. Comp. Physiol. B Biochem. Syst. Environ. Physiol., 188, 163–176.

Mumford, R.E. (1958). Population Turnover in Wintering Bats in Indiana. J. Mammal., 39, 253–261.

Murdoch, W.W. (2014). Switching in General Predators: Experiments on Predator Specificity and Stability of Prey Populations. Ecol. Monogr., 39, 335–354.

O'Keefe, J.M., Pettit, J.L., Loeb, S.C. & Stiver, W.H. (2019). White-nose syndrome dramatically altered the summer bat assemblage in a temperate southern Appalachian forest. Mamm. Biol., 98, 146–153.

Pedersen, A.B., Jones, K.E., Nunn, C.L. & Altizer, S. (2007). Infectious diseases and extinction risk in wild mammals. Conserv. Biol., 21, 1269–1279.

Pedersen, T.L. (2020). patchwork: The Composer of Plots, R package.

Pettit, J.L. & O'Keefe, J.M. (2017). Impacts of White-Nose Syndrome Observed During Long-Term Monitoring of a Midwestern Bat Community. J. Fish Wildl. Manag., 8, 69–78.

Phillips, G.L. (1966). Ecology of the Big Brown Bat (Chiroptera: Vespertilionidae) in Northeastern Kansas. Am. Midl. Nat., 75, 168–198.

Puechmaille, S.J., Wibbelt, G., Korn, V., Fuller, H., Forget, F., Mühldorfer, K., et al. (2011). Pan-European distribution of white-nose syndrome fungus (*Geomyces destructans*) not associated with mass mortality. PLoS One, 6, e19167.

Püttker, T., Barros, C.S., Pinotti, B.T., Bueno, A.A. & Pardini, R. (2019). Co-occurrence patterns of rodents at multiple spatial scales: Competitive release of generalists following habitat loss? J. Mammal., 100, 1229–1242.

R Core Team. (2021). R: A language and environment for statistical computing.

Ratz, T., Monteith, K.M., Vale, P.F. & Smiseth, P.T. (2021). Carry on caring: Infected females maintain their parental care despite high mortality. Behav. Ecol., 32, 738–746.

Reeder, D.M., Frank, C.L., Turner, G.G., Meteyer, C.U., Kurta, A., Britzke, E.R., et al. (2012). Frequent Arousal from Hibernation Linked to Severity of Infection and Mortality in Bats with White-Nose Syndrome. PLoS One, 7, e38920.

Retschnig, G., Williams, G.R., Mehmann, M.M., Yañez, O., De Miranda, J.R. & Neumann, P. (2014). Sex-specific differences in pathogen susceptibility in honey bees (*Apis mellifera*). PLoS One, 9, e85261.

Richardson, C.S., Heeren, T. & Kunz, T.H. (2018). Seasonal and sexual variation in metabolism, thermoregulation, and hormones in the big brown bat (*Eptesicus fuscus*). Physiol. Biochem. Zool., 91, 705–715.

Roznik, E.A., Sapsford, S.J., Pike, D.A., Schwarzkopf, L. & Alford, R.A. (2015). Condition-dependent reproductive effort in frogs infected by a widespread pathogen. Proc. R. Soc. B Biol. Sci., 282, 20150694.

Ruoss, S., Becker, N.I., Otto, M.S., Czirják, G. & Encarnação, J.A. (2019). Effect of sex and reproductive status on the immunity of the temperate bat *Myotis daubentonii*. Mamm. Biol., 94, 120–126.

Russell, R.E., Halstead, B.J., Mosher, B.A., Muths, E., Adams, M.J., Grant, E.H.C., et al. (2019). Effect of amphibian chytrid fungus (*Batrachochytrium dendrobatidis*) on apparent survival of frogs and toads in the western USA. Biol. Conserv., 236, 296–304.

Rysgaard, G.N. (1942). A Study of the Cave Bats of Minnesota with Especial Reference to the Large Brown Bat, *Eptesicus fuscus fuscus* (Beauvois). Am. Midl. Nat., 28, 245–267.

Schowalter, D.B. & Gunson, J.R. (1979). Reproductive biology of the big brown bat (*Eptesicus fuscus*) in Alberta. Can. F. Nat., 93, 48–54.

Siddon, C.E. & Witman, J.D. (2004). Behavioral indirect interactions: Multiple predator effects and prey switching in the rocky subtidal. Ecology, 85, 2938–2945.

Simonis, M.C., Brown, B.B. & Bahn, V. (2020). Mobile bat acoustic routes indicate cavity-roosting species undergo compensatory changes in community composition following white-nose syndrome. Acta Chiropterologica, 22, 315–326.

Skerratt, L.F., Berger, L., Speare, R., Cashins, S., McDonald, K.R., Phillott, A.D., et al. (2007). Spread of chytridiomycosis has caused the rapid global decline and extinction of frogs. Ecohealth, 4, 125–134.

Smith, K.F., Sax, D.F. & Lafferty, K.D. (2006). Evidence for the role of infectious disease in species extinction and endangerment. Conserv. Biol., 20, 1349–1357.

Stan Development Team. (2020). RStan: the R interface to Stan, R package.

Swanson, G. & Evans, C. (1936). The Hibernation of Certain Bats in Southern Minnesota. J. Mammal., 17, 39–43.

Todd, B.D., Scott, D.E., Pechmann, J.H.K. & Whitfield Gibbons, J. (2011). Climate change correlates with rapid delays and advancements in reproductive timing in an amphibian community. Proc. R. Soc. B Biol. Sci., 278, 2191–2197.

Trewby, I.D., Wilson, G.J., Delahay, R.J., Walker, N., Young, R., Davison, J., et al. (2008). Experimental evidence of competitive release in sympatric carnivores. Biol. Lett., 4, 170–172.

Turner, G.G., Reeder, D. & Coleman, J.T.H. (2011). A Five-year Assessment of Mortality and Geographic Spread of White-Nose Syndrome in North American Bats, with a look to the future. Bat Res. News, 52, 13–27.

VanderWaal, K.L. & Ezenwa, V.O. (2016). Heterogeneity in pathogen transmission: mechanisms and methodology. Funct. Ecol., 30, 1606–1622.

Vlad, M.O. (1989). The optimal sex ratio for age-structured populations. Math. Biosci., 93, 181–190.

Voyles, J., Young, S., Berger, L., Campbell, C., Voyles, W.F., Dinudom, A., et al. (2009). Pathogenesis of Chytridiobycosis, a Cause of Catastrophic Amphibian Declines. Science, 326, 582–586.

Wagner, D.L., Fox, R., Salcido, D.M. & Dyer, L.A. (2021a). A window to the world of global insect declines: Moth biodiversity trends are complex and heterogeneous. PNAS, 118, 1–8.

Wagner, D.L., Grames, E.M., Forister, M.L., Berenbaum, M.R. & Stopak, D. (2021b). Insect decline in the Anthropocene: Death by a thousand cuts. PNAS, 118, 1–10.

Whitaker, J.O. & Gummer, S.L. (1992). Hibernation of the Big Brown Bat, *Eptesicus fuscus*, in Buildings. J. Mammal., 73, 312–316.

Whitaker, J.O. & Gummer, S.L. (2000). Population Structure and Dynamics of Big Brown Bats (*Eptesicus fuscus*) Hibernating in Buildings in Indiana. Am. Midl. Nat., 143, 389–396.

White Nose Syndrome Response Team. (2022). White-nose syndrome occurrence map by year. Hadley, Massachusetts. https://www.whitenosesyndrome.org/.

Wibbelt, G., Kurth, A., Hellmann, D., Weishaar, M., Barlow, A., Veith, M., et al. (2010). White-nose syndrome fungus (*Geomyces destructans*) in bats, Europe. Emerg. Infect. Dis., 16, 1237–1242.

Wickham, H. (2009). ggplot2: Elegant Graphics for Data Analysis. Springer-Verlag, New York, New York.

Wickham, H., François, R., Henry, L. & Müller, K. (2021). dplyr: A Grammar of Data Manipulation, R package.

Williams, G.C. (1966). Natural Selection, the Costs of Reproduction, and a Refinement of Lack's Principle. Am. Nat., 100, 687–690.

Wilson, E.O. (1961). The Nature of the Taxon Cycle in the Melanesian Ant Fauna. Am. Nat., 95, 169–193.

Wimsatt, W.A. (1945). Notes on Breeding Behavior, Pregnancy, and Parturition in Some Vespertilionid Bats of the Eastern United States. J. Mammal., 26, 23–33.

Yaremych, S.A., Warner, R.E., Mankin, P.C., Brawn, J.D., Raim, A. & Novak, R. (2004). West Nile Virus and High Death Rate in American Crows. Emerg. Infect. Dis., 10, 709–711.

Young, H.S., Parker, I.M., Gilbert, G.S., Sofia Guerra, A. & Nunn, C.L. (2017). Introduced Species, Disease Ecology, and Biodiversity–Disease Relationships. Trends Ecol. Evol., 32, 41–54.

Zurowski, K., Janmaat, A.F., Kabaluk, T. & Cory, J.S. (2020). Modification of reproductive schedule in response to pathogen exposure in a wild insect: Support for the terminal investment hypothesis. J. Evol. Biol., 33, 1558–1566.

CHAPTER 5

CONCLUSION

The overarching goal of this dissertation was to identify changes in energy-based traits of hosts during prolonged exposure to an introduced pathogen, and relate those traits to long-term host population level impacts of the pathogen. Pathogen introductions and emerging infectious diseases that impact wildlife are becoming increasingly prevalent (Daszak *et al.* 2001). To better understand their effect on host population dynamics, it is critical we have a better understanding for how wildlife not only respond to pathogen exposure and infections, but also persist despite long-term pathogen exposure and infections. This dissertation expands our knowledge for how long-term pathogen exposure impact less susceptible host traits over time, and also highlights how these hosts can have indirect ecological consequences due to a pathogen introduction.

The aim of Chapter 2 was to understand how energy intake traits change in hosts with long-term pathogen exposure. To address this aim, I used host body mass as a proxy for energy intake and quantified changes to adult *E. fuscus* body mass across the eastern US and *Pd* exposure time-steps. *Eptesicus fuscus* progressively decreased mass with increasing latitude following the introduction of *Pd.* First, this work highlights how the responses of less susceptible wildlife hosts under long-term pathogen pressures can be spatially manifested. This is most clearly seen through the identification of spatial gradients for *E. fuscus* body mass over pathogen exposure time that were nonexistent

prior to *Pd* introduction. Further, results from this chapter also suggest that long-term pathogen exposure may also alter thermoregulatory patterns of *E. fuscus* across space. Chapter 2 emphasizes the notion that the responses of hosts less susceptible to pathogen infections should not be overlooked. While species highly susceptible to infection receive the most study (Altizer *et al.* 2004; Voyles *et al.* 2007; McGuire *et al.* 2017), less susceptible hosts are also impacted by pathogen pressures but those impacts may take longer periods of time to recognize.

In Chapter 3, I aimed to understand how host energy-expenditure traits change with long-term pathogen exposure. To address this aim, I quantified the torpid energy expenditures of *E. fuscus* across a wide range of ambient temperatures using whole-animal respirometry. Depending on the values used for pre-*Pd* exposure, *E. fuscus* either had no change to their torpid metabolic rates following long-term *Pd* exposure, or *E. fuscus* had increases to their torpid metabolic rates following long-term *Pd* exposure. If *E. fuscus* have increases to torpid energy expenditures, it could be due to an energetic cost of resistance to *Pd* infection and additional torpid energy expenditures would need accommodated. In warmer temperatures, it is likely *E. fuscus* can account for additional energy expenditures because food is more widely available. However, in colder temperatures, finding food to offset additional energy losses during torpor could be challenging even though *E. fuscus* are known to forage in winter (Dunbar *et al.* 2007; Reynolds *et al.* 2017). Outcomes from this work suggest the need for future studies which: 1) investigate the winter foraging activity of *E. fuscus* and 2) re-examine *E. fuscus'* torpid metabolic rates in the lab and in the field. Although I found conflicting results, Chapter 3 reiterates the importance of understanding the responses of less

susceptible hosts under long-term pathogen pressures, and outlines the ecological implications of inconsistent outcomes.

In Chapter 4, I aimed to understand the long-term population level impacts of pathogen exposure on less susceptible hosts. To address this aim, I quantified changes to adult *E. fuscus* capture rates with long-term *Pd* exposure across the eastern US. Overall capture rates of *E. fuscus* almost doubled with increasing *Pd* exposure time, with greater increases to female capture rates than male capture rates. Further, the capture rates of lactating and post-lactating *E. fuscus* increased with latitude across the eastern US with long-term *Pd* exposure. These shifts in *E. fuscus* capture rates following long-term pathogen exposure suggest a competitive release from highly susceptible bat species that have high mortality rates (Cheng *et al.* 2021). However, such rapid increases to host capture rates, when considered as a proxy for abundance, can reflect increases to intraspecific competition, and may impact the persistence of less susceptible hosts in the future. Chapter 4 highlights that hosts less susceptible to pathogen infections may incur additional ecological pressures in response to long-term pathogen exposure.

Taken together, results from the research presented here suggests hosts that are less susceptible to pathogen infections may undergo a combination of pathogen and ecological pressures following a pathogen introduction and long-term exposure. *Eptesicus fuscus* traits for body mass and torpid energy expenditures were negatively impacted by long-term *Pd* exposure, particularly in northern latitudes above 39.6 °N. However, these trait changes in less susceptible and resistant *E. fuscus* were paired with increases to their capture rates across the eastern US. Therefore, I would suggest that *E. fuscus* undergo changes within their populations due to a combination of pathogen (*Pd*)

and intraspecific competitive pressures. Because *E. fuscus* are less susceptible to *Pd*, competitive pressures may be stronger than pathogen pressures in regulating their population size. However, if *E. fuscus* reach their carrying capacity, pathogen pressures could contribute to steeper population declines to regulate their population. Overall, this dissertation highlights the importance of how introduced pathogens can cause spatially driven responses in less susceptible hosts over time, and how other ecological pressures may contribute to those responses. Future efforts for understanding the degree of persistence of less susceptible wildlife host populations are critical for predicting how and why their populations change following emerging infectious disease outbreaks and epidemics.

REFERENCES

Altizer, S., Davis, A.K., Cook, K.C. & Cherry, J.J. (2004). Age, sex, and season affect the risk of mycoplasmal conjunctivitis in a southeastern house finch population. Can. J. Zool., 82, 755–763.

Cheng, T.L., Reichard, J.D., Coleman, J.T.H., Weller, T.J., Thogmartin, W.E., Reichert, B., et al. (2021). The scope and severity of White-nose Syndrome on hibernating bats in North America. Conserv. Biol., 35, 1586–1597.

Daszak, P., Cunningham, A.A. & Hyatt, A.D. (2001). Anthropogenic environmental change and the emergence of infectious diseases in wildlife. Acta Trop., 78, 103–116.

Dunbar, M.B.., Whitaker, J.O.. & Robbins, L.W. (2007). Winter feeding by bats in Missouri. Acta Chiropterologica, 9, 305–322.

McGuire, L.P., Mayberry, H.W. & Willis, C.K.R. (2017). White-nose syndrome increases torpid metabolic rate and evaporative water loss in hibernating bats. Am. J. Physiol. - Regul. Integr. Comp. Physiol., 313, R680–R686.

Reynolds, D.S., Shoemaker, K., Von Oettingen, S. & Najjar, S. (2017). High Rates of Winter Activity and Arousals in Two New England Bat Species: Implications for a Reduced White-Nose Syndrome Impact? Northeast. Nat., 24, B188–B208.

Voyles, J., Berger, L., Young, S., Speare, R., Webb, R., Warner, J., et al. (2007). Electrolyte depletion and osmotic imbalance in amphibians with chytridiomycosis. Dis. Aquat. Organ., 77, 113–118.

APPENDIX A

CHAPTER 2 SUPPORTING INFORMATION

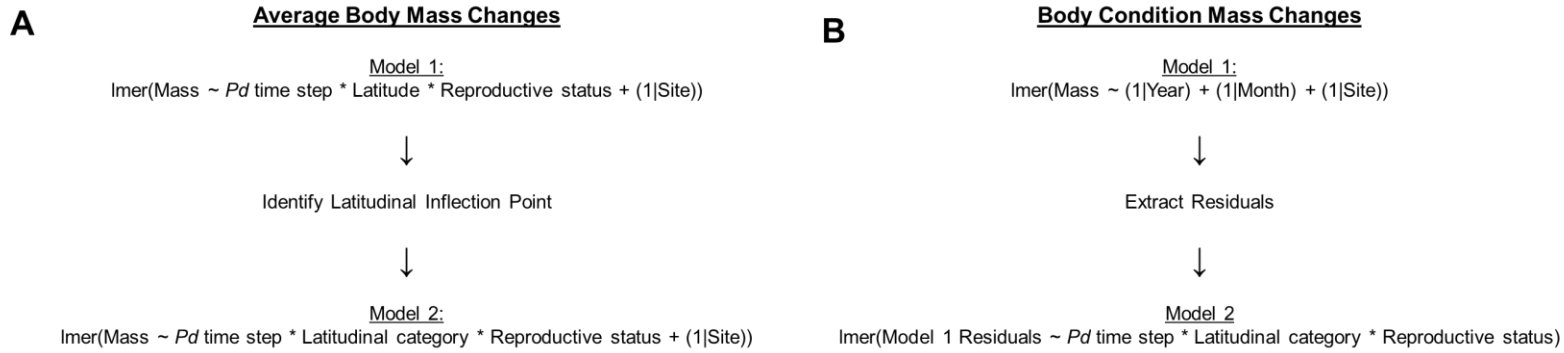

Figure S2.1. Linear model creation for female *E. fuscus* mass (**A**) or mass variation (**B**). Male linear models were created in the same fashion but without the interaction term for reproductive status. Models were created using the lme4 package in R (Bates *et al.* 2015; R Core Team 2021).

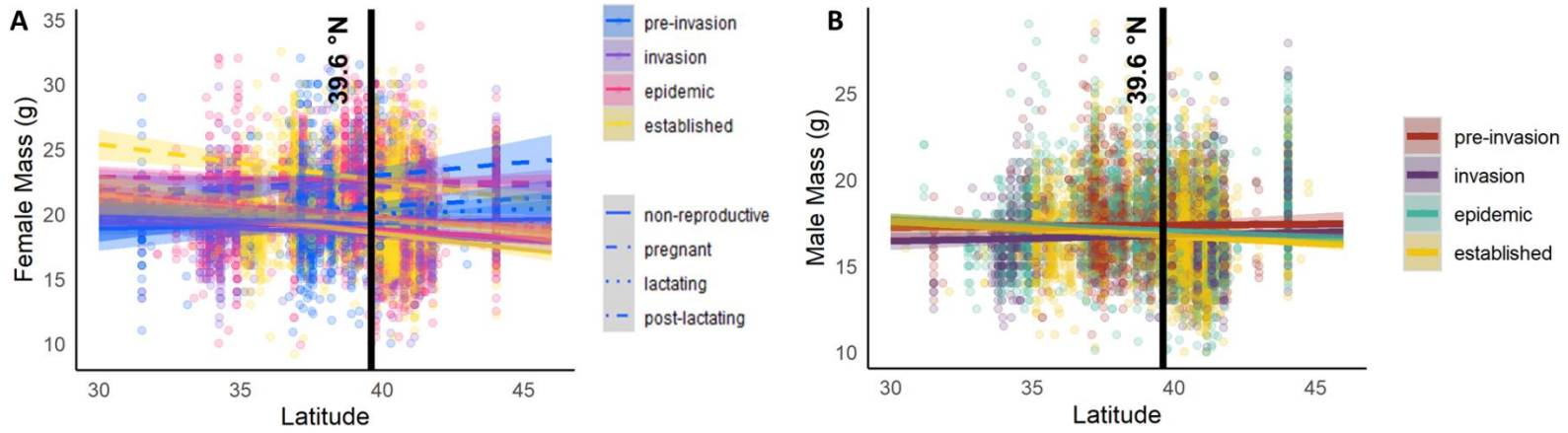

Figure S2.2. The effects of progressive *Pd* exposure on female (**A**) and male (**B**) big brown bat mass depended on latitude and reproductive status (females only). The interaction of *Pd* time-steps and reproductive status occurred at 39.6 °N (vertical black line) such that values south of 39.6 °N varied compared to values north of 39.6 °N (**A**, females, $F_{9, 2646} = 2.626$, $P = 0.0049$, $R^2 = 0.70$; **B**, males, $F_{3, 2729} = 5.474$, $P < 0.0001$, $R^2 = 0.58$;). Circles represent raw data points and lines represent predicted values with shaded 95% confidence intervals.

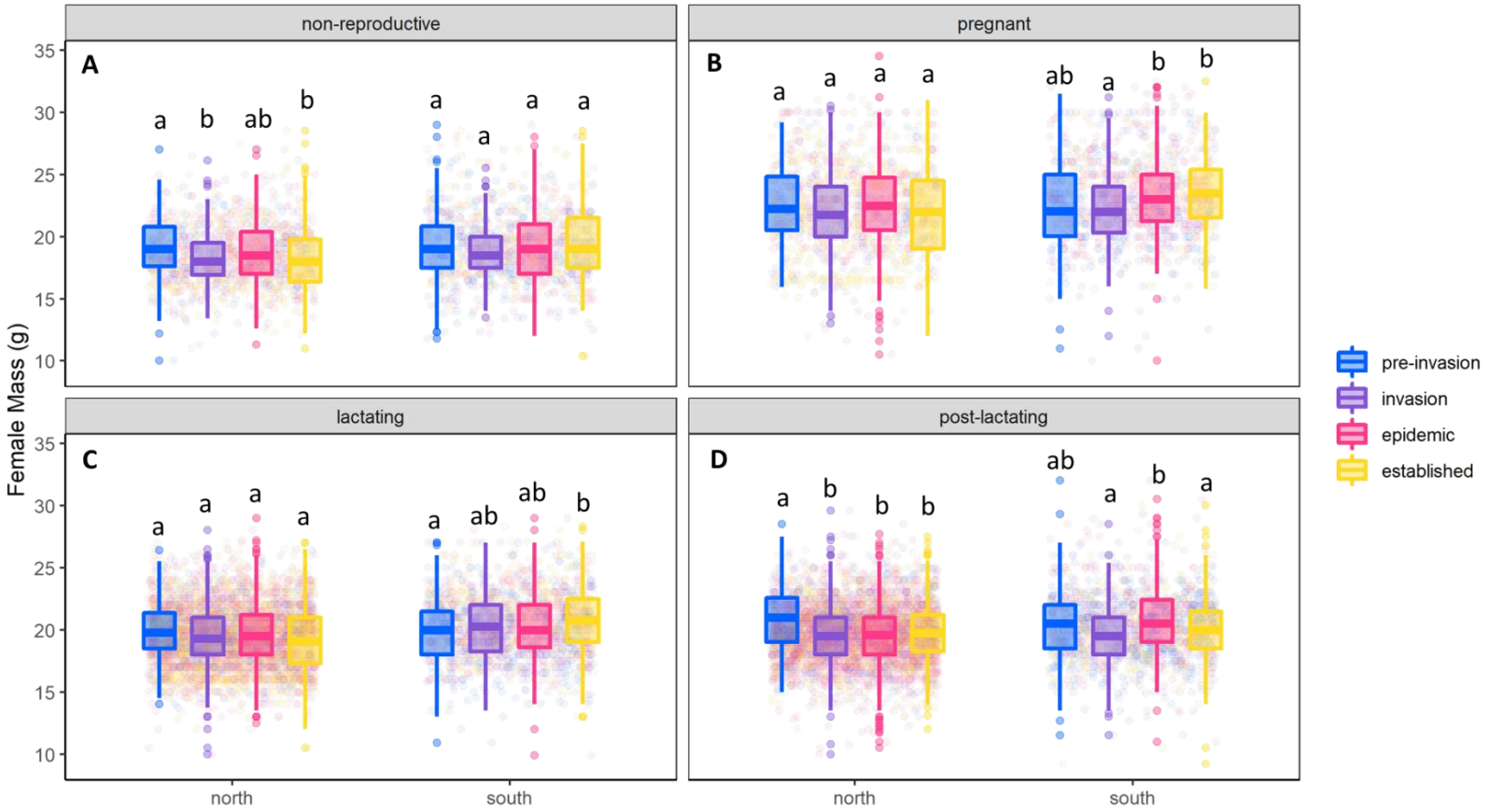

Figure S2.3. *E. fuscus* mass for northern and southern female bats varied across *Pd* exposure time-steps for non-reproductive (**A**), pregnant (**B**), lactating (**C**), and post-lactating (**D**) bats. Circles are raw data points for female mass and boxes represent

50% of data. Thick lines within the boxes represent median mass and vertical whiskers above and below each box represent an additional 25% of data each. Lowercase letters indicate significant differences based off Tukey tests for female mass across four comparisons for *Pd* exposure time-steps within simple groupings for reproductive status and latitudinal category of north/south.

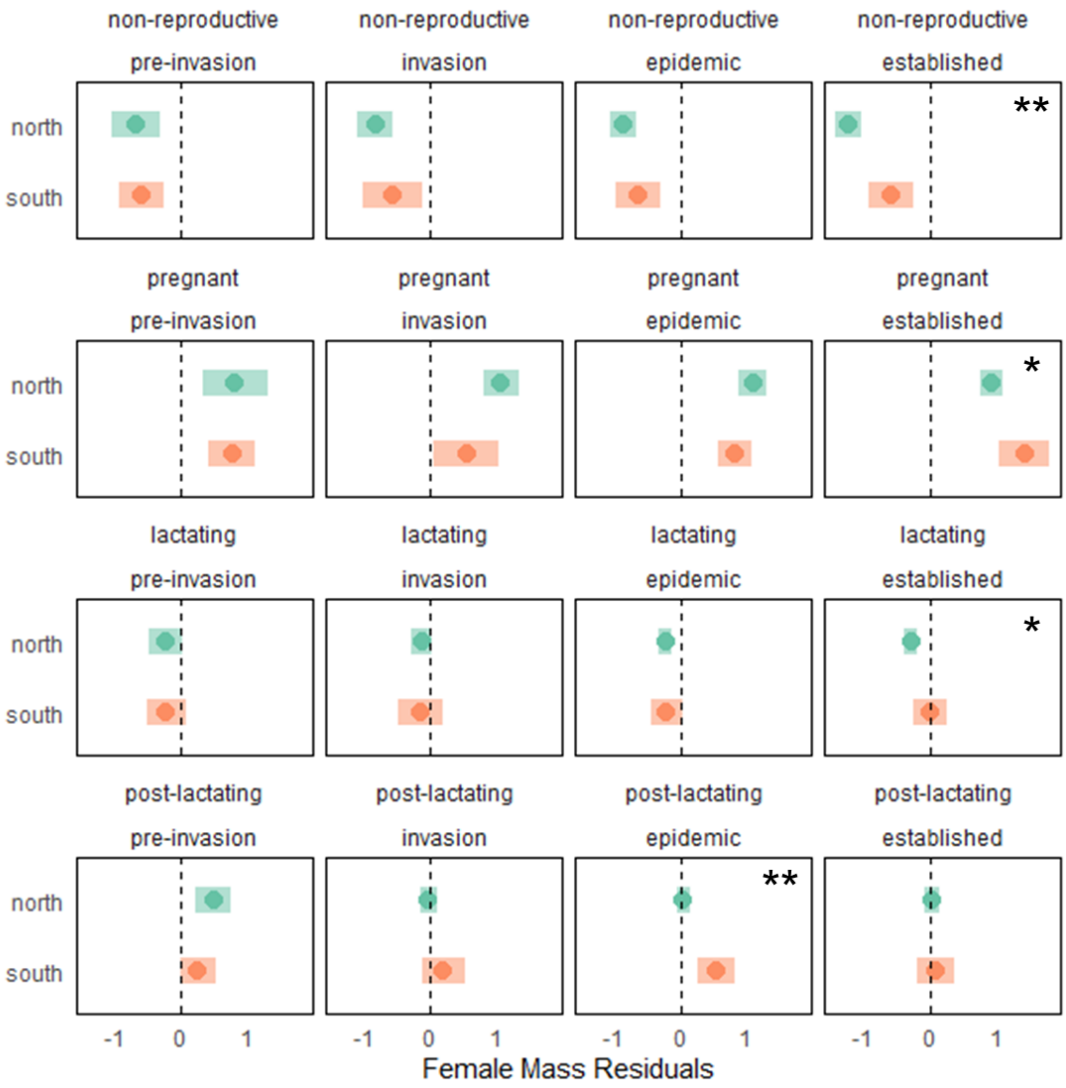

Figure S2.4. Female *E. fuscus* mass variation differs north to south for non-reproductive, pregnant and lactating bats by *Pd* establishment, and for post-lactating bats by *Pd* epidemic ($F_9 = 1.986$, $P = 0.0367$, $R^2 = 0.05$). Circles represent mean mass variation and bars represent 95% confidence intervals. Vertical dashed lines mark a zero value for mass residuals, or no mass variation. *P < 0.05; **P < 0.01; ***P < 0.001.

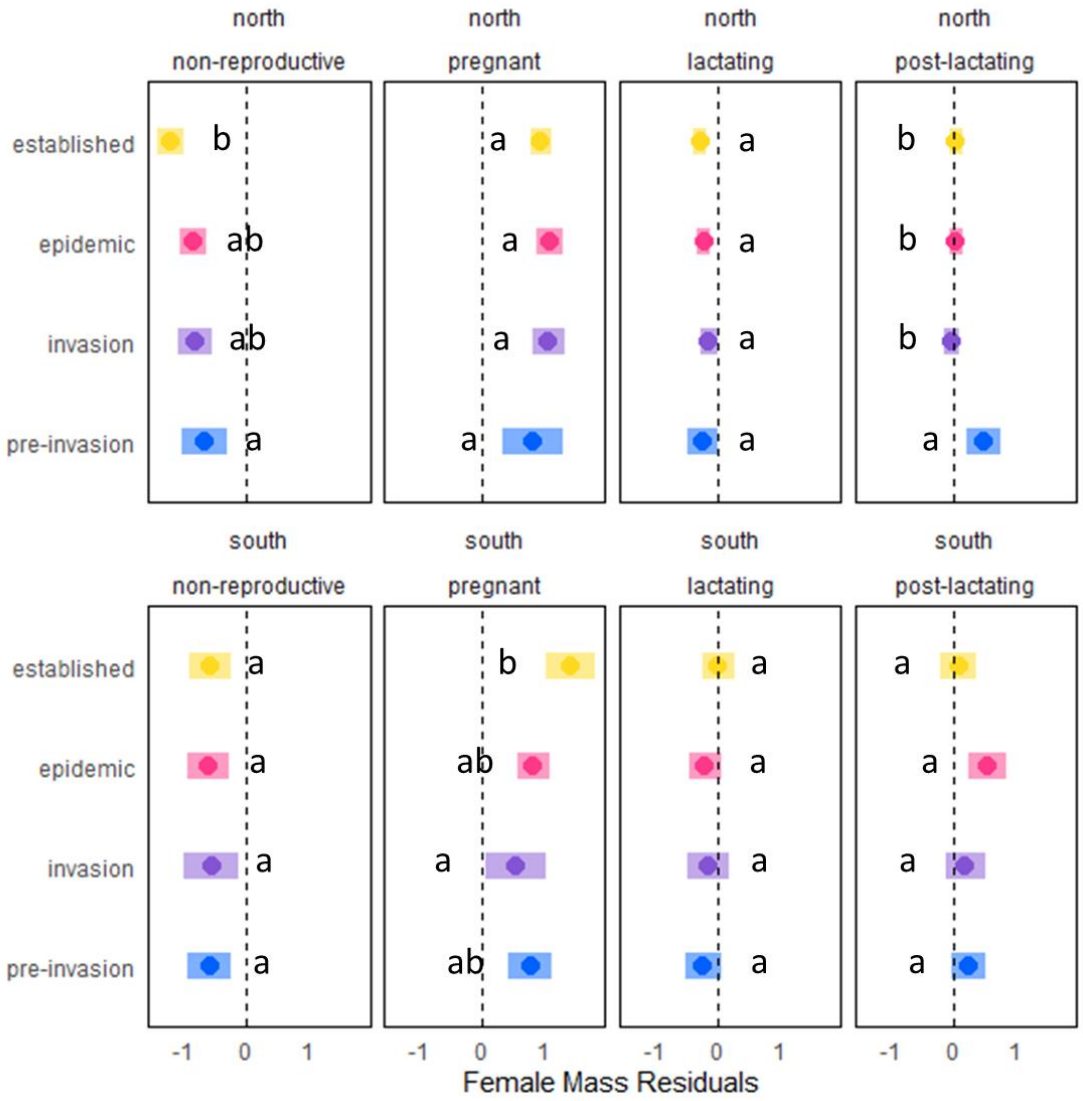

Figure S2.5. *E. fuscus* mass variation for northern and southern female bats varied by reproductive status across *Pd* exposure time-steps. Circles represent mean mass variation and bars represent 95% confidence intervals. Vertical dashed lines mark a zero value for mass residuals, or no mass variation. Lowercase letters indicate significant differences

based off Tukey tests for female mass across four comparisons for *Pd* exposure time-steps within simple groupings for reproductive status and latitudinal category.

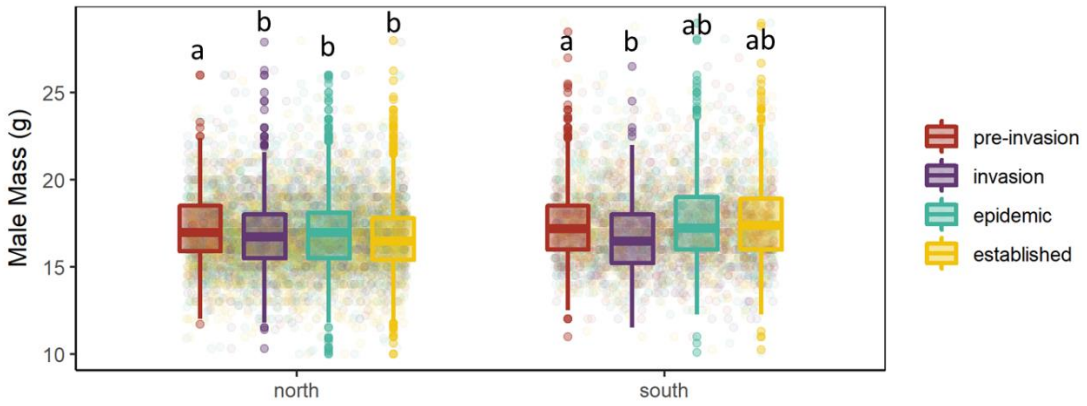

Figure S2.6. Male *E. fuscus* mass varied by *Pd* exposure time-steps north and south. Circles are raw data points and boxes represent 50% of data. Thick lines within the boxes represent median values and vertical whiskers above and below each box represent an additional 25% of data each. Lowercase letters indicate significant differences based off Tukey tests for data across four comparisons for *Pd* exposure time-steps within simple groupings for latitudinal category.

Table S2.1. Variance (σ^2) and standard deviations (SD) for random effects of month, site and year for female and male mass. Table values are from initial mass variation models (Fig 2.2B, Model 1).

Model	Random Effect	σ^2	SD
Female	Month	3.6769	1.9167
	Site	2.1794	1.4763
	Year	0.2609	0.4805
	Residual	5.3534	2.3137
Male	Month	4.2006	2.0495
	Site	0.9976	0.9988
	Year	0.0479	0.2188
	Residual	3.3210	1.8224

APPENDIX B
CHAPTER 3 SUPPORTING INFORMATION

Torpid metabolism to fat calculations

I converted torpid $\dot{V}_{O_2}$ (mL O_2 min^{-1} g^{-1}) to grams of fat burned in an 18.78 g bat in a day for post-*Pd* and pre-*Pd* average mass-specific $\dot{V}_{O_2}$ from Szewczak & Jackson (1992) at each temperature setpoint. To do so, I used the following standard conversion factors:

To convert mL to L, I used 1 L = 1000 mL.

To convert min to days, I used 60 min = 1 hr and 24 hr = 1 day.

To convert L of O_2 to grams of fat, I used 1.96 L O_2 = 1 g of fat (Brown & Brengelmann 1966).

Therefore, for any given average $\dot{V}_{O_2}$, conversions to grams of fat burned in 180 days Ire as follows:

$$\frac{mL\ O2}{\min g} * \frac{60\ min}{1\ hr} * \frac{24\ hr}{1\ day} * \frac{1\ L}{1000\ mL} * \frac{18.78\ g}{1} * \frac{1\ g\ fat}{1.96\ L\ O2}$$

For pre-*Pd* data from Szewczak & Jackson (1992) at a T_{sk} setpoint of 5 ℃:

$$\frac{0.0005\ mL\ O2}{\min g} * \frac{60\ min}{1\ hr} * \frac{24\ hr}{1\ day} * \frac{1\ L}{1000\ mL} * \frac{18.78\ g}{1} * \frac{1\ g\ fat}{1.96\ L\ O2} = 0.006\ g\ fat$$

For pre-*Pd* data from Szewczak & Jackson (1992) at a T_{sk} setpoint of 10 ℃:

$$\frac{0.0006\ mL\ O2}{\min g} * \frac{60\ min}{1\ hr} * \frac{24\ hr}{1\ day} * \frac{1\ L}{1000\ mL} * \frac{18.78\ g}{1} * \frac{1\ g\ fat}{1.96\ L\ O2} = 0.008\ g\ fat$$

For pre-*Pd* data from Szewczak & Jackson (1992) at a T_{sk} setpoint of 20 ℃:

$$\frac{0.0018\ mL\ O2}{\min g} * \frac{60\ min}{1\ hr} * \frac{24\ hr}{1\ day} * \frac{1\ L}{1000\ mL} * \frac{18.78\ g}{1} * \frac{1\ g\ fat}{1.96\ L\ O2} = 0.03\ g\ fat$$

For pre-*Pd* data from Szewczak & Jackson (1992) at a T_{sk} setpoint of 30 ℃:

$$\frac{0.0069\ mL\ O2}{\min g} * \frac{60\ min}{1\ hr} * \frac{24\ hr}{1\ day} * \frac{1\ L}{1000\ mL} * \frac{18.78\ g}{1} * \frac{1\ g\ fat}{1.96\ L\ O2} = 0.10\ g\ fat$$

For pre-*Pd* data from Szewczak & Jackson (1992) at a T_{sk} setpoint of 37 ℃:

$$\frac{0.0159\ mL\ O2}{\min g} * \frac{60\ min}{1\ hr} * \frac{24\ hr}{1\ day} * \frac{1\ L}{1000\ mL} * \frac{18.78\ g}{1} * \frac{1\ g\ fat}{1.96\ L\ O2} = 0.22\ g\ fat$$

For post-*Pd* data at a T_a setpoint of 5 ℃:

$$\frac{0.0067\ mL\ O2}{\min g} * \frac{60\ min}{1\ hr} * \frac{24\ hr}{1\ day} * \frac{1\ L}{1000\ mL} * \frac{18.78\ g}{1} * \frac{1\ g\ fat}{1.96\ L\ O2} = 0.11\ g\ fat$$

For post-*Pd* data at a T_a setpoint of 10 ℃:

$$\frac{0.0043\ mL\ O2}{\min g} * \frac{60\ min}{1\ hr} * \frac{24\ hr}{1\ day} * \frac{1\ L}{1000\ mL} * \frac{18.78\ g}{1} * \frac{1\ g\ fat}{1.96\ L\ O2} = 0.07\ g\ fat$$

For post-*Pd* data at a T_a setpoint of 20 ℃:

$$\frac{0.0082\ mL\ O2}{\min g} * \frac{60\ min}{1\ hr} * \frac{24\ hr}{1\ day} * \frac{1\ L}{1000\ mL} * \frac{18.78\ g}{1} * \frac{1\ g\ fat}{1.96\ L\ O2} = 0.13\ g\ fat$$

For post-*Pd* data at a T_a setpoint of 30 ℃:

$$\frac{0.0190\ mL\ O2}{\min g} * \frac{60\ min}{1\ hr} * \frac{24\ hr}{1\ day} * \frac{1\ L}{1000\ mL} * \frac{18.78\ g}{1} * \frac{1\ g\ fat}{1.96\ L\ O2} = 0.26\ g\ fat$$

For post-*Pd* data at a T_a setpoint of 37 ℃ and 37.5 ℃:

$$\frac{0.0159\ mL\ O2}{\min g} * \frac{60\ min}{1\ hr} * \frac{24\ hr}{1\ day} * \frac{1\ L}{1000\ mL} * \frac{18.78\ g}{1} * \frac{1\ g\ fat}{1.96\ L\ O2} = 0.31\ g\ fat$$

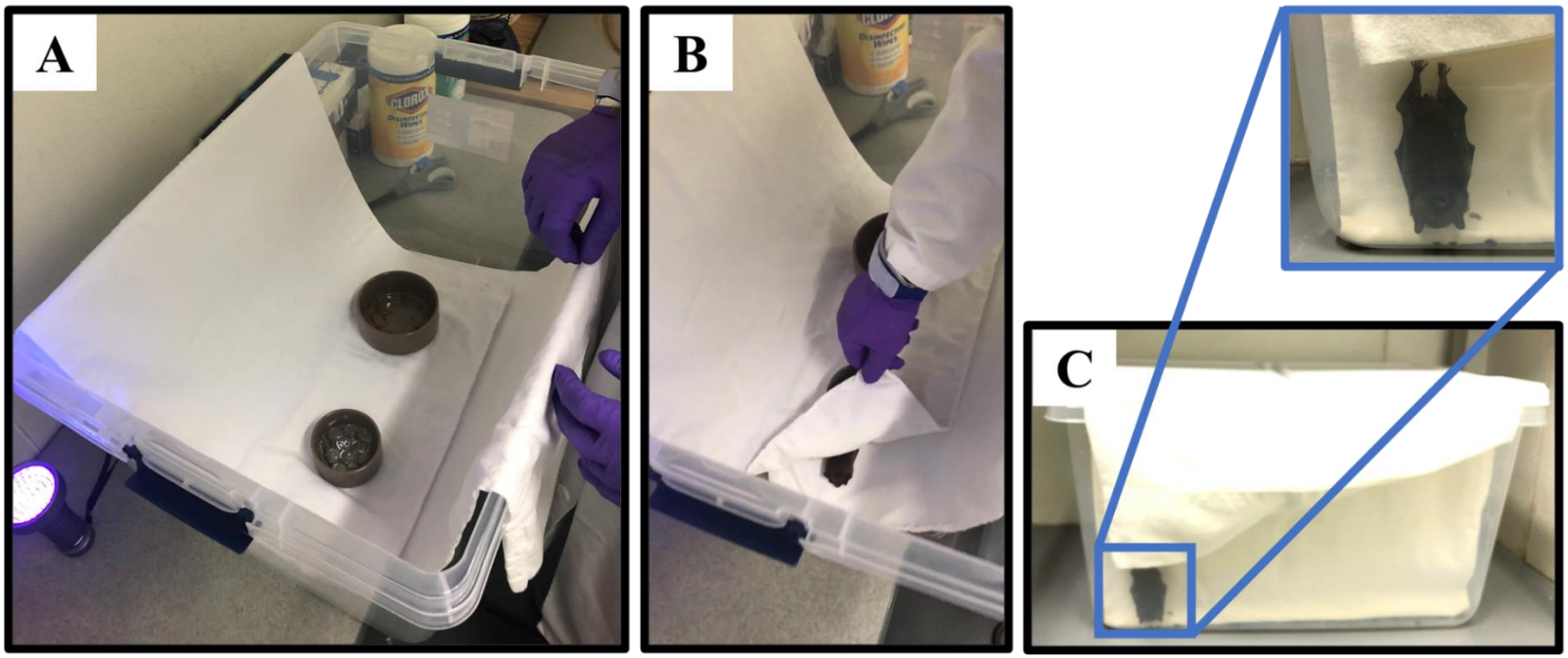

Figure S3.1. Bats Ire housed at Wright State University in 62.5 L plastic enclosures with two pillow cases draped over the long sides of the enclosure (A). Bats typically roosted underneath pillowcases (B) or hung vertically on the pillowcases (C).

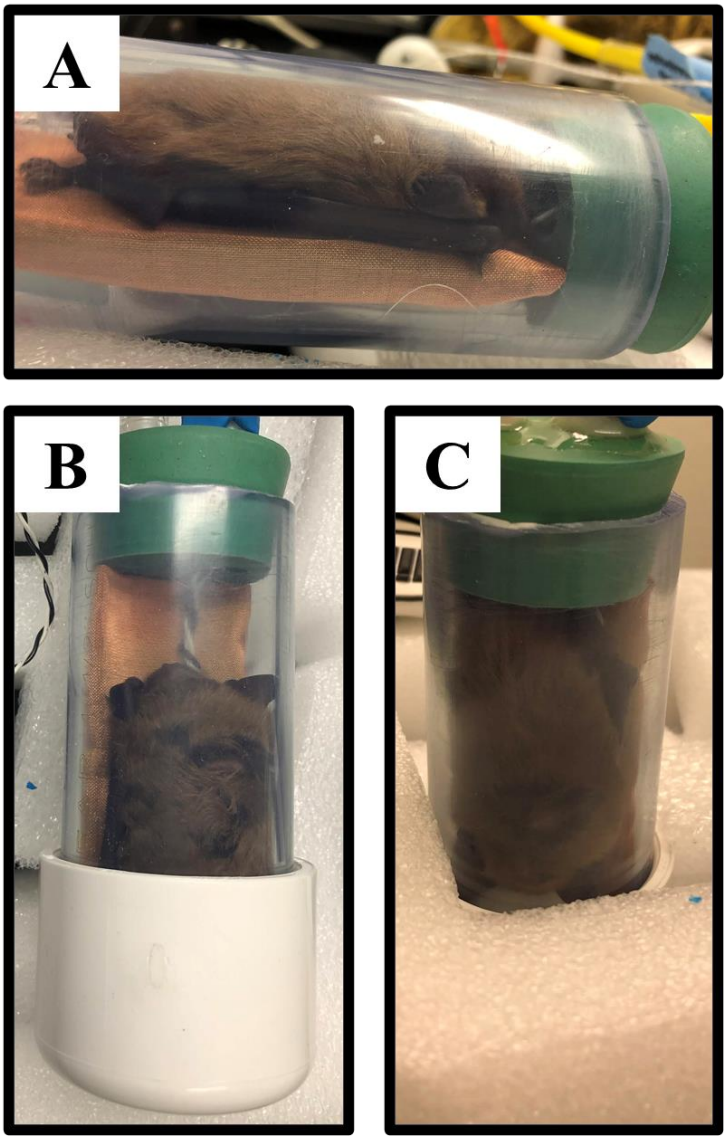

Figure S3.2. Bats Ire placed in a 0.9 L metabolic chamber for O_2 data collection. This chamber allowed bats to roost sternal (A and B) or vertical (C) depending on individual bat preference. A foam panel wrapped in copper mesh provided bats with material to hold on to with their hind limbs and allowed skin temperature probes to press on bat abdomens.

Table S3.1. Sex, average mass (g), average forearm length (mm) and *Pd* detection results via PCR for each individual bat collected in winters 2020 and 2021.

UID	Swab Collection Date	Sex	Mass (g)	Forearm Length (mm)	*Pd* nucleaic acid
20191748	6-Jan-20	F	22.85	46.00	not detected
20191750	30-Jan-20	F	24.58	49.00	not detected
20191753	14-Jan-20	M	20.92	48.00	not detected
20191754	5-Feb-20	M	16.81	47.50	not detected
20191759	19-Feb-20	M	16.61	43.50	not detected
20200022	11-Mar-20	F	21.82	47.50	not detected
20201736	15-Jan-21	F	19.29	47.50	not detected
20201738	4-Feb-21	M	17.77	50.50	not detected
20201746	15-Mar-21	F	15.62	46.00	not detected
20201747	26-Feb-21	M	16.96	49.50	not detected
20201748	1-Mar-21	F	17.41	47.50	not detected
20201749	10-Feb-21	M	23.98	50.00	not detected
20201750	19-Feb-21	F	18.83	49.00	not detected
20210010	12-Mar-21	M	15.14	45.25	not detected
20210012	3-Mar-21	F	20.89	48.75	not detected
20210013	8-Mar-21	M	15.30	46.50	not detected
20210024	19-Mar-21	M	19.15	48.25	not detected
20210029	24-Mar-21	M	14.07	48.00	not detected
20210035	8-Mar-21	F	18.55	47.50	not detected

Table S3.2. Average torpid metabolic rates, skin temperatures and ambient temperatures of each individual *E. fuscus* sampled in 2020 and 2021 at each ambient temperature set point and collection day. NAs represent where individual *E. fuscus* data was not collected and 'removed' values indicate where individual values were removed from analyses due to small signal to noise ratios.

	Ta Setpoint 0 ℃			Ta Setpoint 5 ℃			Ta Setpoint 10 ℃			Ta Setpoint 15 ℃			Ta Setpoint 20 ℃ Day 1			Ta Setpoint 20 ℃ Day 2		
UID	**VO2**	**Tsk**	**Ta**	**VO2**	**Tsk**	**Ta**	**VO2**	**Tsk**	**Ta**	**VO2**	**Tsk**	**Ta**	**VO2**	**Tsk**	**Ta**	**VO2**	**Tsk**	**Ta**
20191748	NA	NA	NA	NA	NA	NA	0.0005	11.1808	10.8825	NA	NA	NA	0.0006	19.9037	19.7705	0.0011	20.0233	19.6342
20191750	0.0067	5.4090	4.3958	removed	7.8350	7.2956	0.0011	9.7366	9.9209	removed	14.9419	14.8082	NA	NA	NA	0.0003	20.6848	19.8184
20191753	0.0144	3.6540	2.8414	0.0028	6.6399	6.5057	0.0011	8.8198	9.2262	0.0025	16.3996	15.8820	removed	21.0759	20.3237	-0.0003	20.0990	19.9667
20191754	0.0637	11.8577	5.1534	0.0311	8.0476	6.3754	0.0109	10.1216	9.2764	0.0020	14.8359	14.3932	0.0080	20.6839	19.7341	0.0019	20.9975	20.0409
20191759	0.0327	7.4814	5.0116	0.0166	9.2257	7.0893	0.0080	9.5007	9.6867	0.0185	20.2561	15.6021	0.0497	29.1073	22.6548	0.0479	26.8713	21.4757
20200022	0.0101	4.8975	3.7257	0.0028	7.6378	6.6070	0.0007	8.8131	8.8420	0.0036	15.7732	14.8559	0.0057	25.0396	21.3037	0.0100	24.9458	21.7465
20201736	0.0025	5.7811	4.3034	0.0038	7.9393	8.2002	0.0039	10.1940	11.6766	0.0022	15.5996	16.7424	0.0198	22.0031	21.9369	0.0288	20.5117	21.4768
20201738	0.0223	7.3105	5.5047	0.0025	8.6874	8.8719	0.0080	11.6905	12.7165	0.0013	15.5045	16.8515	0.0095	19.2428	20.7561	0.0064	20.5393	21.1256
20201746	0.0165	4.3148	2.5453	removed	6.3230	6.6121	0.0016	9.0888	10.3030	removed	13.9796	15.8087	0.0006	19.1003	20.9392	0.0058	19.4951	20.3382
20201747	0.0022	3.2410	0.1762	0.0026	6.4797	5.3546	0.0010	9.1698	9.9179	removed	15.3282	17.0190	0.0056	20.1007	22.7012	0.0061	20.4790	21.0356
20201748	0.0181	5.1545	-0.5448	0.0015	6.6034	4.0561	0.0002	8.8031	8.3108	0.0027	14.7277	15.0863	0.0028	19.7867	20.5869	0.0036	19.8813	20.4994
20201749	0.0171	5.5031	4.4393	0.0023	7.3917	6.9484	0.0054	9.9596	11.4102	0.0025	15.4218	16.5337	0.0040	19.9585	21.4335	0.0075	20.8508	20.8060
20201750	0.0130	4.8034	1.3493	0.0021	7.4412	6.2854	0.0018	10.0243	9.7068	0.0052	14.8119	15.4655	0.0021	19.5838	20.9061	0.0034	19.8051	20.6277
20210010	0.0128	19.0303	7.5108	0.0326	13.9049	7.9290	0.0114	14.1360	11.8034	0.0043	15.0551	15.4977	0.0035	19.9371	20.9074	0.0084	20.3040	20.9498
20210012	0.0738	8.6790	4.8075	0.0021	7.6831	7.6838	0.0029	11.4855	13.0662	0.0028	15.2344	16.6844	0.0062	20.4307	21.6739	0.0062	20.6736	21.4257
20210013	0.0528	9.1678	2.5097	0.0127	9.2139	7.1049	0.0233	11.4699	10.5511	removed	16.0194	16.6294	0.0024	20.1132	21.5258	0.0080	19.9135	19.8377
20210024	0.0085	3.0244	1.1647	0.0029	6.1314	5.8943	removed	8.5291	9.3979	0.0048	14.5195	16.2611	removed	20.2566	22.2351	0.0232	20.3907	21.5119
20210029	0.0103	3.9101	1.3948	0.0006	6.7051	5.9366	0.0023	9.1321	9.2424	0.0010	14.5362	15.4767	0.0071	19.5150	20.4650	0.0030	19.7455	20.1620
20210035	0.0292	5.4967	1.0616	0.0023	7.0145	5.2490	0.0035	9.8013	10.7769	0.0044	15.5162	16.1594	0.0025	20.0132	21.5062	0.0145	21.9150	21.2795

Table S3.2. Continued

	Ta Setpoint 20 ℃ Day 3			Ta Setpoint 25 ℃			Ta Setpoint 30 ℃			Ta Setpoint 35 ℃			Ta Setpoint 37 ℃			Ta Setpoint 37.5 ℃		
UID	VO2	Tsk	Ta	VO2	Tsk	Ta	VO2	Tsk	Ta	VO2	Tsk	Ta	VO2	Tsk	Ta	VO2	Tsk	Ta
20191748	NA	NA	NA	0.0055	26.9356	26.1095	0.0117	31.3678	30.3853	0.0120	35.8828	35.2915	NA	NA	NA	NA	NA	NA
20191750	NA	NA	NA	0.0088	26.7476	25.3227	0.0182	32.6463	30.7463	0.0112	35.0769	34.6530	NA	NA	NA	NA	NA	NA
20191753	0.0018	19.6396	19.2740	0.0401	26.9107	26.4370	0.0255	31.9216	31.2265	0.0152	34.6647	34.6404	NA	NA	NA	NA	NA	NA
20191754	NA	NA	NA	0.0104	29.3520	26.4090	0.0224	31.5677	30.0930	0.0122	34.4111	34.0191	0.0163	36.4151	36.1017	NA	NA	NA
20191759	NA	NA	NA	0.0091	28.3135	25.6759	0.0116	32.9071	30.9151	0.0156	34.6685	34.3700	0.0136	37.2409	36.8495	NA	NA	NA
20200022	NA	NA	NA	0.0074	30.4539	28.1310	0.0210	36.3098	33.7721	0.0860	38.3834	37.1036	0.0177	41.0977	39.8652	NA	NA	NA
20201736	NA	NA	NA	0.0088	25.2754	25.9047	0.0163	31.6302	31.0238	0.0216	35.1209	35.0048	NA	NA	NA	0.0271	37.7267	37.5670
20201738	NA	NA	NA	0.0097	24.9478	26.4140	0.0359	29.8939	30.9494	0.0214	34.8397	34.8739	NA	NA	NA	0.0221	37.0681	37.5169
20201746	NA	NA	NA	0.0069	24.5364	25.9312	0.0105	30.7666	31.5242	0.0211	34.5788	36.4257	NA	NA	NA	0.0370	36.2255	38.7030
20201747	NA	NA	NA	0.0061	24.5907	25.3910	0.0137	30.2651	30.5533	0.0165	35.4372	35.9273	NA	NA	NA	0.0204	37.3565	38.0237
20201748	NA	NA	NA	0.0094	25.2479	26.6115	0.0150	31.3957	31.7426	0.0091	35.3302	35.7745	NA	NA	NA	0.0218	37.8612	38.4659
20201749	NA	NA	NA	0.0133	25.0643	26.1883	0.0091	31.3170	32.5938	0.0150	35.9495	37.7413	NA	NA	NA	0.0168	37.7671	40.4228
20201750	NA	NA	NA	0.0224	25.2250	25.2785	0.0149	31.5921	30.7022	0.0163	35.3930	35.1234	NA	NA	NA	0.0233	38.3827	37.5823
20210010	NA	NA	NA	0.0081	25.0279	24.5956	0.0129	30.3496	29.7535	0.0190	35.2977	34.4009	NA	NA	NA	0.0200	37.9044	36.7564
20210012	NA	NA	NA	0.0130	25.2908	26.0591	0.0300	31.0236	31.1908	0.0193	35.6549	36.4191	NA	NA	NA	0.0212	38.4191	38.7498
20210013	NA	NA	NA	0.0125	24.3412	24.4368	0.0426	31.1989	29.3875	0.0044	34.3486	34.1182	NA	NA	NA	0.0224	36.6188	36.7699
20210024	NA	NA	NA	0.0273	24.6734	25.3555	0.0226	33.0127	32.1655	0.0263	35.3068	35.9535	NA	NA	NA	0.0248	38.2114	39.5243
20210029	NA	NA	NA	0.0161	25.5430	25.4541	0.0112	31.3891	30.5599	0.0194	35.3646	35.2035	NA	NA	NA	0.0280	38.0731	37.5177
20210035	NA	NA	NA	0.0069	25.6684	24.2234	0.0155	31.1575	29.8831	0.0124	35.8322	34.9749	NA	NA	NA	0.0232	38.3021	36.8529

APPENDIX C
CHAPTER 4 SUPPORTING INFORMATION

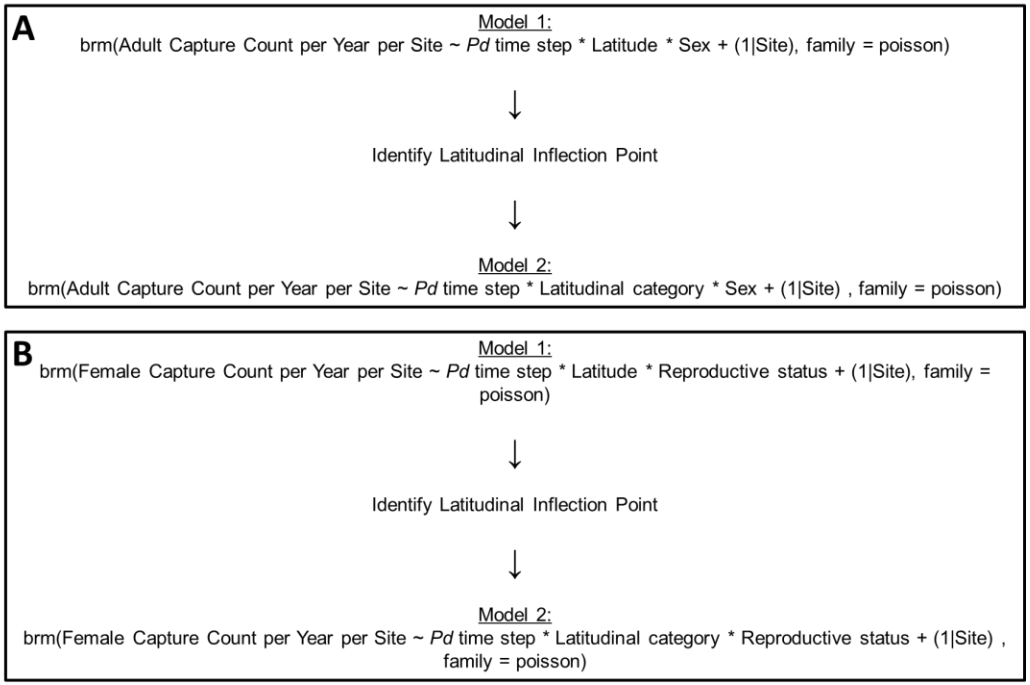

Figure S4.1. Bayesian generalized linear mixed model creation occurred in two steps to determine differences in adult demographics (A) or female reproductive demographics (B). Models Ire created using the *brms* package in R (Bürkner 2017; R Core Team 2021).

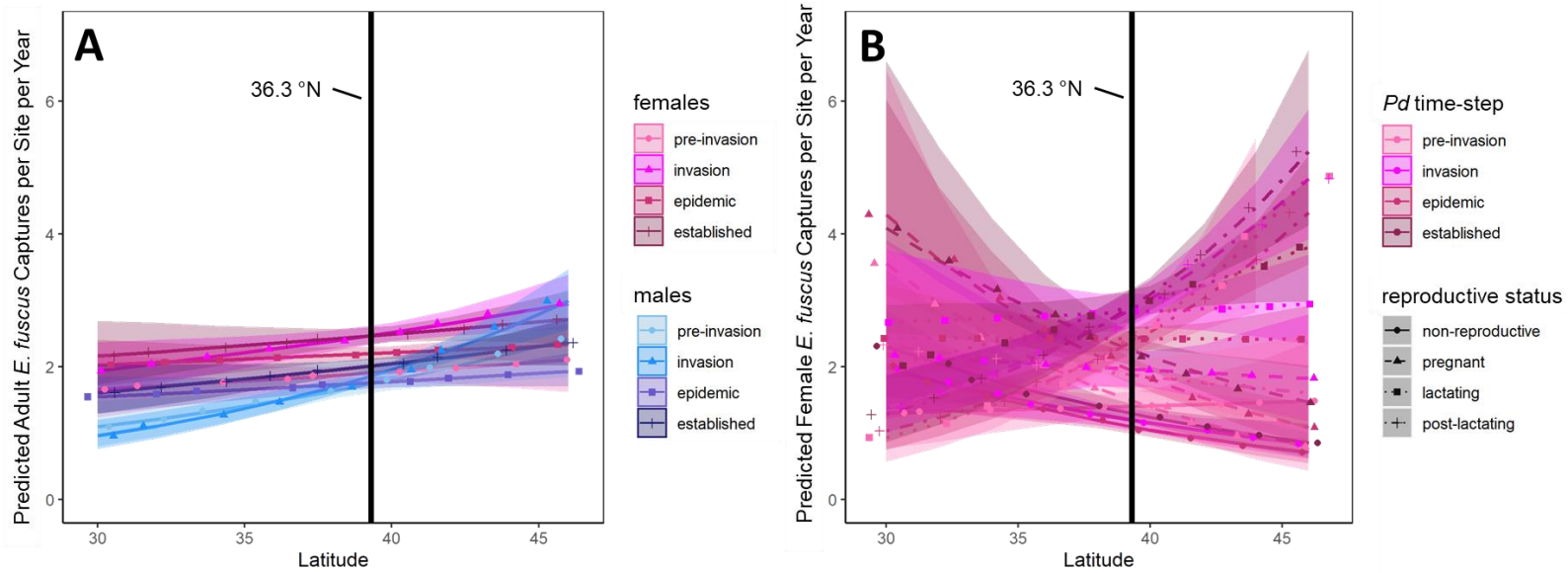

Figure S4.2. Demographic changes to the abundance of *E. fuscus* occurred over *Pd* exposure time-steps with latitude for adults [R^2 = 0.36 (0.34, 0.37); A] and females-only [R^2 = 0.49 (0.46, 0.51); B] and males. The interaction of *Pd* time-steps, latitude and sex (A) or female reproductive status (B) occurred at 39.3 °N for adult and female-only models (vertical black line). Values south of spatial thresholds varied compared to values north of spatial thresholds. Circles are predicted posterior mean estimates for whole number latitudes from 30-45 °N. Lines represent predicted values for posterior mean estimates with shaded

95% credible intervals. Color reflects *Pd* exposure time-steps for males (blue hues) or females (pink hues), and line type reflects reproductive status (females only, A).

END.